
Application of the Second Generation Intact Stability Criteria in Freeboard assessment

Auteur : Josipovic, Marko

Promoteur(s) : Rigo, Philippe

Faculté : Faculté des Sciences appliquées

Diplôme : Master : ingénieur civil mécanicien, à finalité spécialisée en "Advanced Ship Design"

Année académique : 2022-2023

URI/URL : <http://hdl.handle.net/2268.2/18228>

Avertissement à l'attention des usagers :

Tous les documents placés en accès ouvert sur le site le site MatheO sont protégés par le droit d'auteur. Conformément aux principes énoncés par la "Budapest Open Access Initiative"(BOAI, 2002), l'utilisateur du site peut lire, télécharger, copier, transmettre, imprimer, chercher ou faire un lien vers le texte intégral de ces documents, les disséquer pour les indexer, s'en servir de données pour un logiciel, ou s'en servir à toute autre fin légale (ou prévue par la réglementation relative au droit d'auteur). Toute utilisation du document à des fins commerciales est strictement interdite.

Par ailleurs, l'utilisateur s'engage à respecter les droits moraux de l'auteur, principalement le droit à l'intégrité de l'oeuvre et le droit de paternité et ce dans toute utilisation que l'utilisateur entreprend. Ainsi, à titre d'exemple, lorsqu'il reproduira un document par extrait ou dans son intégralité, l'utilisateur citera de manière complète les sources telles que mentionnées ci-dessus. Toute utilisation non explicitement autorisée ci-avant (telle que par exemple, la modification du document ou son résumé) nécessite l'autorisation préalable et expresse des auteurs ou de leurs ayants droit.



Created with MidjourneyAI, published under creative commons license

Master's Thesis

Application of the Second Generation Intact Stability Criteria in Freeboard Assessment

by Marko Josipović

Supervisors:

Dr.-Ing. Igor Bačkalov

Dr.-Ing. Florian Sprenger



Duisburg, 2023

Application of the Second Generation Intact Stability Criteria in Freeboard Assessment

© Marko Josipović, 2023

All rights reserved, text, pictures, and graphics are protected material.

The work in this thesis was carried out in the:



DST Entwicklungszentrum für Schiffstechnik und Transportsysteme e. V.

Duisburg, Germany

Direct Supervisor: Dr.-Ing. Igor Bačkalov (DST, Duisburg)

Faculty Supervisor: Dr.-Ing. Florian Sprenger (University of Rostock, Germany)

M.Sc. Iven Sponholz (University of Rostock, Germany)

Universität
Rostock



Traditio et Innovatio



SOLENT
UNIVERSITY
SOUTHAMPTON



Zachodniopomorski
Uniwersytet
Techniczny
w Szczecinie



With the support of the
Erasmus+ Programme
of the European Union



Application of the Second Generation Intact Stability Criteria in Freeboard Assessment

Master Thesis

Submitted on August 7, 2023

by Marko JOSIPOVIĆ

Teodora Hercla 3, 11080 Belgrade, Serbia
marko.josipovic@uni-rostock.de
Student ID No.: 222202274

Reviewer

Dr.-Ing. Igor BAČKALOV
backalov@dst-org.de
DST - Development Centre for Ship
Technology and Transport Systems
Oststrasse 77, 47057 Duisburg,
Germany

Reviewer

Dr.-Ing. Florian SPRENGER
florian.sprenger@uni-rostock.de
University of Rostock
Albert-Einstein-Str 2, 18059 Rostock,
Germany

EMSHIP+ PROGRAM
ADVANCED DESIGN OF SHIPS AND OFFSHORE STRUCTURES
ACADEMIC YEAR 2022-2023

Тјело стење под силом душевном,
колеба се душа у тијелу:
море стење под силом небесном,
колебљу се у мору небеса...

- Petar II Petrović Njegoš, Gorski Venac

Declaration of Authorship

I, Marko Josipovic, declare that this thesis and the work presented in it are my own and have been generated by me as the result of my own original research.

Where I have consulted the published work of others, this is always clearly attributed.

Where I have quoted from the work of others, the source is always given. With the exception of such quotations, this thesis is entirely my own work.

I have acknowledged all main sources of help.

Where the thesis is based on work done by myself jointly with others, I have made clear exactly what was done by others and what I have contributed myself.

This thesis contains no material that has been submitted previously, in whole or in part, for the award of any other academic degree or diploma.

I cede the copyright of the thesis in favor of the University of Rostock and DST - Development Centre for Ship Technology and Transport Systems.

Date: 7 August 2023

Signature:

Location: Duisburg, Germany

Acknowledgement

First and foremost, I want to express my deepest gratitude to my family. Their endless patience, support, and faith in me throughout my education journey, and particularly through this rigorous master's program, have been invaluable. It didn't turn out so bad!

I would also like to express my sincere gratefulness to my professor, Igor Bačkalov, who has been an actuator in the whole process of writing this thesis. During this period he significantly contributed to my academic and personal growth. Next to sparking my interest in stability and seakeeping, he interested me also in German models. With lots of cups of coffee, I am hoping that we will continue the shared journey in the same way.

I am grateful to Prof. Stefan Rudaković, for his advice, and assistance to cross-check the developed code. His doctoral dissertation made the process of writing this thesis significantly smoother.

Special thanks to Prof. Florian Sprenger and Mr. Iven Sponholz for their insightful reviews and comments during the development of this thesis.

Finally, I would like to thank my friends and colleagues, who have contributed to my journey with their support.

Abstract

The goal of the thesis is to evaluate the influence of freeboard on the dynamic stability of ships in intact condition in seaway using a probabilistic approach. Currently, the assessment of freeboard is governed by deterministic regulations of the International Convention on Load Lines which are mostly based on the damage stability and shipping of green water considerations. The investigation presented in this thesis is based on the evaluation of the vulnerability of a sample container ship to stability failure in Dead Ship Condition whereby the freeboard of the examined ship was systematically varied. For the purpose of this assessment, Vulnerability Level 1 and 2 are considered as given in Second Generation Intact Stability Criteria (SGISC), the state-of-the-art intact stability criteria put forward by the International Maritime Organization. An original computer code for assessment of stability in Dead Ship Condition was developed and the analysis is performed on a small container vessel (feeder) considering two container arrangements and the presence/absence of bilge keels. The thesis also presents the full procedure for the calculation of the long-term index of probability of stability failure in Dead Ship Condition.

The thesis outcomes indicate that the increase of freeboard within the realistic boundaries may reduce the probability of stability failure by up to two orders of magnitude. The research shows that the probabilistic calculations done at Vulnerability Level 2 give a range of acceptable metacentric heights, limited by lower and upper boundaries, as well as an "optimal" metacentric height corresponding to the lowest probability index of stability failure. Such results cannot be achieved at Level 1 which results in the minimum value of metacentric height only. The calculations also confirm the existence of inconsistencies in stability assessment in Dead Ship Condition according to the SGISC framework. Finally, some recommendations for defining precise approaches in specific stages of the methodology for Level 2 are suggested, which could reduce the possibility of calculation errors.

Keywords: Second Generation Intact Stability Criteria, roll motion,
Dead Ship Condition, freeboard assessment

Scientific field: Mechanical Engineering

Scientific branch: Naval Architecture

Zusammenfassung

Das Ziel der Abschlussarbeit ist die Bewertung des Einflusses des Freibords auf die dynamische Stabilität von Schiffen im unbeschädigten Zustand und in Seebedingungen unter Verwendung eines probabilistischen Ansatzes. Derzeit wird die Beurteilung des Freibords von den Vorschriften der Internationalen Freibord-Übereinkommen bestimmt, welche hauptsächlich auf der Leckstabilität und der Berücksichtigung von Wasser an Deck basieren. Die in dieser Arbeit präsentierte Untersuchung basiert auf der Bewertung der Anfälligkeit eines beispielhaften Containerschiffs für Stabilitätsversagen im Zustand dead ship, wobei der Freibord des untersuchten Schiffs systematisch variiert wurde. Für diese Bewertung werden die vulnerability level 1 und 2 gemäß den Kriterien der Second Generation Intact Stability Criteria (SGISC) berücksichtigt, die von der International Maritime Organization als die aktuellsten Kriterien für die Intaktstabilität vorgestellt wurden. Ein Computercode zur Beurteilung der Stabilität im Zustand dead ship wurde entwickelt und die Analyse wurde an einem kleinen Containerschiff (feeder) durchgeführt, wobei zwei Containeranordnungen und das Vorhandensein sowie Fehlen von Bilgenkielen berücksichtigt wurden. Zusätzlich wird das vollständige Verfahren zur Berechnung des Langzeit-Index der Wahrscheinlichkeit eines Stabilitätsversagens im Zustand dead ship präsentiert.

Die Ergebnisse der Arbeit zeigen, dass eine Erhöhung des Freibords innerhalb realistischer Grenzen die Wahrscheinlichkeit eines Stabilitätsversagens um bis zu zwei Größenordnungen verringern kann. Die Untersuchungen zeigen, dass die probabilistischen Berechnungen, die auf vulnerability level 2 durchgeführt wurden, einen Bereich akzeptabler Metazentrischerhöhen liefern, begrenzt durch untere und obere Grenzen, sowie eine optimale Metazentrischehöhe, die dem niedrigsten Index der Wahrscheinlichkeit eines Stabilitätsversagens entspricht. Solche Ergebnisse können auf Stufe 1 nicht erzielt werden, was lediglich zu einem minimalen Wert der Metazentrischenhöhe führt. Die Berechnungen bestätigten auch fehlende Konsistenz bei der Stabilitätsbewertung im Zustand dead ship gemäß der SGISC. Schließlich werden einige Empfehlungen zur Festlegung präziser Ansätze in bestimmten Phasen der Methodik für Stufe 2 vorgeschlagen, die die Möglichkeit von Berechnungsfehlern reduzieren könnten.

Schlüsselwörter:	Second Generation Intact Stability Criteria, Rollbewegung, dead ship Zustand, Bewertung des Freibords
Wissenschaftliches Feld:	Maschinenbau
Wissenschaftlicher Zweig:	Schiffsarchitektur

Table of Contents

Acknowledgement	v
Abstract	vii
Zusammenfassung	ix
Nomenclature	xi
1 Introduction	1
2 The Role of Freeboard	3
2.1 Possibilities for Improvement of Intact Stability	3
2.2 Freeboard as a Critical Element of Ship Stability and Safety	4
2.3 International Convention on Load Lines	6
3 Second Generation Intact Stability Criteria	7
3.1 Overview	8
3.2 Fundamentals of Stability Failure Modes	9
4 Dead Ship Condition	17
4.1 Vulnerability Level 1	17
4.2 Vulnerability Level 2	19
5 Sample Ship - Multipurpose Cargo Vessel	29
5.1 Model of the Ship	29
5.2 Modifying Freeboard on a Sample Ship	30
6 Application of the Vulnerability Level 2 of SGISC for Dead Ship Condition	35
6.1 Wind Impact and Associated Relevant Angles	38
6.2 Environments Impact	40
6.3 Equivalent Linear Roll Damping Coefficients	42
6.4 Long-term Failure Index of Worked Example	45
7 Analysis and Interpretation of Results	49
7.1 Research Outcome	49
7.2 Interpretation	52
8 Conclusions and Future Work	57
Bibliography	61

Nomenclature

Symbols

Symbol	Definition	Unit
A_K	Total area of bilge keels	$[m^2]$
A_L	Projected lateral area	$[m^2]$
B	Breadth of the ship	$[m]$
C_B	Block coefficient	$[-]$
C_{DSC}	Long-term DSC failure index	$[-]$
$C_{DSC,s}$	Short-term DSC failure index	$[-]$
C_M	Midship section coefficient	$[-]$
C_P	Prismatic coefficient	$[-]$
C_{whm}	Wind heeling moment coefficient	$[-]$
C_W	Waterplane area coefficient	$[-]$
D	Depth of the ship	$[m]$
g	Gravity acceleration, taken as 9.81	$[m/s^2]$
\overline{GM}	Metacentric height	$[m]$
\overline{GM}_{res}	Residual metacentric height	$[m]$
\overline{GZ}	Righting lever	$[m]$
\overline{GZ}_{res}	Residual righting lever	$[m]$
H	Absolute roll transfer function	$[-]$
H_{rel}	Relative roll transfer function	$[-]$
H_s	Significant wave height	$[m]$
\overline{KG}	Vertical centre of gravity	$[m]$
L	Length of the ships	$[m]$
$l_{wind,tot}$	Wind heeling lever	$[m]$
m_0	Zeroth spectral moment	$[-]$
m_2	Second spectral moment	$[-]$
\overline{OG}	Vertical distance between waterline and center of gravity	$[m]$
P	Pressure	$[Pa]$
r	Effective wave slope coefficient	$[-]$
S	Spectrum of relative roll angle	$[rad^2/(rad/s)]$
s	Wave steepness factor	$[-]$
S_v	Spectrum of the wind gust	$[(m/s)^2/(rad/s)]$
S_{zz}	Spectrum of sea elevation	$[m^2/(rad/s)]$
$S_{\alpha\alpha}$	Spectrum of wave slope	$[rad^2/(rad/s)]$
$S_{\alpha\alpha,c}$	Spectrum of effective wave slope	$[rad^2/(rad/s)]$
$S_{\delta M_{wind,tot}}$	Spectrum of the wind gust moment	$[(Nm)^2/(rad/s)]$

TABLE OF CONTENTS

Symbol	Definition	Unit
d	Draught of the ship	[m]
t	Time	[s]
$T_{z,CDSC,s}$	Zero-crossing wave period	[s]
T_{exp}	Exposure time	[s]
$T_{z,\varphi}$	Zero-crossing roll period	[s]
T_r	Natural roll period	[s]
U_w	Mean wind speed	[m^2/s]
V	Displaced volume	[m^3]
W_i	Weighting factor	[-]
Z	Vertical distance from the center of windage area to the center of the underwater lateral area	[m]
β	Quadratic damping coefficient	[$1/s$]
Δ	Displacement force	[N]
δ	Cubic damping coefficient	[s/rad^2]
$\Delta\varphi_{res,EA+}$	Residual range of stability to leeward side	[$rad,^\circ$]
$\Delta\varphi_{res,EA-}$	Residual range of stability to windward side	[$rad,^\circ$]
μ	Linear damping coefficient	[$1/s$]
ν	Viscosity, taken as $1.14 \cdot 10^{-6}$	[m^2/s]
μ_e	Equivalent linear roll damping coefficient	[-]
ρ	Density of water, taken as 1025	[kg/m^3]
ρ_{air}	Density of air, taken as 1.222	[kg/m^3]
$\sigma_{z,CDSC,s}$	Standard deviation of roll	[rad]
$\sigma_{\dot{x}}$	Standard deviation of roll angular velocity	[rad/s]
$\varphi_{cap,EA+}$	Virtual capsize angle to leeward side	[$rad,^\circ$]
$\varphi_{cap,EA-}$	Virtual capsize angle to windward side	[$rad,^\circ$]
$\varphi_{crit,+}$	Critical angle to leeward side	[$rad,^\circ$]
$\varphi_{crit,-}$	Critical angle to windward side	[$rad,^\circ$]
φ_d	Angle of deck immersion	[$rad,^\circ$]
$\varphi_{fail,+}$	Failure angle to leeward side	[$rad,^\circ$]
$\varphi_{fail,-}$	Failure angle to windward side	[$rad,^\circ$]
φ_f	Angle of down-flooding	[$rad,^\circ$]
φ_s	Static heel angle	[$rad,^\circ$]
$\varphi_{VW,+}$	Angle of vanishing stability to leeward side	[$rad,^\circ$]
$\varphi_{VW,-}$	Angle of vanishing stability to windward side	[$rad,^\circ$]
φ_1	Angle of roll	[$rad,^\circ$]
χ	Aerodynamic admittance function	[-]
ω	Circular frequency	[rad/s]
ω_e	Encounter wave frequency	[rad/s]
$\omega_{z,CDSC,s}$	Zero-crossing roll frequency	[rad/s]
ω_0	Natural roll frequency	[rad/s]
$\omega_{0,e}$	Modified natural roll frequency	[rad/s]

Abbreviations

Abbreviation	Definition
BK	Bilge Keel
DSA	Direct Stability Assessment
DSC	Dead Ship Condition
ICLL	International Convention on Load Lines
IMO	International Maritime Organisation
2008 IS CODE	Intact Stability Code 2008
LC1	Loading Condition 1
LC2	Loading Condition 2
L1	Level 1
L2	Level 2
OG	Operational Guidance
OL	Operational Limitation
SGISC	Second Generation Intact Stability Criteria
SOLAS	International Convention for the Safety of Life at Sea
TEU	twenty-foot equivalent unit
1DOF	one-degree-of-freedom

Introduction

The sea environment is characterized by strong winds and waves which can create challenging but sometimes also unsustainable conditions for the ships, resulting in capsizing and sinking. Without having the possibility to influence external factors, it is the design and operation of the ship that can be utilized to avoid or at least reduce to some extent the undesirable consequences.



Figure 1.1: Katsushika Hokusai, *The Great Wave off Kanagawa*, 1831.

The general idea of the thesis is to assess how the freeboard, which is an essential ship design parameter, affects the intact stability of a ship in rough weather. To do this, the Second Generation Intact Stability Criteria (SGISC) which represent the state-of-the-art approach in the stability field, will be used.

Intact and damage stability, as well as the seakeeping performance of the ship, are significantly influenced by the freeboard. Nowadays, the freeboard assessment of seagoing vessels is regulated by the deterministic International Convention on Load Lines (ICLL), which is going to be addressed in *Chapter 2*. On the other hand, the importance of freeboard from the safety point of view is often suppressed for economic reasons: a smaller freeboard results in smaller enclosed spaces (i.e. in lower gross tonnage (GT)) and decreased steel weight of the ship which leads to lower capital and operational costs. A compromise between stability, safety, and economics should be carefully defined, and the determination of the freeboard plays an especially important role in this process.

Second Generation Intact Stability Criteria represent a different approach to intact stability assessment based on "first principles", where interaction between environmental conditions and ships is better related to underlying physics and does not contain as many empirical elements, as is the case with the rules given in the International Code on Intact Stability (2008 IS CODE). SGISC are finalized by International Maritime Organization (IMO) in 2020 but are still not mandatory in the shipbuilding industry. The criteria address five stability failure modes: Dead Ship Condition, Excessive Acceleration, Pure Loss of Stability, Parametric Rolling, and Surf-Riding/Broaching-to. The failure modes will be described in *Chapter 3*. IMO gives an opportunity for a multi-tier concept, where the assessment of a ship's vulnerability to each failure mode consists of three different levels: Vulnerability Level 1, Vulnerability Level 2, and Direct Stability Assessment. While the complexity of calculations increases with each level, the accuracy should increase as well, and consequently, the conservativeness should decrease.

The main objective of this thesis is to analyze the ship's vulnerability to Dead Ship Condition for different freeboard heights, using the procedure of SGISC Vulnerability Level 2 (L2). L2 is a probabilistic analysis that provides an optimal balance between complexity and accuracy for the purpose of this study. Dead Ship Condition implies the failure of the ship's main propulsion plant, with the master and the crew having no possibility to intervene and affect the ship's position with respect to the dominant wind and wave conditions. It is assumed that in such circumstances, the ship would be exposed to beam winds and waves which may lead to a large amplitude of roll motion and even capsizing. Ship rolling represents a complex physical phenomenon; the simplifications used in IMO criteria to address the ship roll motion are going to be addressed in *Chapter 4*. The study will be performed on a small container vessel (a feeder) described in *Chapter 5*, which is selected as a sample ship due to its large lateral surface, which makes it vulnerable to beam wind. The freeboard of the sample ship will be systematically varied, and the SGISC L2 will be applied with the goal to isolate the influence of this single parameter on the intact stability of the ship in a seaway, which is the subject of *Chapter 6*. This influence will be described in probabilistic terms in *Chapter 7*.

The Role of Freeboard

2.1. Possibilities for Improvement of Intact Stability

Stability improvement may be considered in various phases of a ship's life. Ideally, the intended stability performance would be accomplished in the design phase, reducing the need for future steps and saving additional expenses while preventing accidents caused by insufficient stability. However, the measures for stability improvement are sometimes considered in the course of ship reconstruction. The potential reasons behind this include complying with newly implemented regulations (which in some cases may apply in retrospect) or correcting errors made during the design and/or construction phase.

It is essential to identify the parameters involved in formulating the moment of stability to determine the appropriate measures for improving ship stability. The moment of stability $M_{st}(\varphi)$ can be calculated as follows:

$$M_{st}(\varphi) = g \cdot \Delta \cdot \overline{GZ}(\varphi). \quad (2.1)$$

From the equation above it can be noticed that the stability may be improved by raising either the displacement Δ or the righting lever \overline{GZ} , as both parameters are directly proportional to the moment of stability. Changing displacement is not often the solution for this type of problem. Increasing displacement results in higher prices of construction costs and expenses of exploitation (larger and more powerful engines to reach a certain speed compared to initial displacement). Raising the weight of the steel on the ship will also increase the weight of the lightship, which will reduce the payload capacity. On the other hand, modification of the righting lever is well one of the solutions which open more space for the creativity of engineers. According to Steinen, the righting lever can be divided into two parts:

$$\begin{aligned} \overline{GZ}(\varphi) &= \overline{GZ}_c(\varphi) + \overline{GZ}_{res}(\varphi) \\ \overline{GZ}(\varphi) &= \overline{GM}_0 \cdot \sin(\varphi) + \overline{M}_0 \overline{M}_\varphi \cdot \sin(\varphi) \end{aligned} \quad (2.2)$$

where $\overline{GZ}_c(\varphi)$ corresponds to the righting lever of the ship which has a circular arc section and $\overline{GZ}_{res}(\varphi)$ is the residual righting lever. Regarding the first term which is a function

of the distribution of the masses and the hull form, it can be noticed that higher values of metacentric heights result in higher values of the righting lever. It is well known that greater metacentric heights result in better (hydrostatic) stability, but it will be shown that it may not always be like that in the case of dynamic stability in waves. Without going too much into detail, it may be stated that lowering the ship masses, loading the ballast, or increasing the ship beam are some of the measures that could be beneficial for a greater \overline{GM}_0 . The second term $\overline{GZ}_{res}(\varphi)$ is a function of the hull form only and the benefit of this term will be explained in the following section.

2.2. Freeboard as a Critical Element of Ship Stability and Safety

As noted above, the second term in the *Equation (2.2)* is the only function of the hull form. *Figure 2.1* illustrates variation $\overline{GZ}_{res}(\varphi)$ with different hull forms. For a ship with a circular arc cross-section, the residual righting lever does not exist ($\overline{GZ}_{res}(\varphi) = 0$). This implies that the equation is only influenced by the initial metacentric height \overline{GM}_0 . A ship whose hull form has a tumble-home section shows a negative residual righting lever. In contrast, ships with U and V cross-sections have a positive residual righting lever. Between these two, the V-section demonstrates slightly superior residual stability. The shape of the ship's hull above the waterline, which can either be narrowed or widened is very important because it dictates how the center of buoyancy shifts (B-curve) when it submerges. The way of shifts of buoyancy force directly influences the righting lever, affecting the overall stability of the ship. More details can be found in *Ribar, 1986*.

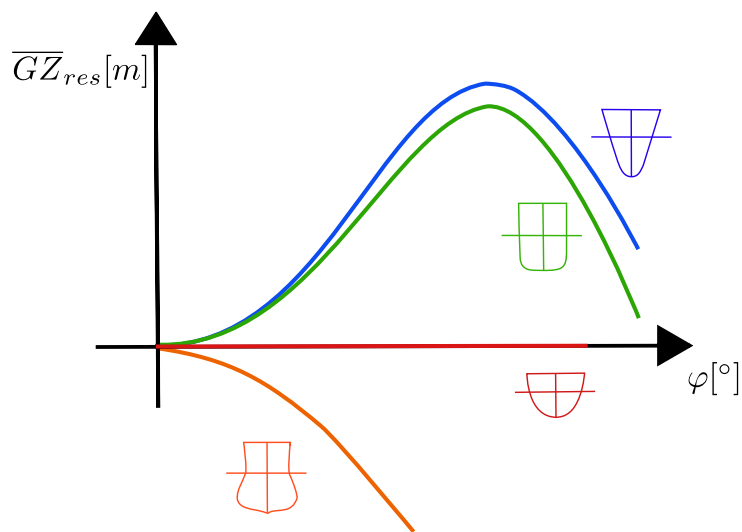


Figure 2.1: Residual righting lever for different hull forms (*Ribar, 1986*).

Apart from the hull shape influence on $\overline{GZ}_{res}(\varphi)$, the freeboard height also plays a critical role. Increasing the freeboard height has a significant impact on various aspects of ship safety and stability. From the intact stability point of view, the residual righting lever increases with the higher freeboard which is directly associated with the righting lever. Increased freeboard height has a positive effect on damage stability as well because it provides additional reserve buoyancy. An increase of freeboard is also an effective measure in mitigating the impact of green water which can damage the structure and equipment on the deck.

2.2. FREEBOARD AS A CRITICAL ELEMENT OF SHIP STABILITY AND SAFETY

Figure 2.2 illustrates the case where the ship has the same submerged hull form, while the freeboard height is different. It may be noticed that up to a certain heeling angle, the trends of the residual righting lever are the same for both freeboard heights. This angle corresponds to the angle where the deck of the ship with the lower freeboard submerges (green-shaded area) after which its submerged geometry sharply changes which results in the decline of $\overline{GZ}_{res}(\varphi)$. The same process applies to the ship with the higher freeboard as well, but the residual righting lever will start to decline at a much higher angle of the heel (blue-shaded area).

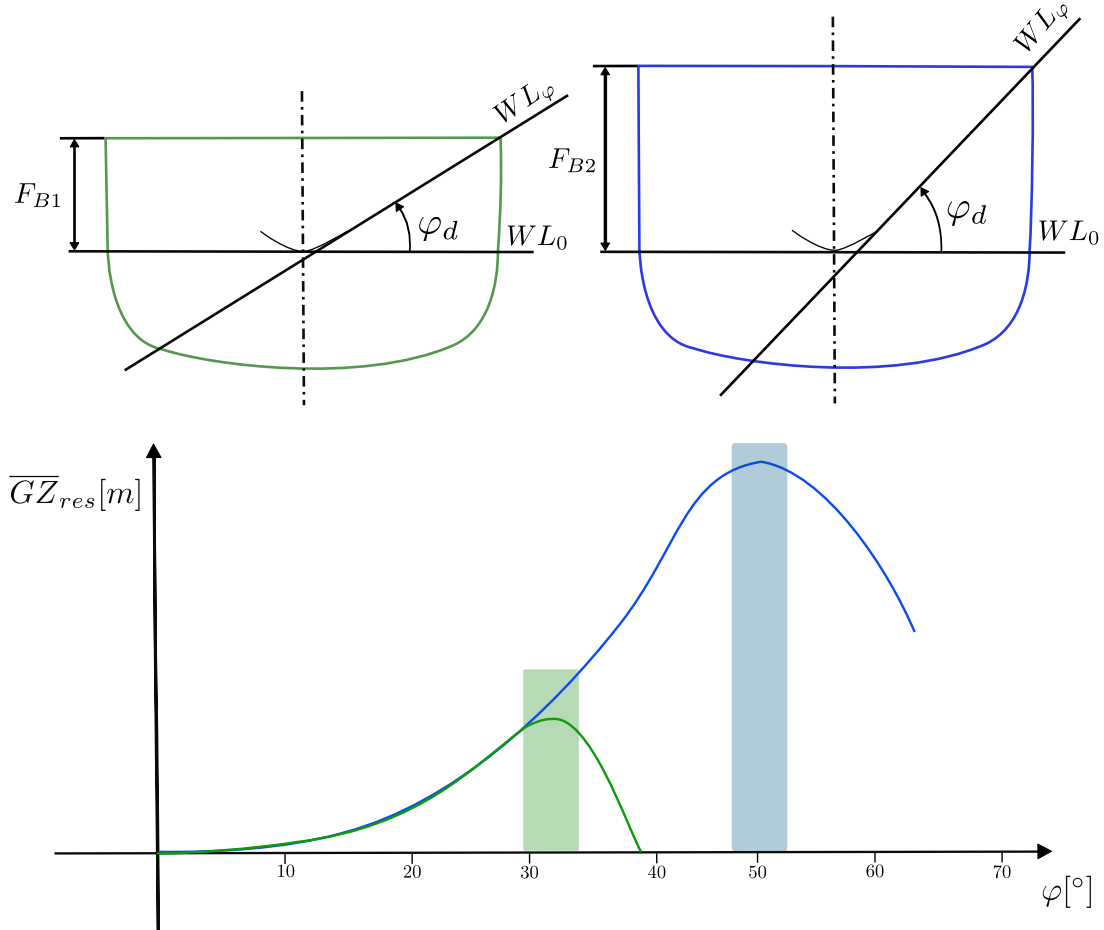


Figure 2.2: Simplified representation of residual righting lever for different freeboard heights (*Ribar, 1986*).

In general, the righting lever significantly depends on the freeboard: with higher freeboards the maximum values of \overline{GZ} appear at higher values, the range of stability is increasing, and so does the energy required to capsize the ship, either statically or dynamically. However, it should be kept in mind that with the increase of freeboard for the same draft, the mass of the steel and the volume of enclosed spaces increase as well; the former results in an increase in production costs and a decrease in payload, while the latter affects the increase of gross tonnage. Thus, both the construction and operation of the ship become more costly. On the other hand, the safety of the ship is significantly improved. These two aspects have to be balanced.

2.3. International Convention on Load Lines

The International Convention on Load Lines (ICLL) is the regulatory instrument used to determine the minimum freeboard for seagoing ships. The ICLL also prescribes the minimum bow height and the corresponding reserve buoyancy. ICLL also provides a set of essential conditions regarding watertightness and strength from a safety point of view which need to be satisfied before determining minimum freeboard. The freeboard is defined as the vertical distance from the upper edge of the deck line to the related load line (the maximum permissible load limit for a ship). Load lines mainly depend on the zone of sailing and season. The origins of ICLL date back to 1930. The present convention (including the tables for freeboard designation) was adopted by IMO in 1966. The most significant modifications were introduced by the Protocol of 1988 and the amendments of 2003. More details about the convention can be found in *IACS/LL, 2008*.

It should be noted that the ICLL requirements are mostly based on the need to improve reserve buoyancy (which has a positive impact on ship stability in damaged condition) and mitigate the effects of green water (which was the main subject of the 2003 amendments). Such decisions were mostly motivated by the major accidents in the period of establishment of the convention; the minimum bow height requirements can be traced back to a series of bulk carrier accidents in the 1980s. As a consequence, the influence of the freeboard on intact stability was left out of focus.

On the other hand, a higher freeboard may be undesirable as it leads to greater enclosed spaces as mentioned above. Therefore, the designer's main objective is typically to satisfy the minimum safety requirements and reduce costs. The freeboard assignment rules have been criticized for being based on outdated hull forms and, as such, unsuitable for modern seagoing ships (a similar deficiency is also noted in the first generation of stability criteria which will be discussed in the following chapter). Next to this, according to ICLL, smaller ships will have relatively smaller freeboards, which means that, in the same wave environment, a small ship will be experiencing relatively higher waves than a large ship. More details on the historical background of the ICLL regulations and the critical analysis of ICLL may be found at *Schneekluth and Bertram, 1998* and *Bačkalov, 2017*.

Second Generation Intact Stability Criteria

The creation of the International Convention for the Safety of Life at Sea (SOLAS), two years after the sinking of the Titanic in April 1912 marks a key moment in the history of maritime regulations. The adequacy of safety measures and regulations is typically reconsidered after accidents, especially if those involve fatalities. The initial international regulations were mainly focused on the stability of ships in damaged condition where the attention was put on the efficiency of the ship's subdivision. As a consequence, the intact stability was largely out of focus, and the corresponding criteria were not mandatory for a very long time.

One of the most important contributions to the field of intact stability in the 20th century was given by Jaakko Rahola. Starting from the earlier research on this topic until 1939, in his doctoral dissertation (*Rahola, 1939*) Rahola proposed a set of criteria for a "good" righting lever, taking into account factors such as a maximum lever, stability range, potential energy of stability, etc. The main idea behind this approach was to compare the righting levers of the ships involved in accidents with those of ships that had no known intact stability problems until then.

International Maritime Organization (IMO) developed the first intact stability provisions in the form of recommendations in 1968 based on the Rahola criterion. The provision was modified in 1985 which concerned the expansion of the database of analyzed ships, from 14 analyzed by Rahola up to 166 ships. The length of the examined ships did not exceed more than 100 *m* and only one passenger and merchant vessel were included. This criterion is included in International Code on Intact Stability (2008 IS CODE) for all seagoing ships which have a length above 24 *m*. More details about the history and development of 2008 IS CODE can be found in *Francescutto, 2023*.

Presently, 2008 IS CODE (*IMO, 2008*) consists of three parts: Part A (statistical criteria and the severe wind and rolling criterion), Part B (provision for specific types of ships and other additional recommendations), and Explanatory Notes. In view of the presented brief historical overview, the question arises: is the tool to assess the stability of an intact ship suitable for modern ships? The hull form, capacity as well as other features have significantly changed compared to vessels analyzed by Rahola which were built between 1870 and 1938. Even the term "unconventional ships" which is nowadays

being used to refer to some contemporary ships, can perhaps be avoided because the present global trade cannot be imagined without ultra-large container vessels (which are regarded as unconventional) that mainly exceed lengths more than three times greater than the ships used for defining the 1985 criteria. In general, even modern merchant inland vessels have lengths greater than 100 *m*. Notwithstanding the oversimplified description of physical phenomena relevant to the stability of ships in waves (weather criterion), the consideration of righting lever in the calm water only, and relying on old empirical data are indicators of deficiencies in these regulations.

3.1. Overview

According to *Kobyliński, 2014*, during the late 1970s and early 1980s, there was a discussion regarding the potential replacement of the existing intact stability criteria with the new ones which would rely on more precise physical modeling and a more rigorous mathematical approach. However, due to the lack of adequate computational tools, this process had to be postponed. The Second Generation Intact Stability Criteria was finalized in 2020 by IMO. The main objective was to provide an assessment framework comprising mathematical models which are independent of empirical data, such as historical accident records or hull forms. IMO gives the procedure for assessing five stability failure modes to which a ship can be vulnerable:

1. Parametric Rolling
2. Pure Loss of Stability
3. Surf-Riding/Broaching
4. Excessive Accelerations
5. Dead Ship Condition

Within the SGISC framework, intact stability failure is defined as a condition of the vessel which is unable to remain within specified limits of roll angle and/or accelerations. Two types of failure are considered, total stability failure (capsizing) or partial failure (an unacceptable condition for normal operation of the crew, passenger, cargo, or ship equipment related to large amplitude roll motions and accelerations). Each of the five failure modes has a multi-tier concept, where the assessment of a ship's vulnerability consists of three different levels:

1. Vulnerability Level 1 (L1)
2. Vulnerability Level 2 (L2)
3. Direct Stability Assessment (DSA)

Direct Stability Assessment gives an opportunity to get a realistic picture i.e. to use numerical simulations or physical model tests to evaluate the dynamic stability and safety of an advanced ship model. Due to the complexity, price, time required to perform the assessment, and limitations of human resources and facilities, failure modes may be assessed using simpler procedures, L1 and L2. L1 and L2 are less accurate but the level of conservatism is increased (L1 should be the most conservative but the least accurate).

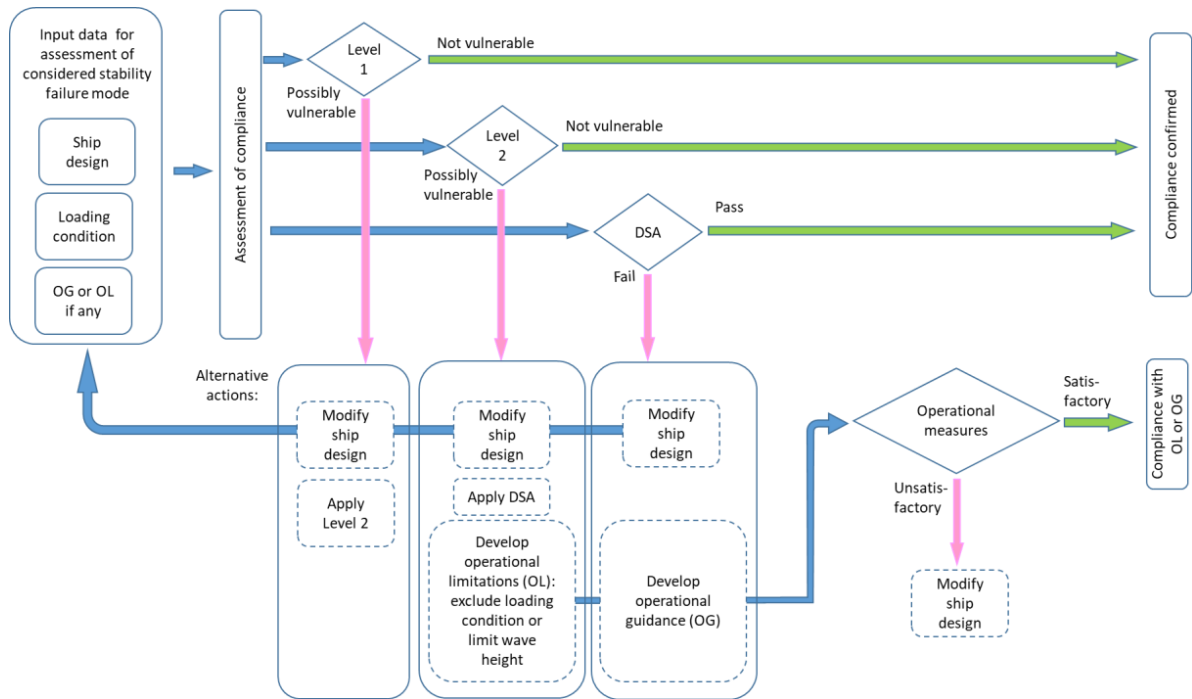


Figure 3.1: Simplified scheme of the application structure of SGISC (IMO, 2019).

As an alternative solution to the mentioned levels which are ship design and loading condition dependent, an additional level - Operational Guidance/Operational Limitations (OG/OL) is added to the framework (see Figure 3.1). Furthermore, each level can be used as a starting point and can be used stand-alone, independently of other levels. In such a way, the end-users have two possibilities to achieve compliance with the criteria: to change the design of the ship or to apply the operational measures. Currently, the use of SGISC is not mandatory.

3.2. Fundamentals of Stability Failure Modes

In this Section, all modes of stability failures will be briefly explained. A detailed description of these failure modes can be found in IMO, 2022. Understanding the relationship between wave frequencies and ship motions is a vital initial step before explaining potential failure modes. The frequency of the waves, denoted by ω , undoubtedly plays a significant role in influencing a ship's motions. Nevertheless, these motions are actually dependent on the encounter frequency which depends on the ship's speed and the angle between the ship's heading and the direction of wave propagation.

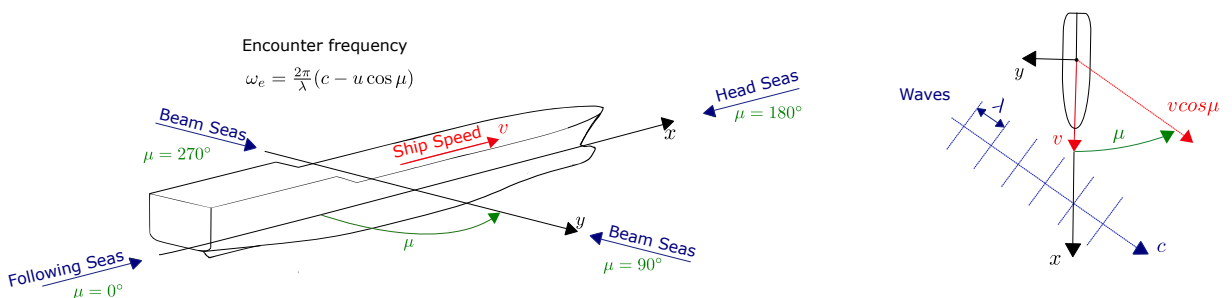


Figure 3.2: Wave propagation in an encounter with a heading of the ship.

Figure 3.2 describes the relationship between the ship's heading and the propagation of waves, from where the encounter frequency (ω_e) can be defined. The figure includes a mathematical formulation of ω_e . In this context, the $x - y$ coordinate system is connected to the ship, while the x axis represents the ship's direction of sailing. The constant speed of the ship is represented as v , while the heading angle relative to the waves is denoted as μ . The term λ refers to the wavelength, while c stands for the celerity of the waves.

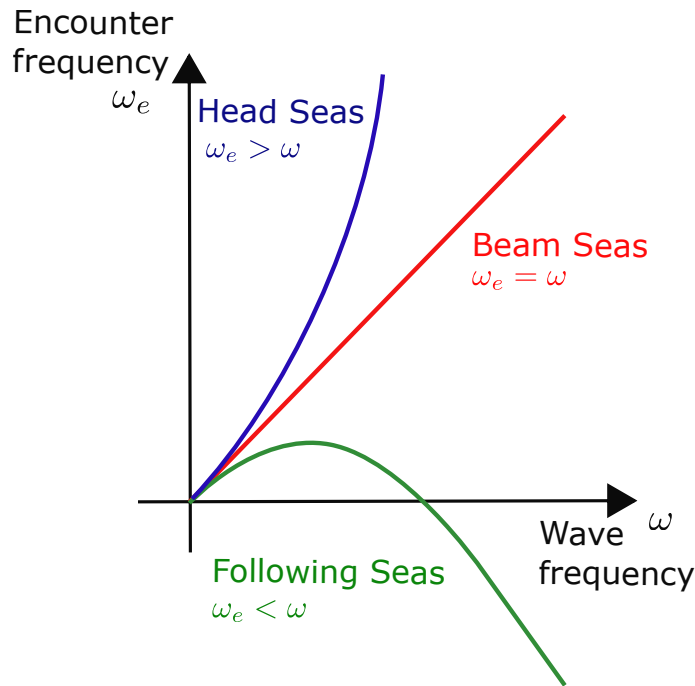


Figure 3.3: Encounter frequency (*Lloyd, 1998*).

In the μ range from 90° up to 270° , the encounter frequency is always greater than the wave frequency. Parametric rolling can appear in these circumstances, while next to this failure mode also slamming or green water could be potentially dangerous scenarios. Excessive rolling is a dangerous scenario that occurs in beam ways ($\mu = 90^\circ$ or $\mu = 270^\circ$). Encounters frequency is equal to wave frequency which means the ship experienced the wave frequency. Parametric Rolling, Pure Loss of Stability, and Surf-Riding/Broaching are appearing in the case of the following seas ($\mu = 0^\circ$) or stern-quartering waves ($0^\circ < \mu < 90^\circ$ or $270^\circ < \mu < 360^\circ$). The encounter frequency is reduced, but for the high waves frequency becomes even negative. A negative frequency means that the ship is overtaking the waves, while a positive encounter frequency means that the waves are overtaking the ship (*Lloyd, 1998*). Slamming also can occur next to those failure stability modes. Explained relations of the frequencies can be found in *Figure 3.3*. Those relations are derived from linear wave theory, which is considered in SGISC. However, more details about linear wave theory can be found in mentioned reference *Lloyd, 1998* or in *Hofman, 2020*.

3.2.1. Parametric Rolling

While sailing in the head, following, bow, and stern-quartering seas, if certain conditions are met, the ship can experience undesirable rolling motions, known as Parametric Rolling. The motions can quickly become extremely violent, resulting in large roll amplitudes and (sometimes) significant lateral accelerations.

The basic conditions of the parametric resonance imply that the encounter frequency is approximately twice the natural roll frequency of the ship and that the wavelength is close to the ship's length. These conditions, as a consequence, lead to fluctuation in righting lever (\overline{GZ}) because, as the wave passes by the ship, the midship is positioned at the wave crest at one instance, and at the wave trough at another. This causes the fluctuating changes of stability-related parameters of ship underwater hull geometry.

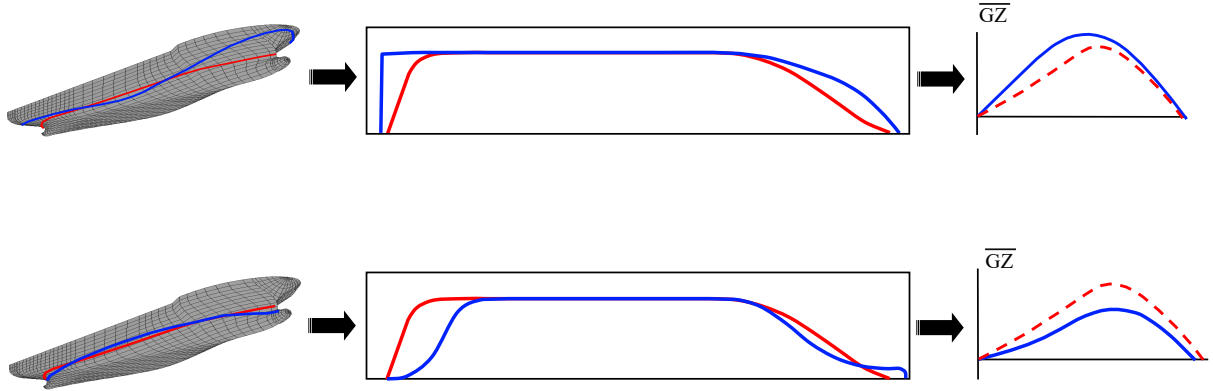


Figure 3.4: Changes of stability in one wave cycle (*IMO, 2023*). The figure above is showing the situation where the wave trough is amidships, and below when the wave crest is located amidships. With (—) is represented changes in the waterplane and righting lever. With (—) is represented waterplane while with (---) righting lever in calm water.

Large container vessels are more prone to these changes in hydrostatic properties in waves, and consequently to Parametric Rolling, because of their hull forms. In order to provide more space for containers on deck, the aft part of the ship has a pronounced flare. Mentioned changes of stability can be visible in *Figure 3.4* while a simplified scenario of Parametric Rolling is represented in *Figure 3.5*.

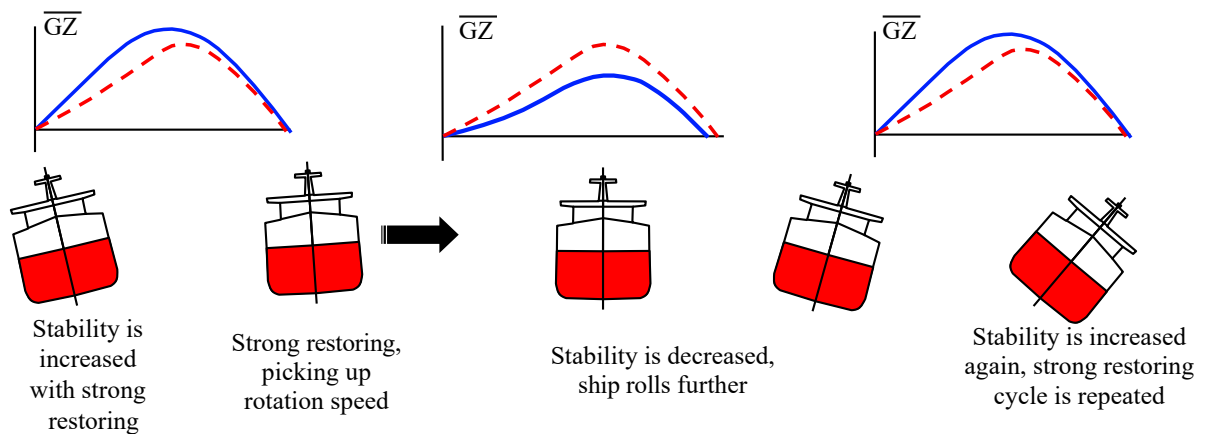


Figure 3.5: Simplified scenario of parametric roll resonance - one and a half wave cycle (*IMO, 2023*). The left side shows ship rolls while in the wave trough, in the middle in the wave crest, and on the right again in the wave trough. With (---) is represented righting lever in calm water while with (—) changes of a righting lever due to a variation of waterplane.

Therefore, due to differences in the underwater hull geometry, the roll motion amplitudes increase gradually with each wave cycle. Roll damping is an important factor in the inception of Parametric Rolling; the lower the damping, the greater the chances for the onset of this stability failure mode.

3.2.2. Pure Loss of Stability

Pure Loss of Stability is a stability failure mode that is also induced by a change of ship hydrostatics properties on the wave crest but it is considered to be a single-wave event.

In this scenario, the wave propagates from astern (following or stern-quartering wave) whereby the wave celerity is slightly higher than the ship speed. Again, the wavelength should be similar to the ship length. As a result, the ship is being "captured" by the wave (the encounter frequency is almost zero) and may remain for a prolonged period (an order of magnitude greater than the natural roll period) at the wave crest. From the stability point of view, the extended time spent at the wave crest may result in a significant decrease in the righting lever.

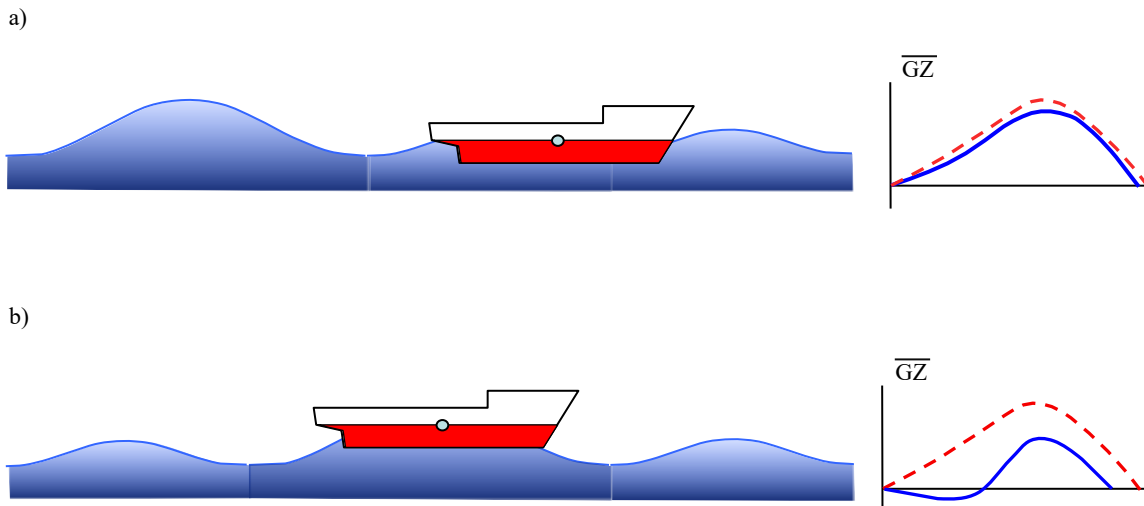


Figure 3.6: Pure Loss of Stability (*IMO, 2023*). a) Typical changes of stability caused by relatively small waves. b) Large decrease of \overline{GZ} curve, caused by the crest of a large wave. With (---) is represented righting lever in calm water while with (—) changes of a righting lever due to a variation of waterplane.

The actual reduction of stability in case of Pure loss of stability may vary as shown in *Figure 3.6*, and so will the energy required to heel the ship. Pure loss of stability may not even occur in the absence of a (sufficiently high) heeling moment unless the ship has attained a negative metacentric height.

3.2.3. Surf-Riding/Broaching-to

Surf-Riding is a phenomenon that occurs under specific conditions. The waves approach from the stern (following or stern-quartering), and steepness should be sufficiently high. Additionally, the wavelength must be similar to the ship's length while the speed of the ship should be equal to, or higher than wave celerity (the so-called "stationary sailing").

This is a single-wave event where the waves capture a ship on the front slope, which is leading to matching the speeds of the waves and vessel.

Surf-Riding often precedes Broaching-to which represents a violent, uncontrollable turn accompanied by a large heel angle that may lead to capsizing. However, larger and slower ships are not considered vulnerable to this stability failure mode.

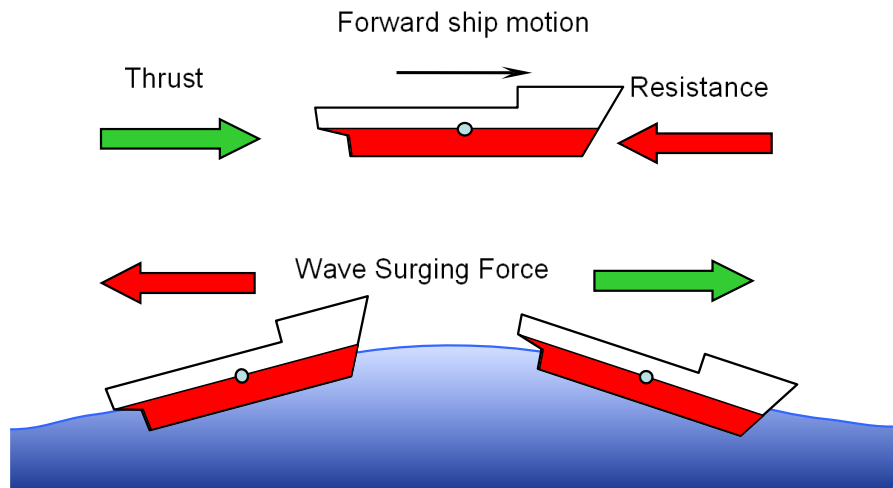


Figure 3.7: Direction of the forces (IMO, 2023). Thrust is the force produced by the propulsion system that enables the ship to move forward against resistance forces. Wave surfing force pushes the ship forward (denoted with green color) or backward (denoted with red color) depending on its position relative to the waves.

Depending on the position relative to the waves, ship speed can vary. The surging force can contribute positively to the thrust when the vessel is located at the face of the wave (higher speed) while on the back of the wave, the force is pushing back the ship (see Figure 3.7).

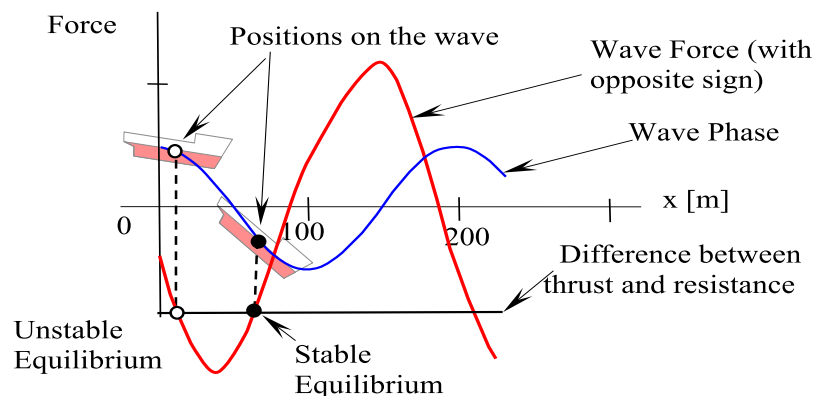


Figure 3.8: Equilibrium positions for Surf-Riding relative to the waves (IMO, 2023). The ship can be disturbed backward or forwards due to the external effect, but depending on the location will define the equilibrium condition of the ship, either stable or unstable.

To experience the Surf-Riding the vessel should be in an equilibrium state and that can be achieved when the surging forces, the resistance of the hull, and the thrust force (thrust), are balanced otherwise the ship will just experience the surging motions. Regarding this matter, the stable equilibrium is when a ship after being unbalanced, naturally returns to the position where only Surf-Riding is possible. Contrarily, in a state of unstable equilibrium, the ship may experience either Surf-Riding conditions or surging motions. The balance between those forces for different ship positions on the waves is represented in *Figure 3.8*.

3.2.4. Excessive Acceleration

Lateral accelerations can mainly occur on the vessel in the ballast condition with high metacentric height. Smaller metacentric heights in terms of rolling motions are more favorable as they are associated with higher values of the rolling period. Excessive Acceleration is included last on the list of stability failures. Accidents of the container vessels Chicago Express in September 2008 and Guayas in September 2009 make this phenomenon included as a failure mode. Nevertheless, as an example, the values of \overline{GM} of those vessels are 7.7 m and 5.6 m, respectively.

During rolling motions, the rolling period is the same for every position on the ship but not the travel distance. The object located at higher positions needs a longer distance to cover for the same time compared to when it is located lower. To satisfy this condition, linear velocity i.e. linear acceleration needs to be larger at the higher positions (see *Figure 3.9*). Large linear acceleration causes larger inertial forces, which can be fatal for the crew members and cargo. Moreover, experiencing Excessive Acceleration does not depend on the vessel speed but it is necessary for the wave to propagate from the beam direction.

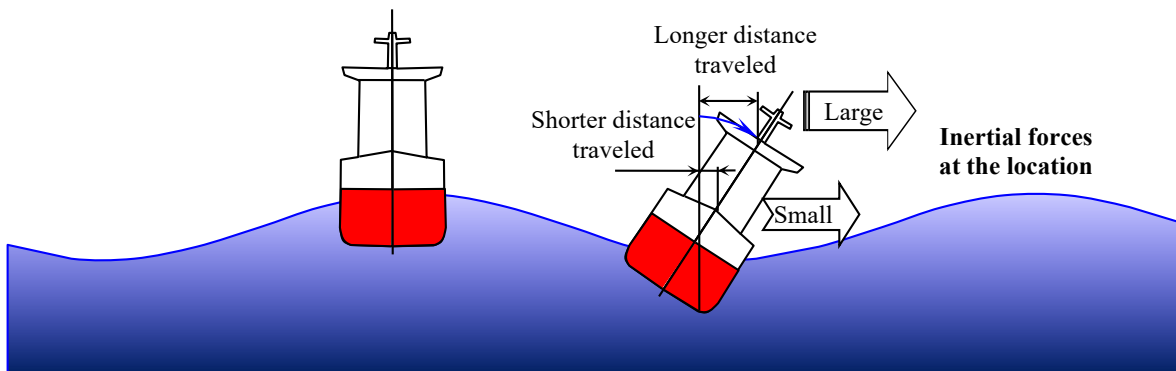


Figure 3.9: Simplification of a scenario - Excessive Acceleration (IMO, 2023).

3.2.5. Dead Ship Condition

Dead Ship Condition refers to a scenario where a ship has lost its power and has turned into beam seas, where it is rolling under the action of waves as well as heeling and drifting under the action of wind. Under these circumstances, the vessels with large lateral surfaces are most vulnerable to DSC, such as container vessels, RO-RO, etc. The simplified scenario of the stability failure mode DSC is represented in *Figure 3.10*.

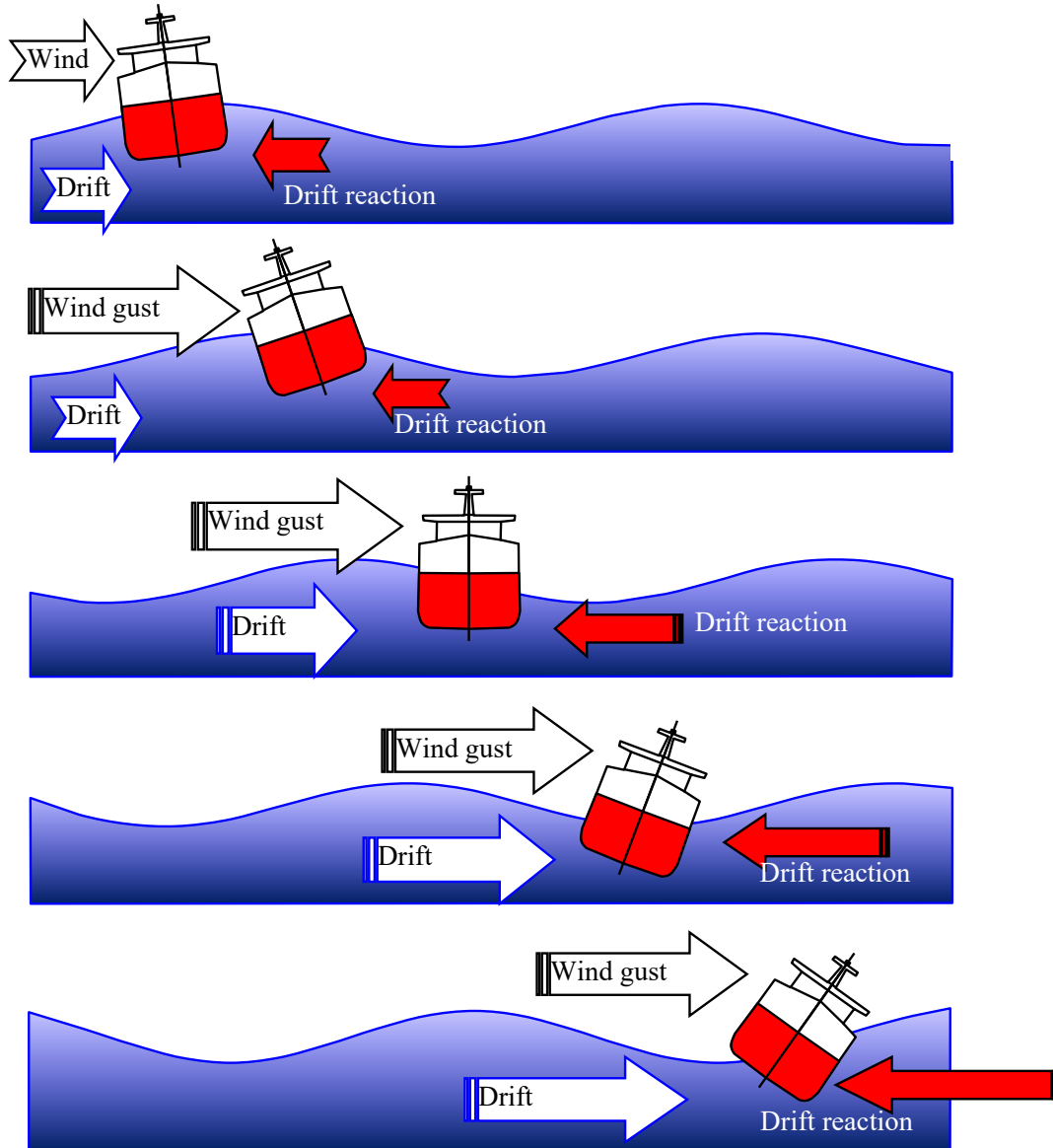


Figure 3.10: Simplified scenario of Dead Ship Condition (IMO, 2023). Firstly, it is assumed that the ship would turn the beam to wind and waves due to the loss of propulsion, which is followed by drifting and rolling. Secondly, the ship is exposed to a sudden gust of wind when it reaches the windward roll amplitude. In this condition, the ship starts to roll back to leeward where the velocity of drift and drift reaction start to grow. As the ship rolls further to the leeward side, the velocity and reaction of the drift continue to escalate, resulting in an extra heeling force. Eventually, the ship will reach its maximum roll angle on the leeward side, which may result in stability failure.

To prevent or mitigate stability failure modes described herein, the crew could consider taking appropriate operational measures, such as a change of course and/or speed. This is not the case with the Dead Ship Condition. Due to the loss of systems providing thrust and control, the master and the crew are unable to react, so the ship is "on its own". Both conventional and non-conventional ships can experience this condition, which emphasizes the need for comprehensive assessment methods.

Dead Ship Condition

This Chapter explains the procedures for stability assessment at Level 1 and Level 2 of SGISC for Dead Ship Condition stability failure mode. Detailed descriptions of the procedures for both L1 and L2, as well as all the formulas and expressions used in this Chapter, may be found in *IMO, 2020*.

The Level 1 vulnerability criterion of SGISC is based on the "Severe wind and rolling criterion" (i.e., "Weather Criterion") with the correction of factor s . Weather Criterion represents a semi-empirical approach that is based on the dynamic stability criteria used in Japan and USSR in the 1950s. Weather Criterion incorporates the experiences in the operation of ship types and hull forms which could be nowadays considered outdated to a large extent. Nevertheless, due to simplicity and long experience in their application, Weather Criteria are still used, despite their deficiencies.

Vulnerability Level 2 of SGISC is a probabilistic criterion based on the evaluation of the long-term stability failure index C_{DSC} . Compared to L1, L2 takes more precisely into account the physical phenomena of ships in environmental conditions. This makes L2 more complex, but also less conservative and more universally applicable, even to unconventional vessels.

4.1. Vulnerability Level 1

Assessment of the vulnerability at Level 1 for dead ship stability failure mode is evaluated using the "Severe wind and rolling criterion (weather criterion)" outlined in section 2.3 of part A of the 2008 Intact Stability Code (the wave steepness values (s) have been expanded). The vessel should withstand the combined effects of beam wind and rolling (due to the waves) in the following scenario:

1. The ship is subjected to a steady wind pressure acting perpendicular to the ship's centreline which results in a steady wind heeling lever, l_{w1} . Due to the l_{w1} , the ship is heeled up to a static angle of equilibrium φ_0 which should not exceed 16° or 80 % of the angle of the deck edge immersion, whichever is less.
2. From the resultant angle of equilibrium, φ_0 , the ship is assumed to roll owing to wave action to an angle of roll, φ_1 .

3. The ship is then subjected to a gust of wind which results in a gust wind heeling lever, l_{w2} .
4. As indicated in *Figure 4.1*, under these circumstances, area b (hatched with green color) should be equal to or greater than area a (hatched with blue color).

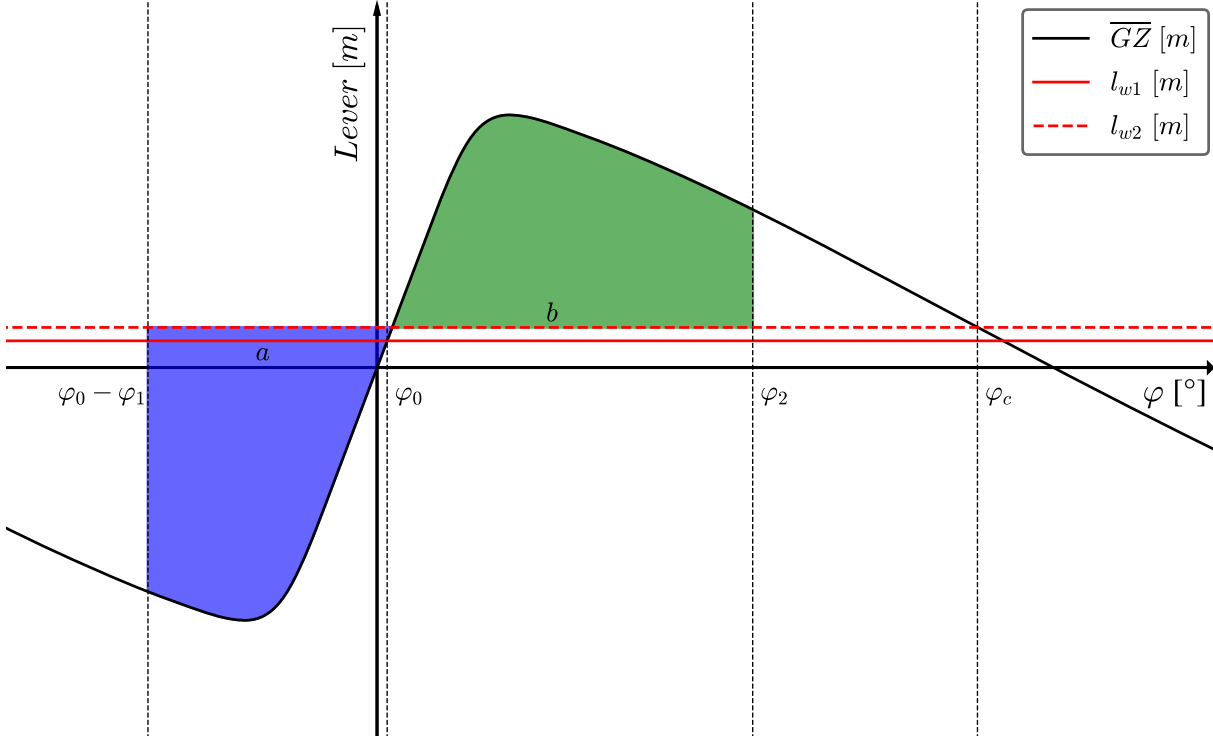


Figure 4.1: Graphical representation of "Weather Criterion". The angle of heel under the action of the steady wind l_{w1} is φ_0 and the angle of a roll to windward due to wave action is φ_1 . Angle φ_2 is defined as minimum among 50° , the angle of downloading φ_f , and the angle of capsizing φ_c (the second intercept between l_{w2} and \overline{GZ} curves).

The wind heeling levers l_{w1} and l_{w2} are constant values at all angles of inclination and should be calculated as follows:

$$l_{w1} = \frac{P \cdot A_L \cdot Z}{1000 \cdot g \cdot \Delta} \quad (4.1)$$

$$l_{w2} = 1.5 \cdot l_{w1} \quad (4.2)$$

where P is wind pressure of $504 [Pa]$, $Z [m]$ is the vertical distance from the center of lateral windage area $A_L [m^2]$ to the center of the underwater lateral area, g is the gravity constant (taken as $9.81 [m/s^2]$) and displacement of the vessel is denoted with $\Delta [t]$.

The angle of roll, φ_1 , should be calculated as follows:

$$\varphi_1 = 109 \cdot k \cdot X_1 \cdot X_2 \cdot \sqrt{r \cdot s}. \quad (4.3)$$

Values of factors X_1 , X_2 , k , and s can be found in *Table 4.1*, where intermediate values should be calculated using linear interpolation. For the rounded-bilge ships having no bilge or bar keel factor k value is 1, or for the ships which have a sharp bilge value is 0.7. Otherwise, factor k can be estimated using the table where A_k [m^2] represents the total overall area of bilge keels or the area of the lateral projection of the bar keel or the sum of these areas. Factor r can be calculated as follows:

$$r = 0.73 + 0.6 \cdot \frac{\overline{KG} - d}{d}. \quad (4.4)$$

Table 4.1: Values of factor X_1 , X_2 , k and s

Factor X_1		Factor X_2		Factor k		Factor s	
B/d	X_1	C_B	X_2	$\frac{A_k \cdot 100}{L_{WL} \cdot B}$	k	$T_r(s)$	s
≤ 2.4	1.0	≤ 0.45	0.75	0	1.0	≤ 6	0.100
2.5	0.98	0.50	0.82	1.0	0.98	7	0.098
2.6	0.96	0.55	0.89	1.5	0.95	8	0.093
2.7	0.95	0.60	0.95	2.0	0.88	12	0.065
2.8	0.93	0.65	0.97	2.5	0.79	14	0.053
2.9	0.91	≥ 0.70	1.00	3.0	0.74	16	0.044
3.0	0.90			3.5	0.72	18	0.038
3.1	0.88			≥ 4.0	0.70	20	0.032
3.2	0.86					22	0.028
3.4	0.82					24	0.025
≥ 3.5	0.80					26	0.023
						28	0.021
						≥ 30	0.020

An alternative solution for determining the wind heeling lever l_{w1} , wave steepness factor s , and the angle of roll φ_1 under certain circumstances, can be found in mentioned document (*IMO, 2020*).

4.2. Vulnerability Level 2

Compared to Level 1, the methodology of Level 2 is more complex but the accuracy of vulnerability to Dead Ship Conditions is improved. The procedure of L2 is a probabilistic approach, where a measure of the stability failure mode is long-term probability index C_{DSC} which is obtained as a weighted average of the probability of stability failures in a range of various short-term environmental conditions i.e. a weighted average of short-term index $C_{DSC,s}$. The short-term conditions are defined by the wind and wave spectra, using specific significant wave height H_s and zero-crossing wave period T_z , and the corresponding wind speed. The probability of occurrence of the short-term weather conditions (necessary for the long-term assessment) is defined with a wave scatter table. The short-term index $C_{DSC,s}$ except H_s and T_z also depends on ship characteristics and short-term exposure time.

According to the procedure, the ship roll motion is described with a one-degree-of-freedom mathematical model: a second-order non-linear differential equation given in *Equation (4.5)*:

$$(M_{44} + A_{44}) \ddot{\varphi} + M_{damp}(\dot{\varphi}) + M_{rest}(\varphi) = M_{wave}(t) + M_{wind}(t) \quad (4.5)$$

where M_{44} is a roll mass moment of inertia, A_{44} is a roll added mass moment of inertia, M_{damp} is the damping moment, M_{rest} is restoring moments, $M_{wave}(t)$ is the excitation moment due to the waves, and $M_{wind}(t)$ is the excitation moment due to wind. Additionally, φ represents an angle of the roll where $\dot{\varphi}$ is velocity and $\ddot{\varphi}$ is acceleration with respect to the time t . It is assumed that drifting and heave motion can be neglected. A further convenience in solving this equation is to linearization of \overline{GZ} curve, which will be shown later.

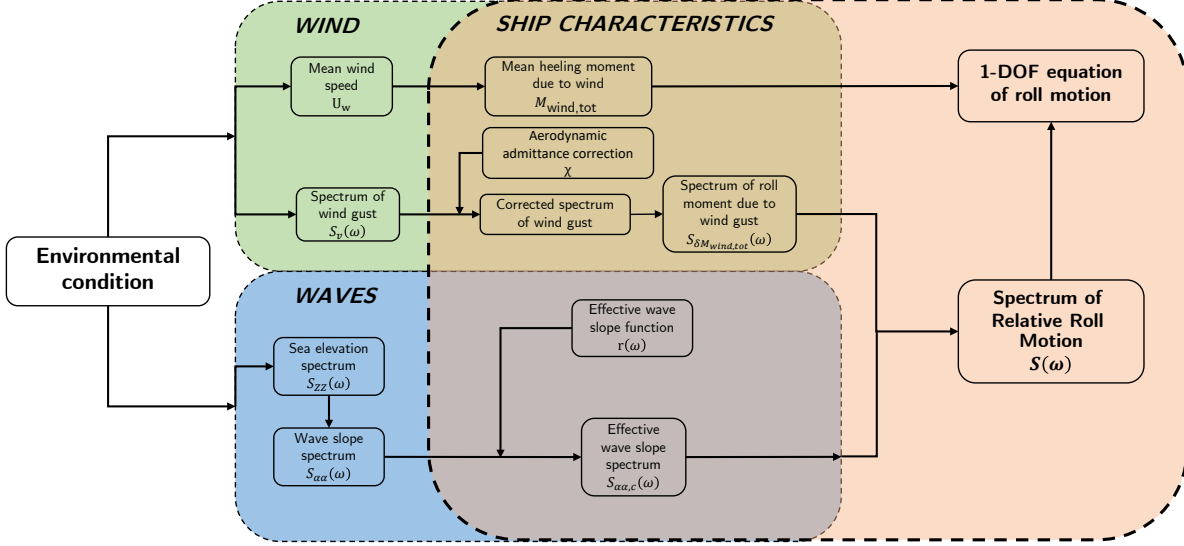


Figure 4.2: Simplified scheme for short-term assessment.

The Equation (4.5) is linearized to make use of the advantages of the linear systems theory. Linear wave theory allows us to represent motions of the considered system (in our case ship) as an excitation oscillated linear system where the excitation frequencies are distinctly defined. More specifically, the excitation forces are defined by the sea state characteristics that have been determined for the considered region, i.e. sea or ocean where the vessel will operate. As a result, the Level 2 approach provides an appropriate tool that employs the 1DOF equation of motions, from which an irregular roll moment can be obtained including environmental influence and ship characteristics. The methodology of defining $C_{DSC,s}$ will be described in follows, where this simplified scheme of this procedure is represented in Figure 4.2.

4.2.1. External Impacts

It is assumed that both wind and waves act from the beam direction while evaluating sea and wind states can be used as an energy spectrum. Firstly, the influence of the waves can be defined using the Bretschneider spectrum which depends on two parameters, H_s and T_z . The spectrum of wave elevation $S_{zz}(\omega)$, as a function of wave frequency ω , can be calculated as follows:

$$S_{zz}(\omega) = \frac{H_s^2}{4\pi} \cdot \left(\frac{2\pi}{T_z}\right)^4 \cdot \omega^{-5} \cdot \exp\left[-\frac{1}{\pi} \cdot \left(\frac{2\pi}{T_z}\right)^4 \cdot \omega^{-4}\right] \quad (4.6)$$

After that, the spectrum of the wave slope $S_{\alpha\alpha}(\omega)$ can be calculated using the following equation:

$$S_{\alpha\alpha}(\omega) = \frac{\omega^2}{g^2} \cdot S_{zz}(\omega) \quad (4.7)$$

where g represents gravity acceleration. As a final step to characterize the sea state, the wave excitation moment can be evaluated using an effective wave slope spectrum:

$$S_{\alpha\alpha,c}(\omega) = r^2(\omega) \cdot S_{\alpha\alpha}(\omega) \quad (4.8)$$

where $r(\omega)$ is the effective wave slope coefficient that describes complex hydrodynamic interaction between waves and a ship hull. The detailed procedure (IMO Method) of determining $r(\omega)$ is given in [Section 4.2.5](#).

Regarding excitation moment due to wind, is necessary first to define the spectrum of the wind gustiness $S_v(\omega)$ which is estimated using the Davenport spectrum:

$$S_v(\omega) = 4K \cdot \frac{U_w^2}{\omega} \cdot \frac{X_D^2}{(1 + X_D^2)^{\frac{4}{3}}} \quad (4.9)$$

with

$$K = 0.003$$

$$X_D = 600 \cdot \frac{\omega}{\pi \cdot U_w}$$

where K is the drag coefficient dependent on the roughness of the surface (in our case water surface). Davenport spectrum is also dependent on the mean wind speed U_w which is given as a function of significant wave height H_s .

$$U_w = \left(\frac{H_s}{0.06717} \right)^{\frac{1}{1.5}} \quad (4.10)$$

The spectrum of the second excitation moment due to gust wind is calculated as follows:

$$S_{\delta M_{wind,tot}}(\omega) = (\rho_{air} \cdot U_w \cdot C_{whm} \cdot A_L \cdot Z)^2 \cdot \chi^2(\omega) \cdot S_v(\omega) \quad (4.11)$$

where ρ_{air} is the density air, C_{whm} is heeling moment coefficient (taken as 1.22), A_L is the lateral windage area, Z is the vertical distance from the center of the lateral windage area A_L to the center of the underwater lateral area (or roughly to a point at one-half the mean draught d) and $\chi(\omega)$ is aerodynamic admittance function. The $\chi(\omega)$ function represents the correction factor in order to consider the absolute dimensions of the windage area for different frequencies. The constant value of 1 for $\chi(\omega)$ is adopted, as it is advised in the mentioned document.

The mean speed of wind is also included in defining the mean heeling moment $M_{wind,tot}$ or lever $l_{wind,tot}$ which induced static heel angle φ_s .

$$M_{wind,tot} = \frac{1}{2} \cdot \rho_{air} \cdot U_w^2 \cdot C_{whm} \cdot A_L \cdot Z \quad (4.12)$$

$$l_{wind,tot} = \frac{M_{wind,tot}}{\Delta}$$

After determining all parameters regarding external effects it is necessary to define some additional characteristics regarding the ship and to relate them to the defined spectrums.

The current method for calculating the natural roll period in L1 is identical to the method used in L2, which lacks a more precise approach. Estimation of the natural roll frequency ω_0 which can be derived from the natural roll period T_r using the following equation:

$$\begin{aligned} T_r &= \frac{2CB}{\sqrt{\overline{GM}}} \\ \omega_0 &= \frac{2\pi}{T_r} \end{aligned} \quad (4.13)$$

where

$$C = 0.373 + 0.023 \cdot \frac{B}{d} - 0.043 \cdot \frac{L_{WL}}{100}$$

Natural roll frequency ω_0 which corresponds to initial metacentric height \overline{GM} (in the upright position) needs to be modified for the static angle of equilibrium φ_s under the action of the constant heeling lever $l_{wind,tot}$ which is determined using *Equation (4.12)*. Therefore, modified natural frequency $\omega_{0,e}$ can be calculated as follows:

$$\omega_{0,e} = \omega_0 \sqrt{\frac{\overline{GM}_{res}(\varphi_s)}{\overline{GM}}} \quad (4.14)$$

where with \overline{GM}_{res} is denoted residual metacentric height. Furthermore, by calculating the first derivative at the static angle of equilibrium φ_s of the \overline{GZ} curve, it's possible to determine the value of \overline{GM}_{res} . The constant heeling lever $l_{wind,tot}$ does not depend on the heeling angle, where the equation below can be simplified.

$$\overline{GM}_{res}(\varphi_s) = \left. \frac{d(\overline{GZ} - l_{wind,tot})}{d\varphi} \right|_{\varphi=\varphi_s} = \left. \frac{d\overline{GZ}}{d\varphi} \right|_{\varphi=\varphi_s} - \left. \frac{dl_{wind,tot}}{d\varphi} \right|_{\varphi=\varphi_s} = \left. \frac{d\overline{GZ}}{d\varphi} \right|_{\varphi=\varphi_s} \quad (4.15)$$

To derive a precise roll angle spectrum estimation, the relative and absolute roll transfer functions are then obtained as follows:

$$\begin{aligned} H_{rel}^2(\omega) &= \frac{\omega^4 + (2 \cdot \mu_e \cdot \omega)^2}{(\omega_{0,e}^2(\varphi_s) - \omega^2)^2 + (2 \cdot \mu_e \cdot \omega)^2} \\ H^2(\omega) &= \frac{\omega_0^4}{(\omega_{0,e}^2(\varphi_s) - \omega^2)^2 + (2 \cdot \mu_e \cdot \omega)^2} \end{aligned} \quad (4.16)$$

where μ_e is the linear roll damping coefficient that needs to be estimated using Simplified Ikeda's method or a more appropriate approach, or through experimentation. Finally, the ship's response to the combined influence of wave and gustiness can be completed by determining the spectrum of the effective relative roll angle $S(\omega)$:

$$S(\omega) = H_{rel}^2(\omega) \cdot S_{\alpha\alpha,c}(\omega) + H^2(\omega) \cdot \frac{S_{\delta M_{wind,tot}}(\omega)}{(\Delta \cdot \overline{GM})^2}. \quad (4.17)$$

Once the relative roll angle spectrum $S(\omega)$ is calculated, several main spectrum characteristics can be evaluated. The zeroth m_0 and second m_2 spectral moment can be calculated as:

$$\begin{aligned} m_0 &= \int_{\omega_{min}}^{\omega_{max}} S(\omega) d\omega, \\ m_2 &= \int_{\omega_{min}}^{\omega_{max}} \omega^2 \cdot S(\omega) d\omega. \end{aligned} \quad (4.18)$$

The standard deviation of the roll motion $\sigma_{C_{DSC,s}}$ around the static angle of equilibrium φ_s is determined as follows:

$$\sigma_{C_{DSC,s}} = \sqrt{m_0} \quad (4.19)$$

The zero-crossing roll period $T_{z,C_{DSC,s}}$ which can be derived from roll zero-crossing frequency $\omega_{z,C_{DSC,s}}$, which is calculated as:

$$\begin{aligned} \omega_{z,C_{DSC,s}} &= \sqrt{\frac{m_2}{m_0}} \\ T_{z,C_{DSC,s}} &= \frac{2\pi}{\omega_{z,C_{DSC,s}}} \end{aligned} \quad (4.20)$$

4.2.2. Short-term Stability Failure Index

Before calculating the short-term stability failure index, it is necessary to determine the critical angles before using an "equivalent area" approach. Due to the action of steady wind, the actual righting lever $\overline{GZ}(\varphi)$ is reduced ($\overline{GZ}_{res}(\xi)$) with constant heeling lever $l_{wind,tot}$.

$$\overline{GZ}_{res}(\xi) = \overline{GZ}(\varphi) - l_{wind,tot} \quad (4.21)$$

After reduction, the linearized righting lever can be defined by residual metacentric height \overline{GM}_{res} at the static heel angle φ_s . The reason why this method is required is due to the differences between the residual areas below the linearized righting lever and the actual residual lever. The energies of restoring, which those areas represent are not the same and some corrections have to be considered to achieve equality. This can be obtained by calculating virtual capsize angles which will give the same area for the linearized righting lever such as the areas obtained below the actual righting lever.

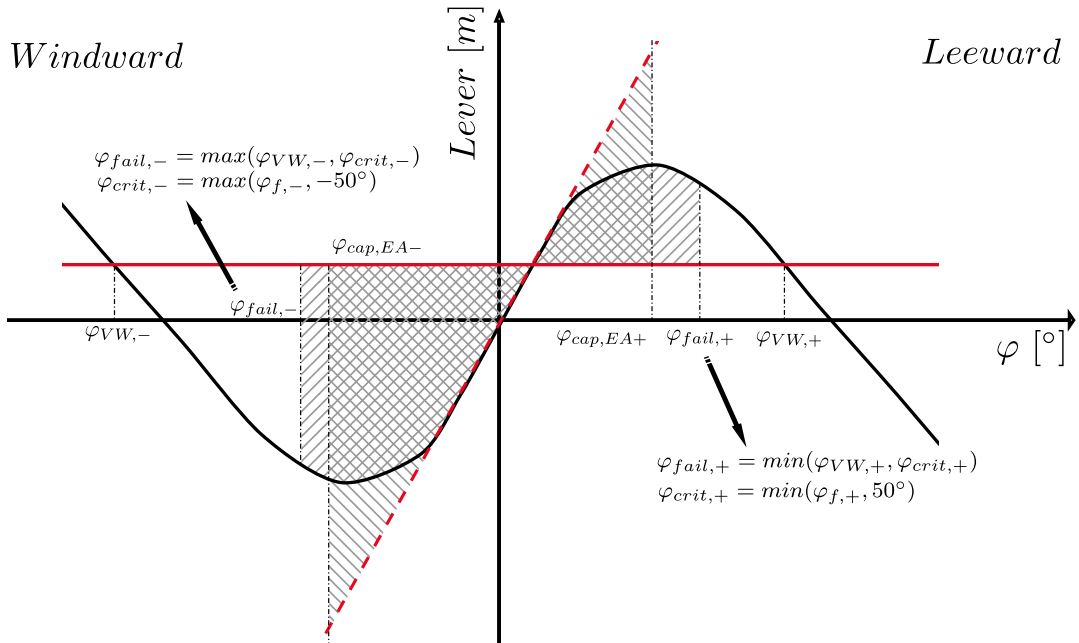


Figure 4.3: Graphical representation of critical angles in DSC-L2. The righting lever \overline{GZ} is denoted with (—), while with (—) is represented the constant heeling lever due to wind $l_{wind,tot}$. The linearised righting lever which is defined by residual metacentric height \overline{GM}_{res} is denoted with (- - -). The grey-hatched area represents the residual energy of a specific lever.

The angle of failure to leeward $\varphi_{fail,+}$ is the minimum between vanishing stability $\varphi_{VW,+}$ under the action of steady wind (second intersection on the positive side) or critical angle $\varphi_{crit,+}$. The angle of failure to windward $\varphi_{fail,-}$ is the maximum between vanishing stability $\varphi_{VW,-}$ under the action of steady wind defined (first intersection on the negative side), and critical angle $\varphi_{crit,-}$. The critical angle $\varphi_{crit,+}$ to leeward is taken as the minimum between downflooding angle $\varphi_{f,+}$ and 50° while to windward $\varphi_{crit,-}$ is taken as the maximum between downflooding angle $\varphi_{f,-}$ (assumed as negative), or -50° . After defining those angles, the residual area under the \overline{GZ} curve at the leeward side is defined from the static heel angle φ_s to the $\varphi_{fail,+}$ while at the windward side from $\varphi_{fail,-}$ to the static heel angle φ_s . In order to achieve equality, the calculation of the virtual capsizing angles $\varphi_{cap,EA+}$ and $\varphi_{cap,EA-}$ is given below:

$$\begin{aligned}\varphi_{cap,EA+} &= \varphi_s + \sqrt{\frac{2}{\overline{GM}_{res}(\varphi_s)} \cdot \int_{\varphi_{fail,+}}^{\varphi_s} \overline{GZ}_{res}(\xi) d\xi}, \\ \varphi_{cap,EA-} &= \varphi_s - \sqrt{\frac{-2}{\overline{GM}_{res}(\varphi_s)} \cdot \int_{\varphi_s}^{\varphi_{fail,-}} \overline{GZ}_{res}(\xi) d\xi}.\end{aligned}\quad (4.22)$$

In *Figure 4.3* is graphically represented the equality between areas under the linearized and the actual residual lever, with respect to specific critical angles. The risk indices to leeward RI_{EA+} and windward RI_{EA-} can be evaluated as follows:

$$\begin{aligned}RI_{EA+} &= \frac{\sigma_{C_{DSC,s}}}{\Delta\varphi_{res,EA+}}; \quad \Delta\varphi_{res,EA+} = \varphi_{cap,EA+} - \varphi_s, \\ RI_{EA-} &= \frac{\sigma_{C_{DSC,s}}}{\Delta\varphi_{res,EA-}}; \quad \Delta\varphi_{res,EA-} = \varphi_{cap,EA-} - \varphi_s\end{aligned}\quad (4.23)$$

where $\Delta\varphi_{res,EA+}$ and $\Delta\varphi_{res,EA-}$ represent a residual range of stability to leeward and windward, respectively. In *Equation (4.24)* is given formulation to calculate r_{EA} which represents the occurrence of capsizing (Poisson process). Taking a reciprocal value of r_{EA} can give us the average time between two capsizing events (measured in seconds), which is more understandable.

$$r_{EA} = \frac{1}{T_{z,C_{DSC,s}}} \cdot \left[\exp\left(-\frac{1}{2 \cdot RI_{EA+}^2}\right) + \exp\left(-\frac{1}{2 \cdot RI_{EA-}^2}\right) \right]. \quad (4.24)$$

The short-term stability failure index of Dead Ship Condition, for the considered short-term environmental condition and exposure time T_{exp} , can be finally calculated as:

$$C_{DSC,s} = 1 - \exp(-r_{EA} \cdot T_{exp}) \quad (4.25)$$

where this short-term exposure period T_{exp} represents the period that the ship has to withstand in Dead Ship Conditions.

4.2.3. Long-term Probability Index

The long-term probability index is based on the probability of occurrence of short-term environmental conditions. The long-term conditions are given in terms of the wave scatter table which is represented in *Table 4.2*. The table corresponds to the North Atlantic characteristics. The long-term probability index can be calculated as follows:

$$C_{DSC} = \sum_{i=1}^n C_{DSC,s,i} \cdot W_i \quad (4.26)$$

where $C_{DSC,s,i}$ is the i – th short-term stability failure index corresponding to i – th sea state, and W_i is the weighting factor for i – th sea state from the scatter table. The weighting factor is given as a function of significant wave height H_s and zero-crossing wave period T_z and it is obtained when the reported number of occurrences from the wave scatter table is divided by the total number of occurrences of all sea states. The total number of occurrences for the North Atlantic is 100000.

Table 4.2: Wave Scatter Table of North Atlantic

		T_z [s] - Average Zero-Crossing Wave Period															
		3.5	4.5	5.5	6.5	7.5	8.5	9.5	10.5	11.5	12.5	13.5	14.5	15.5	16.5	17.5	18.5
H_s [m] - Significant Wave Height	0.5	1.3	133.7	865.6	1186	634.2	186.3	36.9	5.6	0.7	0.1	0	0	0	0	0	0
	1.5	0	29.3	986	4976	7738	5569.7	2375.7	703.5	160.7	30.5	5.1	0.8	0.1	0	0	0
	2.5	0	2.2	197.5	2158.8	6230	7449.5	4860.4	2066	644.5	160.2	33.7	6.3	1.1	0.2	0	0
	3.5	0	0.2	34.9	695.5	3226.5	5675	5099.1	2838	1114.1	337.7	84.3	18.2	3.5	0.6	0.1	0
	4.5	0	0	6	196.1	1354.3	3288.5	3857.5	2685.5	1275.2	455.1	130.9	31.9	6.9	1.3	0.2	0
	5.5	0	0	1	51	498.4	1602.9	2372.7	2008.3	1126	463.6	150.9	41	9.7	2.1	0.4	0.1
	6.5	0	0	0.2	12.6	167	690.3	1257.9	1268.6	825.9	386.8	140.8	42.2	10.9	2.5	0.5	0.1
	7.5	0	0	0	3	52.1	270.1	594.4	703.2	524.9	276.7	111.7	36.7	10.2	2.5	0.6	0.1
	8.5	0	0	0	0.7	15.4	97.9	255.9	350.6	296.9	174.6	77.6	27.7	8.4	2.2	0.5	0.1
	9.5	0	0	0	0.2	4.3	33.2	101.9	159.9	152.2	99.2	48.3	18.7	6.1	1.7	0.4	0.1
	10.5	0	0	0	0	1.2	10.7	37.9	67.5	71.7	51.5	27.3	11.4	4	1.2	0.3	0.1
	11.5	0	0	0	0	0.3	3.3	13.3	26.6	31.4	24.7	14.2	6.4	2.4	0.7	0.2	0.1
	12.5	0	0	0	0	0.1	1	4.4	9.9	12.8	11	6.8	3.3	1.3	0.4	0.1	0
	13.5	0	0	0	0	0	0.3	1.4	3.5	5	4.6	3.1	1.6	0.7	0.2	0.1	0
	14.5	0	0	0	0	0	0.1	0.4	1.2	1.8	1.8	1.3	0.7	0.3	0.1	0	0
	15.5	0	0	0	0	0	0	0.1	0.4	0.6	0.7	0.5	0.3	0.1	0.1	0	0
16.5	0	0	0	0	0	0	0	0.1	0.2	0.2	0.2	0.1	0.1	0	0	0	

As a measure of vulnerability C_{DSC} , a ship is not considered vulnerable to the Dead Ship Condition if:

$$C_{DSC} \leq R_{DSC} \quad (4.27)$$

Remark: Vulnerability Level 2 - Assumptions

Several main assumptions are made to perform calculations :

1. The ship is assumed to be exposed to each short-term environmental condition for an exposure time of 3600 s (1 hour). Proposed by IMO.
2. Heeling angles to the leeward side are assumed to be positive, while heeling angles to the windward side are assumed to be negative. Proposed by IMO.
3. The Simpson's I rule as an integration method has been employed.
4. For the frequency domain, lower frequency limit is $\omega_{min} = 0.000342 \text{ rad/s}$ while for upper frequency limit is taken $\omega_{max} = 3.42 \text{ rad/s}$, and the frequency step is $\Delta\omega = 0.000342 \text{ rad/s}$. The total number of frequencies for the discretization of the spectrum is 10001. Proposed by IMO.

4.2.4. Roll Damping Estimation Method

The estimation of roll damping is performed using Simplified Ikeda's method as proposed within SGISC. Due to its extensiveness, the method will be only briefly explained in the thesis. More details about the procedure can be found in *IMO, 2023* or *Kawahara et al., 2011*. The Simplified Ikeda's method, in general, divides the roll damping coefficient B_{44} into five distinctive damping components: friction (B_F), wave making (B_W), eddy making (B_E), lift (B_L), and bilge keel (B_{BK}). However, according to the definition of Dead Ship Condition, a ship is assumed to have zero forward speed (*IMO, 2020*), thus the lift-damping component (B_L) is excluded from consideration. In addition, it is necessary to compute the roll damping coefficient $B_{44}(\varphi_a)$ as a function of roll amplitude. Using [Equation \(4.28\)](#) enables the extraction of the roll damping coefficients μ , β , and δ through least square fitting. Nevertheless, one or more roll damping coefficients can be neglected, if the final fitting is sufficiently accurate.

$$\frac{B_{44}(\varphi_a) \cdot \omega_0^2}{2 \cdot \Delta \cdot \overline{GM}} \rightarrow \mu + \beta \cdot \frac{4}{3\pi} \cdot \omega_0 \cdot \varphi_a + \delta \cdot \frac{3}{8} \cdot \omega_0^2 \cdot \varphi_a^2 \quad (4.28)$$

The roll damping coefficients are used to define the equivalent linear damping coefficient μ_e , which is also a function of the standard deviation of the roll angular velocity $\sigma_{\dot{x}}$. However, $\sigma_{\dot{x}}$ and μ_e are mutually dependent, which means both are unknown. To determine both parameters, the following iterative procedure can be used:

1. It is assumed for the first iteration ($j = 1$) that the standard deviation of roll angular velocity is $\sigma_{\dot{x},j} = 0$.
2. The equivalent linear roll damping coefficient μ_e is estimated using the following equation:

$$\mu_e(\sigma_{\dot{x},j}) = \mu + \beta \cdot \sqrt{\frac{2}{\pi}} \cdot \sigma_{\dot{x},j} + \delta \cdot \frac{3}{2} \cdot \sigma_{\dot{x},j}^2 \quad (4.29)$$

3. When μ_e is defined, the absolute roll angle spectrum $S_x(\omega)$ can be calculated using the following equation:

$$S_x(\omega) = H^2(\omega) \cdot S_m(\omega) = H^2(\omega) \cdot \frac{S_M(\omega)}{(\Delta \cdot \overline{GM})^2} \quad (4.30)$$

where

$$S_M(\omega) = S_{M, \text{wave}}(\omega) + S_{\delta M_{\text{wind}, \text{tot}}}(\omega)$$

$$S_{M, \text{wave}}(\omega) = (\Delta \cdot \overline{GM})^2 \cdot S_{\alpha\alpha, c}(\omega)$$

4. New standard deviation of roll angular velocity $\sigma_{\dot{x},j+1}$ can be estimated using the following equation:

$$\sigma_{\dot{x},j+1} = \sqrt{\int_0^\infty \omega^2 \cdot S_x(\omega) d\omega} \quad (4.31)$$

5. If the absolute difference $|\sigma_{\dot{x},j} - \sigma_{\dot{x},j+1}|$ is smaller than the given tolerance, the procedure is stopped, and the value of $\sigma_{\dot{x},j+1}$ is assigned to $\sigma_{\dot{x},j}$ where final equivalent linear roll damping coefficient μ_e can be calculated. Otherwise, the process should be repeated from step 2 to step 5.

4.2.5. Effective Wave Slope Coefficient

SGISC proposed the procedure (IMO method) of estimation of the effective wave slope coefficient, and it is given in *IMO, 2023*. In this approach, each transverse section of the ship is transformed into a rectangular shape, maintaining the same dimensions as possible of the original section (*Figure 4.4*). Sections heaving zero breadth at the waterline, such as those in the region of the bulbous bow, are neglected.

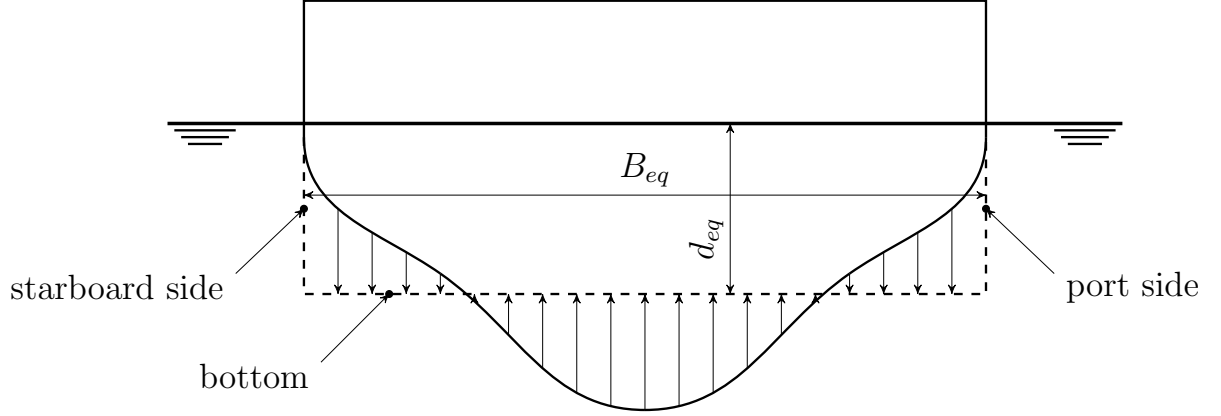


Figure 4.4: Section transformation, IMO method (*Rudaković, 2021*).

This transformation provides an analytical solution for the sectional wave moment (Froude Krylov), and the total wave moment is obtained by integration over the ship length. The algorithm for determining the rectangular section is given in *Equation (4.32)*.

$$\left\{ \begin{array}{l} \text{if } A(x) > 0 \text{ and } B(x) > 0 : \\ \text{otherwise:} \end{array} \right\} \left\{ \begin{array}{l} \text{if } \frac{A(x)}{B(x)} \leq d(x) : \\ \text{if } \frac{A(x)}{B(x)} > d(x) : \\ \left\{ \begin{array}{l} A_{eq}(x) = 0 \\ B_{eq}(x) = 0 \\ d_{eq}(x) = 0 \end{array} \right. \end{array} \right. \left\{ \begin{array}{l} A_{eq}(x) = A(x) \\ B_{eq}(x) = B(x) \\ d_{eq}(x) = \frac{A(x)}{B(x)} \\ d_{eq}(x) = d(x) \\ B_{eq}(x) = B(x) \\ A_{eq}(x) = \frac{A_{eq}(x)}{B_{eq}(x)} \end{array} \right. \quad (4.32)$$

As the shape of the sections changes, various vessel parameters may also be affected. Therefore, the "equivalent vessel" characteristics should be again determined. The displacement volume V_{eq} , transverse metacentric radius $\overline{BM}_{T,eq}$, and the vertical height of the center of buoyancy \overline{KB}_{eq} and gravity \overline{KG}_{eq} of the "equivalent vessel" can be determined using the following equations:

$$\begin{aligned} V_{eq} &= \int_{x_{AE}}^{x_{FE}} A_{eq}(x) dx \\ \overline{BM}_{T,eq} &= \frac{1}{V_{eq}} \int_{x_{AE}}^{x_{FE}} \frac{1}{12} B_{eq}^3(x) dx \\ \overline{KB}_{eq} &= d - \frac{1}{V_{eq}} \int_{x_{AE}}^{x_{FE}} \frac{d_{eq}(x)}{2} A_{eq}(x) dx \\ \overline{KG}_{eq} &= \overline{KB}_{eq} + \overline{BM}_{T,eq} - \overline{GM} \end{aligned} \quad (4.33)$$

where x_{AE} and x_{FE} are the longitudinal coordinates of the aft and forward ends of the ship, respectively.

The effective wave slope coefficient is defined as follows:

$$r(\omega) = \left| \frac{\int_L C(x) dx}{V_{eq} \overline{GM}} \right| \quad (4.34)$$

where,

$$C(x) = \begin{cases} 0 & \text{if } A_{eq}(x) = 0 \text{ and } B_{eq}(x) = 0 \\ A_{eq}(x) \cdot [K_1(x) + K_2(x) + F_1(x) \cdot \overline{OG}_{eq}] & \end{cases} \quad (4.35)$$

and where

$$\begin{aligned} k_w &= \omega^2/g ; \quad \overline{OG}_{ea} = \overline{KG}_{eq} - d \\ K_1(x) &= \frac{\sin\left(k_w \cdot \frac{B_{eq}(x)}{2}\right)}{\left(k_w \cdot \frac{B_{eq}(x)}{2}\right)} \cdot \frac{(1 + k_w \cdot d_{eq}(x)) e^{-k_w \cdot d_{eq}(x)} - 1}{k_w^2 \cdot d_{eq}(x)} \\ K_2(x) &= -\frac{e^{-k_w \cdot d_{eq}(x)}}{k_w^2 \cdot d_{eq}(x)} \cdot \left[\cos\left(k_w \cdot \frac{B_{eq}(x)}{2}\right) - \frac{\sin\left(k_w \cdot \frac{B_{eq}(x)}{2}\right)}{\left(k_w \cdot \frac{B_{eq}(x)}{2}\right)} \right] \\ F_1(x) &= -\frac{1 - e^{-k_w \cdot d_{eq}(x)}}{k_w \cdot d_{eq}(x)} \cdot \frac{\sin\left(k_w \cdot \frac{B_{eq}(x)}{2}\right)}{\left(k_w \cdot \frac{B_{eq}(x)}{2}\right)} \end{aligned} \quad (4.36)$$

Sample Ship - Multipurpose Cargo Vessel

5.1. Model of the Ship

The Dead Ship Condition stability failure mode will be investigated using a small multipurpose cargo ship. This type of ships is mainly used at short distances to connect smaller ports with major hubs. A unique feature of these ships is the possibility to carry different cargo such as containers, bulk cargo, and other goods.

Only a ship loaded with containers will be considered in the analysis, as the corresponding loading conditions result in large lateral surface areas that make them particularly vulnerable to beam winds and hence, potentially vulnerable to Dead Ship Condition as well. The selected sample ship (whose main particulars are given in [Table 5.1](#)) is taken from the study of *Bačkalov and Rudaković, 2017*, which investigates the effect of freeboard using a different probabilistic approach than SGISC. The body plan of the sample ship is represented in [Figure 5.1](#). The hull form is characterized by a bulbous bow as well as a stern bulb, which is typical for single-screw ships. A high block coefficient is a consequence of the cargo hold optimized for the carriage of containers.

Table 5.1: Main parameters of a sample ship

Parameter	Symbol	Value	Unit
Waterline length	L_{WL}	121.3	[m]
Length between perpendicular	L_{BP}	120	[m]
Breadth overall	B	21.3	[m]
Depth	D	9	[m]
Draft	d	7.14	[m]
Freeboard	F_B	1.86	[m]
Displacement	Δ	14504	[t]
Block coefficient	C_B	0.761	[–]
Prismatic coefficient	C_P	0.765	[–]
Waterplane area coefficient	C_W	0.846	[–]
Midship section coefficient	C_M	0.995	[–]

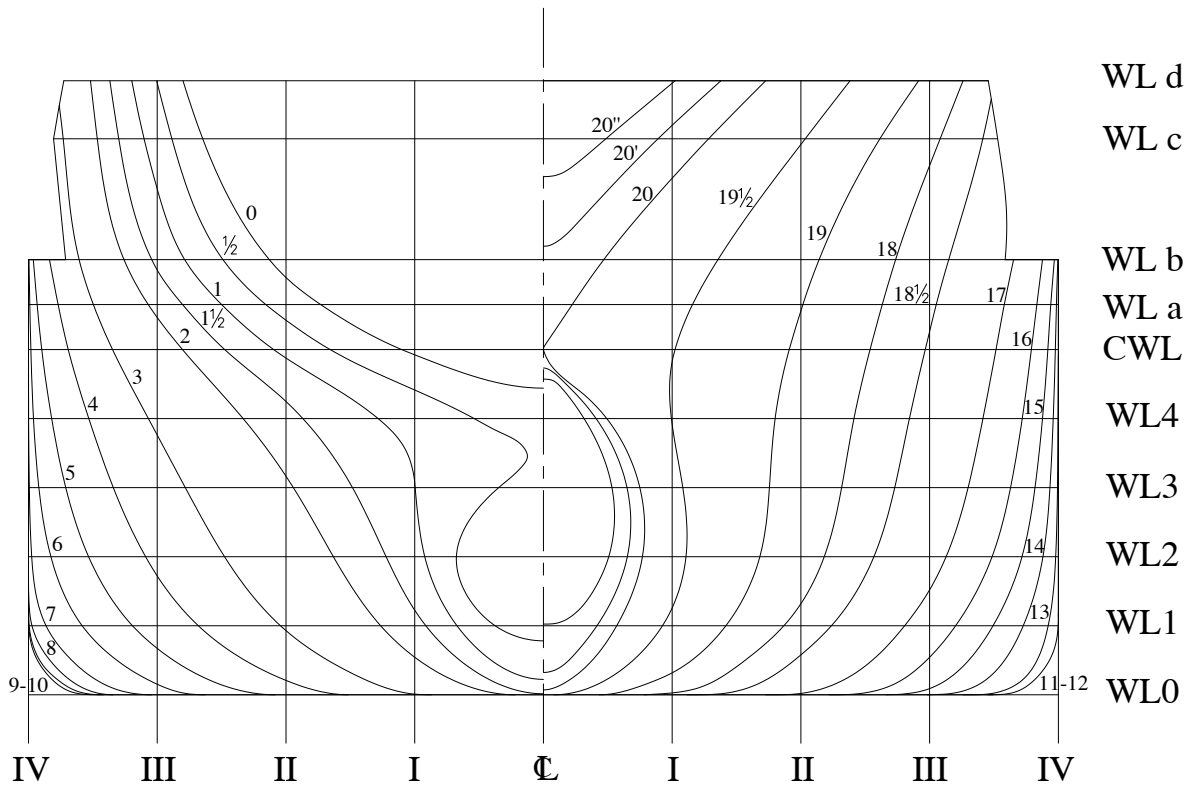


Figure 5.1: Body plan

5.2. Modifying Freeboard on a Sample Ship

A systematic variation of the freeboard in the range from 1.5 m up to 3 m with a step of 0.5 m is performed on the sample ship. The objective is to investigate the impact of the freeboard on the dynamic stability of the ship exposed to stochastic wind and irregular waves. The required modification of the hull is performed using MAXSURF (student license). Figure 5.2 illustrates the changes in the freeboard while maintaining consistency with the remaining elements of the ship.

Table 5.2: Stability characteristics for different freeboard heights - $\overline{GM} = 1.5$ m.

F_B m	D m	\overline{GZ}_{max} m	Range of Stability °	φ_f °	φ_d °
1.5	8.64	0.769	63.6	39.6	8
2	9.14	0.816	64.6	40.2	10.7
2.5	9.64	0.880	65.5	40.2	13.3
3	10.14	0.947	66.8	40.2	15.8

The stability characteristics of the examined ship with different freeboards are reported in Table 5.2. The righting levers \overline{GZ} , and residual righting levers \overline{GZ}_{res} corresponding to the ship with different freeboards are represented in Figure 5.3.

Although the metacentric height is one of the most important ship stability parameters, it is certainly not the only one. The initial stability of the ship can be increased with a larger metacentric height, but it should be noted that at large values the rolling periods

decrease, which is accompanied by high lateral accelerations that can be dangerous for the crew and cargo. The ship's stability significantly depends on the hull form as well which highlights the importance of considering the influence of freeboard in ensuring appropriate stability characteristics. However, as was previously stated, the ICLL does not consider this. While the metacentric height can be influenced to a certain extent during the exploitation of the ship, unfortunately, the freeboard has to be determined in the design phase. The minimum freeboard of the sample ship following ICLL is calculated in *Rudaković, 2014* and stands at 1.236 m. Nevertheless, in study *Munakata et al., 2022* is highlighted that Level 2 does not account in an appropriate manner influence on effective wave slope and roll damping after deck immersion for lower freeboard heights. In addition, as per *Nechaev, 1978*, the effects of green water start to be more pronounced if the height of the freeboard range from 11 % to 17 % of the depth of the vessel. Consequently, it was decided to consider values higher than that determined by ICLL.

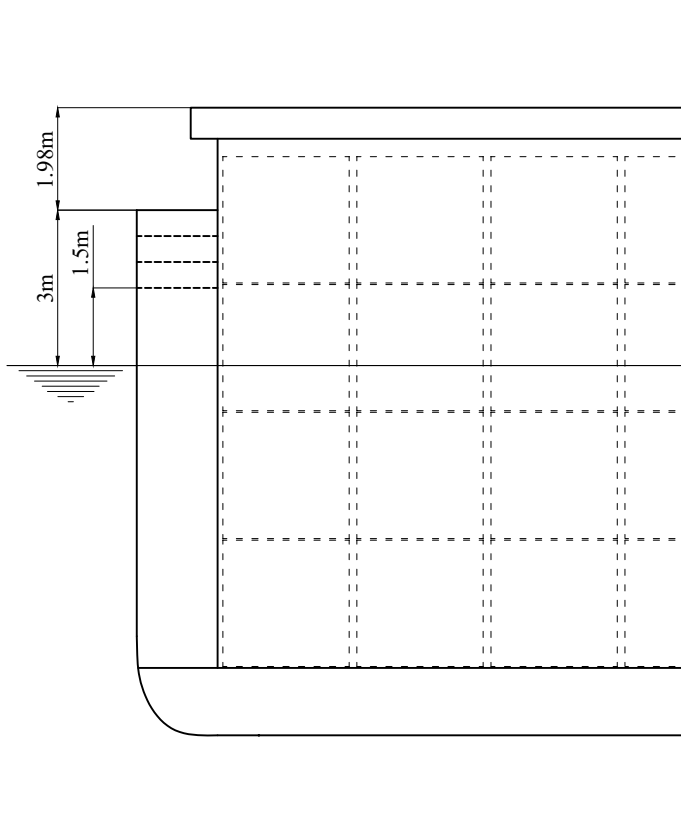
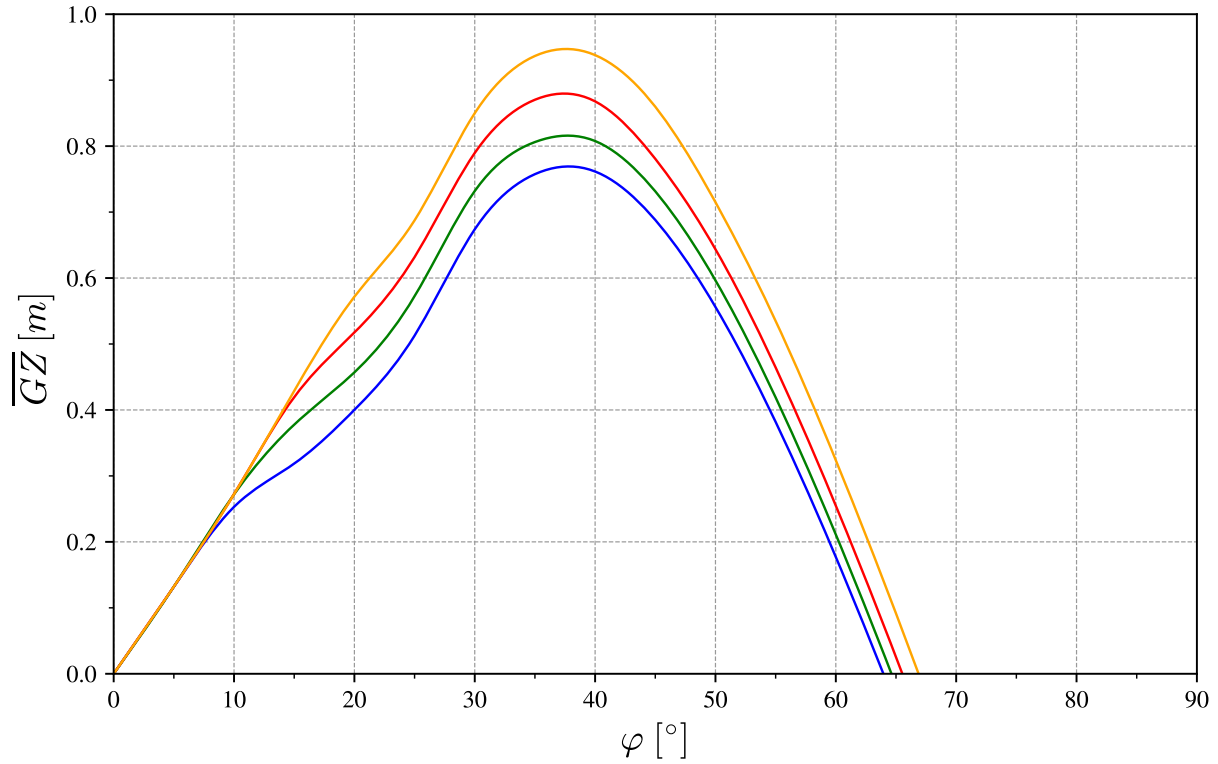
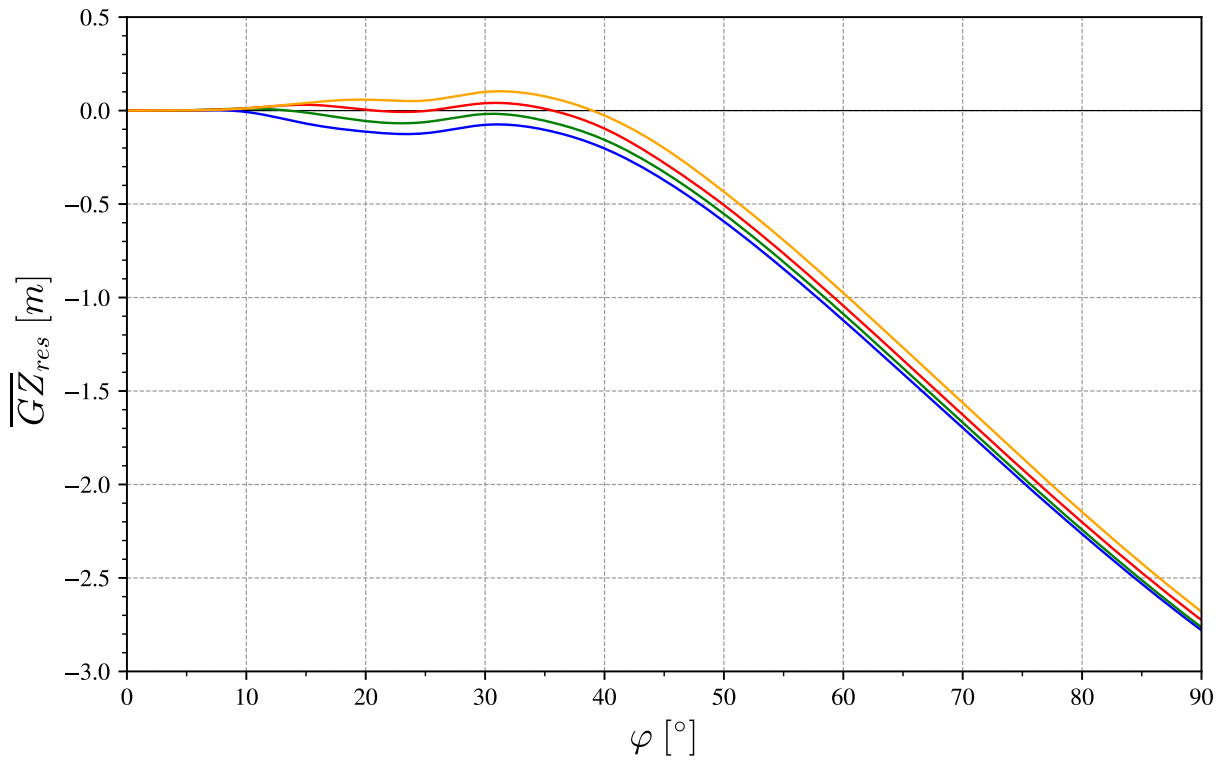


Figure 5.2: Freeboard height variation.

Two different loading conditions (i.e. container arrangement) will be considered for each of the freeboards. It is assumed that the ship displacement remains constant (i.e. the draft does not change). The first loading condition (see *Figure 5.4*) considers 822 TEU (twenty-foot equivalent unit) containers, arranged in four tiers across 13 bays in the cargo hold, five tiers in the first eight bays and four tiers in the remaining five bays on top of the cargo hold along the ship length, and an additional bay with six tiers on the deck, between the accommodation space and the cargo hold. The second loading condition, given in *Figure 5.5*, considers one tier less in the first eight bays on the deck and one tier less in the aft-most positioned bay on the deck.



(a) Righting levers for $\overline{GM} = 1.5 \text{ m}$.



(b) Residual righting lever.

Figure 5.3: Stability characteristic for different freeboard heights. $F_B = 1.5 \text{ m}$ (—), $F_B = 2 \text{ m}$ (—), $F_B = 2.5 \text{ m}$ (—), and $F_B = 3 \text{ m}$ (—).

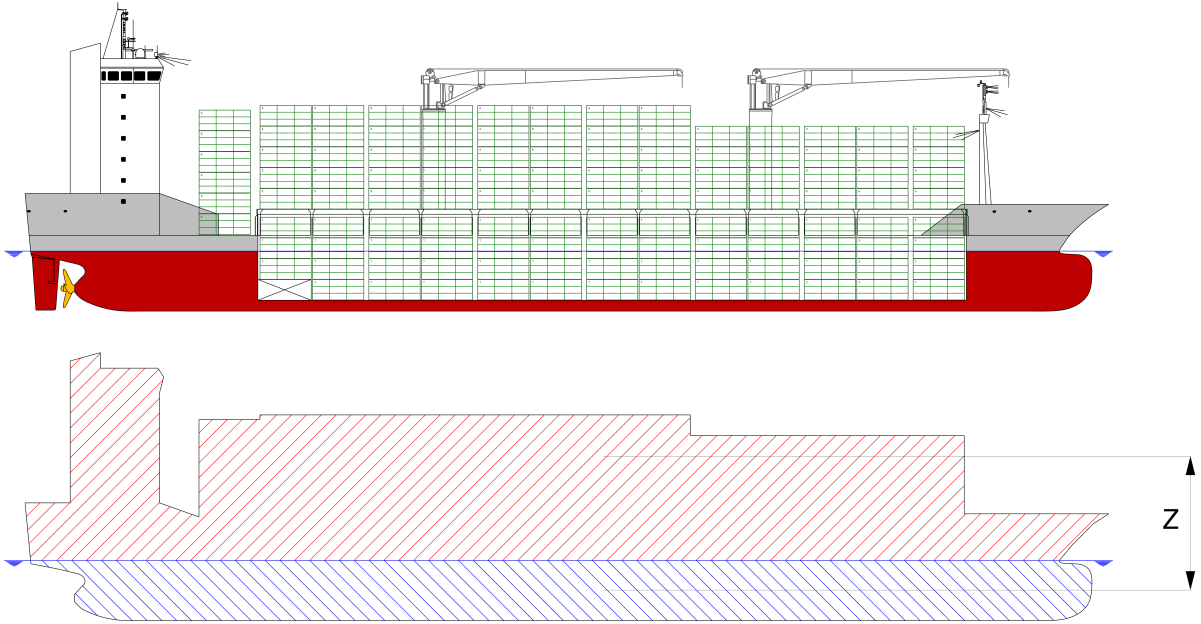


Figure 5.4: Loading Condition 1. The red hatched area represents the projected lateral area exposed to wind ($A_L = 1880.55 \text{ m}^2$), while the blue hatched area represents the underwater lateral area ($A_{UW} = 856.52 \text{ m}^2$). The vertical distance between the centroids of the two areas is $Z = 11.89 \text{ m}$.

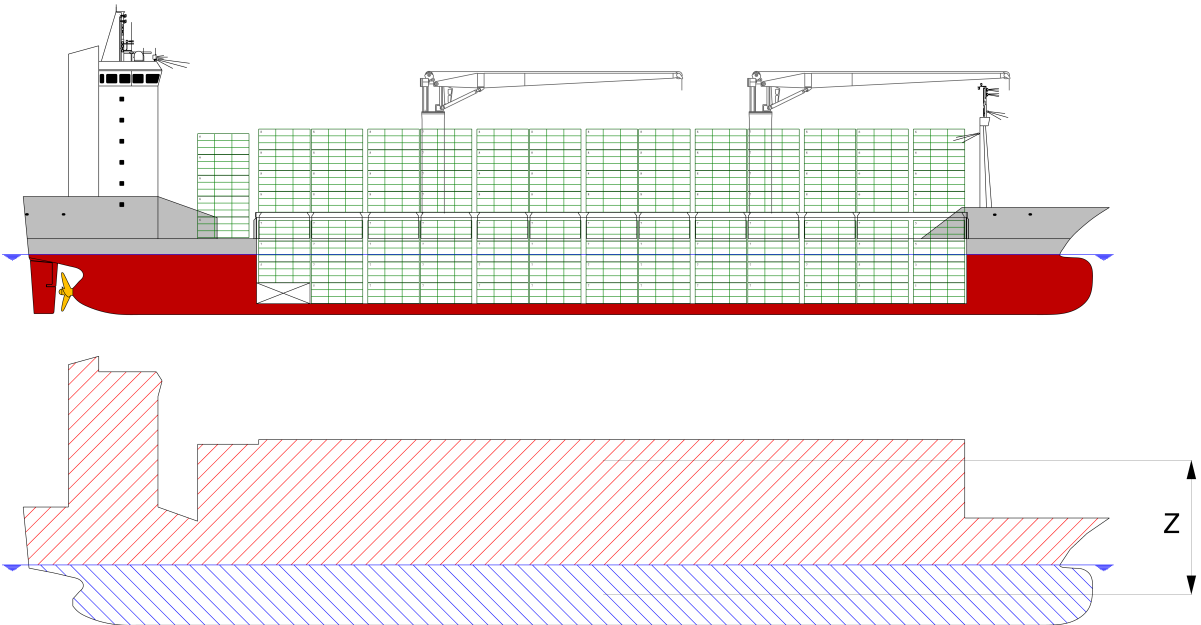


Figure 5.5: Loading Condition 2. The red hatched area represents the projected lateral area exposed to wind ($A_L = 1735.63 \text{ m}^2$), while the blue hatched area represents the underwater lateral area ($A_{UW} = 856.52 \text{ m}^2$). The vertical distance between the centroids of the two areas is $Z = 11.25 \text{ m}$.

Application of the Vulnerability Level 2 of SGISC for Dead Ship Condition

This Chapter presents a worked example of calculating the long-term Dead Ship Condition failure index. The numerical code is written in Python programming language and aligns with the procedure explained in *Section 4.2* (DSC vulnerability at L2). The code is validated with the available IMO data (*IMO, 2013*) and cross-checked with the corresponding code used at the Department of Naval Architecture of the Faculty of Mechanical Engineering, University of Belgrade (*Rudaković, 2021*).

The calculations are performed on the sample ship described in *Chapter 5*. It is important to note that due to extensiveness, the worked example considers only a freeboard height of 2 m and one metacentric height of 1 m. The main particulars used as input for this worked example are listed in *Table 6.1*, while the constants used for all calculations in this thesis can be found in *Table 6.2*. The example considers the ship with bilge keels in Loading Condition 1.

Table 6.1: Considered data for the code of the worked example.

Parameter	Symbol	Value	Unit
Waterline length	L_{WL}	121.3	[m]
Length between perpendicular	L_{BP}	120	[m]
Breadth overall	B	21.3	[m]
Draft	d	7.14	[m]
Freeboard	F_B	2	[m]
Displacement	Δ	14504	[t]
Block coefficient	C_B	0.761	[–]
Midship section coefficient	C_M	0.995	[–]
Metacentric height	\overline{GM}	1	[m]
Centre of gravity	\overline{KG}	6.07	[m]
Downflooding angle	φ_f	40.2	[°]

In *Chapter 7*, the outlined process will be iteratively conducted for each freeboard height and a range of metacentric heights. Furthermore, the long-term stability failure index will be represented as a function of \overline{GM} , where the considered range of metacentric height varies from 0.1 *m* up to 2 *m*, with the step of 0.1 *m*.

Remark: : Worked example - Loading Condition and Bilge Keels Dimensions

1. The projected lateral area for Loading Condition 1 is $A_L = 1880.55 \text{ m}^2$ and the vertical distance between the centroids of the windage area and the underwater area is $Z = 11.89 \text{ m}$.
2. It is assumed that the bilge keel dimensions correspond to the maximum values of applicability of Simplified Ikeda's method. The width is 0.22 *m*, and the length of the bilge keels is 40% of the ship's length.

The righting levers of the sample ship, corresponding to different freeboard heights, are computed using the MAXSURF program (student license) for a specific value of \overline{GM}_0 . The residual righting lever for each freeboard height can then be easily determined, and as previously explained, this term is only dependent on the hull form, making it a constant.

$$\overline{GZ}_{res}(\varphi) = \overline{GZ}(\varphi) - \overline{GM}_0 \cdot \sin(\varphi) \quad (6.1)$$

Therefore, for the range of metacentric height, corresponding righting levers can be obtained using the following equation:

$$\overline{GZ}_i(\varphi) = \overline{GM}_i \cdot \sin(\varphi) + \overline{GZ}_{res}(\varphi) \quad (6.2)$$

The worked example is focused on a single righting lever, but the procedure mentioned above will be carried out in *Chapter 7* in order to analyze ship dynamic stability under various conditions.

In the relevant IMO documents, there is no explicit mention of the required discretization step or interpolation method to define the \overline{GZ} curve, which is necessary to achieve accurate results. In this thesis, a linear interpolation method with a discretization step of 0.005 degree is used to define the \overline{GZ} curve. Comparing available IMO data (*IMO, 2013*) with the mentioned assessment, it is found that a relative error of the short-term failure index $C_{DSC,s}$ is 6.923%. It is important to highlight that the value of $C_{DSC,s}$ of the IMO worked example is extremely small, on the order of 10^{-18} . Despite this, the obtained relative error is deemed satisfactory. A detailed explanation of this observation will be provided in the following section. A smaller discretization step or another more precise interpolation can be used, but to attain a balance between accuracy and computational efficiency it is decided that the current assessment is sufficient.

Table 6.2: Consider constants.

Parameter	Symbol	Value	Unit
Air density	ρ_{air}	1.222	$[m^3/kg]$
Water density	ρ	1025	$[m^3/kg]$
Viscosity	η	$1.14 \cdot 10^{-6}$	$[m^2/s]$
Gravity constant	g	9.81	$[m/s^2]$
Wind healing coefficient	C_{whm}	1.22	$[-]$
Aerodynamic admittance function	λ	1	$[-]$

6.1. Wind Impact and Associated Relevant Angles

The analysis assumes that the ship is subject to the action of the mean wind U_w , which can be calculated according to *Equation (4.10)* as a function of significant wave height H_s . The total heeling moment $M_{\text{wind tot}}$ caused by the mean wind, and the corresponding lever $l_{\text{wind tot}}$, can be calculated using *Equation (4.12)*.

To estimate the static heeling angles φ_s , each intersection of \overline{GZ} with a range of heeling levers $l_{\text{wind tot}}$ (corresponding to each value of U_w) has to be considered. If the mean wind heeling lever exceeds the righting lever i.e. an intersection does not exist, the short-term failure index $C_{DSC,s}$ for that specific significant wave height is equal to 1. Furthermore, the angles of vanishing stability under the action of steady winds to leeward $\varphi_{VW,+}$, and windward $\varphi_{VW,-}$ can also be defined.

If φ_s can be defined, the angles of vanishing stability under the action of steady winds to leeward $\varphi_{VW,+}$, and windward $\varphi_{VW,-}$ can also be determined. The angles of failure to leeward $\varphi_{fail,+}$ are determined as the minimum of the following values $\varphi_{VW,+}$, $\varphi_{f,+}$, 50° , while to windward $\varphi_{fail,-}$ the maximum between $\varphi_{VW,-}$, $\varphi_{f,-}$, -50° . As explained before, these critical angles are illustrated in detail in *Figure 4.3*.

Table 6.3: Relevant angles, residual metacentric heights, and modified natural frequencies for the worked example.

H_s m	l_w m	φ_s °	\overline{GZ}_{res} m	$\omega_{0,e}$ rad/s	φ_{VW+} °	φ_{VW-} °	$\varphi_{fail,+}$ °	$\varphi_{fail,-}$ °	$\varphi_{cap,EA+}$ °	$\varphi_{cap,EA-}$ °	$\Delta\varphi_{res,EA+}$ °	$\Delta\varphi_{res,EA-}$ °
0.5	0.002	0.100	0.968	0.372	55.170	-55.255	40.200	-40.200	38.039	-38.047	37.939	38.147
1.5	0.007	0.430	0.968	0.372	55.045	-55.380	40.200	-40.200	38.017	-38.069	37.587	38.499
2.5	0.014	0.855	0.970	0.373	54.880	-55.540	40.200	-40.200	37.951	-38.045	37.096	38.900
3.5	0.023	1.335	0.975	0.373	54.695	-55.725	40.200	-40.200	37.833	-37.984	36.498	39.319
4.5	0.032	1.860	0.991	0.376	54.485	-55.930	40.200	-40.200	37.499	-37.692	35.639	39.552
5.5	0.041	2.420	1.003	0.379	54.260	-56.145	40.200	-40.200	37.252	-37.498	34.832	39.918
6.5	0.052	3.010	1.016	0.381	54.020	-56.375	40.200	-40.200	36.970	-37.264	33.960	40.274
7.5	0.063	3.615	1.032	0.384	53.765	-56.610	40.200	-40.200	36.641	-36.995	33.026	40.610
8.5	0.074	4.230	1.071	0.391	53.495	-56.860	40.200	-40.200	35.961	-36.300	31.731	40.530
9.5	0.086	4.855	1.094	0.396	53.215	-57.120	40.200	-40.200	35.540	-35.934	30.685	40.789
10.5	0.098	5.485	1.136	0.403	52.920	-57.385	40.200	-40.200	34.869	-35.235	29.384	40.720
11.5	0.111	6.125	1.148	0.405	52.615	-57.660	40.200	-40.200	34.605	-35.093	28.480	41.218
12.5	0.124	6.770	1.153	0.406	52.300	-57.940	40.200	-40.200	34.411	-35.089	27.641	41.859
13.5	0.137	7.435	1.143	0.404	51.965	-58.225	40.200	-40.200	34.391	-35.362	26.956	42.797
14.5	0.151	8.130	1.128	0.402	51.625	-58.515	40.200	-40.200	34.422	-35.722	26.292	43.852
15.5	0.165	8.860	1.077	0.392	51.270	-58.810	40.200	-40.200	34.874	-36.824	26.014	45.684
16.5	0.179	9.645	0.998	0.378	50.900	-59.115	40.200	-40.200	35.698	-38.640	26.053	48.285

After determining the static angles φ_s for each environmental condition, the residual or local metacentric height (see *Equation (4.15)*) \overline{GM}_{res} can be calculated as the first derivative (slope) of the righting arm around an equilibrium point. Later, the modified natural oscillation frequencies can be easily computed using *Equation (4.14)*.

It should be pointed out again that a suggested method to calculate the slope at the angle of equilibrium (φ_s) is not defined in the IMO documents. Furthermore, the value of the local metacentric height is 1.762 m based on the results from *IMO, 2013*, where \overline{GZ} curve differentiation is done using polynomial fitting. In this study, the gradient of the data is computed using the Python NumPy library's "gradient" function (NumPy version 1.21.5). During validation, a relative error of 0.511% occurs for \overline{GM}_{res} which leads to a relative error of 6.923% for the short-term failure index $C_{DSC,s}$. Nevertheless, by utilizing

the value of $\overline{GZ}_{res} = 1.762 \text{ m}$ in the developed code and proceeding with the subsequent calculations, a reduction in the relative error is achieved, reaching a value of 0.081% for $C_{DSC,s}$. This occurrence highlights the significance of defining the specific discretization step of a righting lever or the need for an additional interpolation method. A careful choice of the discretization step ensures accuracy in the calculation process and minimizes potential errors. Furthermore, the proposed method for defining the slope at a static heeling angle also should be provided.

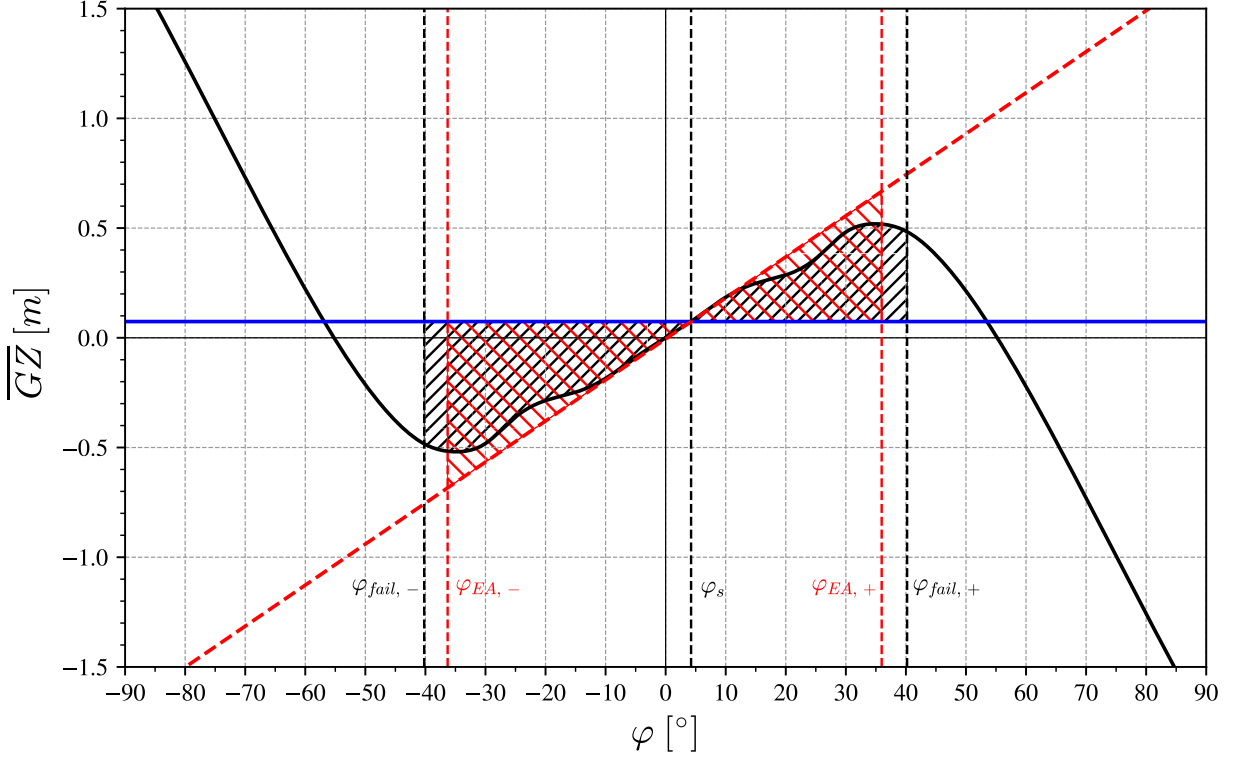


Figure 6.2: Relevant angles for estimating short-term stability failure index using the "equivalent area" approach (with $\overline{GM} = 1\text{m}$, $FB = 2\text{m}$, and Loading Condition 1). Everything associated with the non-linear righting lever \overline{GZ} is denoted with (—) and (---), while with (—) and (---) everything related to a linearized righting lever. With (—) represents the constant heeling lever due to wind $l_{wind,tot}$ which correspond to the $H_s = 8.5 \text{ m}$ ($U_w = 25.21 \text{ m/s}^2$).

Finally, the virtual capsizes angles $\varphi_{cap,EA+}$ and $\varphi_{cap,EA-}$ to leeward and windward, can be defined using Equation (4.22) from "equivalent area" approach. The residual stability range, with respect to each side, can also be computed as a difference with φ_s . The results of relevant angles for worked example are given in Table 6.3, while one case ($H_s = 8.5 \text{ m}$) of using an "equivalent area" approach is represented in Figure 6.2. The virtual capsizes angles $\varphi_{cap,EA+}$ and $\varphi_{cap,EA-}$ may vary in relation to the failure angles $\varphi_{fail,+}$ and $\varphi_{fail,-}$, depending on the characteristics of the residual righting lever. Specifically, in the case of strongly hardening \overline{GZ} , the relation of angles is $\varphi_{cap,EA+} > \varphi_{fail,+}$ and $\varphi_{cap,EA-} < \varphi_{fail,-}$. This occurrence occurs for righting levers corresponding to lower freeboard heights. Conversely, for softening \overline{GZ} , a common scenario is $\varphi_{cap,EA+} < \varphi_{fail,+}$ and $\varphi_{cap,EA-} > \varphi_{fail,-}$.

6.2. Environments Impact

In the SGISC framework for Dead Ship Condition at Vulnerability Level 2, a frequency-dependent effective wave slope coefficient is determined according to *Section 4.2.5*. The hull is divided into 22 equidistant transversal sections along the waterline length L_{WL} , and the integration method is accomplished using Simpson's I rule. In *Table 6.4* can be found inputs of cross-section dimension of a worked example, as well for a sample ship.

Table 6.4: Parameters for estimating the wave slope function $r(\omega)$: $B(x)$, $d(x)$, and $A(x)$ denote the sectional breadth at the waterline, the sectional draught, and underwater sectional area of the sample ship, respectively. x/L indicates the relative location of the section along the ship's length. Cross-section 0' is added in the calculation to perform accurate integration along the length i.e. to include the small portion of the hull aft.

Section	x/L	$B(x)$	$d(x)$	$A(x)$	Section	x/L	$B(x)$	$d(x)$	$A(x)$
	/	m	m	m^2		/	m	m	m^2
0'	0.00	0	0	0	10	0.52	21.30	7.14	151.27
0	0.05	5.86	0.80	2.91	11	0.57	21.30	7.14	151.28
1	0.10	11.16	6.82	37.27	12	0.62	21.30	7.14	151.28
2	0.14	14.93	7.14	67.41	13	0.67	21.30	7.14	150.09
3	0.19	17.82	7.14	96.46	14	0.71	21.17	7.14	145.92
4	0.24	19.66	7.14	117.53	15	0.76	20.86	7.14	139.98
5	0.29	20.75	7.14	132.84	16	0.81	20.18	7.14	131.50
6	0.33	21.20	7.14	142.90	17	0.86	18.72	7.14	118.17
7	0.38	21.30	7.14	148.63	18	0.90	15.79	7.14	96.45
8	0.43	21.30	7.14	150.51	19	0.95	10.17	7.14	60.95
9	0.48	21.30	7.14	151.09	20	1.00	0	7.04	20.35

Wave elevation $S_{zz}(\omega)$ can be obtained using the Bretschneider spectrum (see *Equation (4.6)*). Afterward, a spectrum of the wave slope $S_{\alpha\alpha}(\omega)$ and effective wave slope spectrum $S_{\alpha\alpha,c}(\omega)$ can be determined using *Equation (4.7)* and *Equation (4.8)*, respectively.

The calculation process has to be repeated for each environmental condition (H_s and T_z), and the algorithm which has to be implemented to obtain wave impacts is represented in *Figure 6.3*. For illustrative purposes, the spectrum $S_{zz}(\omega)$, $S_{\alpha\alpha}(\omega)$, estimated effective wave slope coefficient $r(\omega)$ as a function of the wave frequency and $S_{\alpha\alpha,c}(\omega)$ are presented in *Figure 6.4*, respectively. Showcasing results are only for one specific environmental condition.

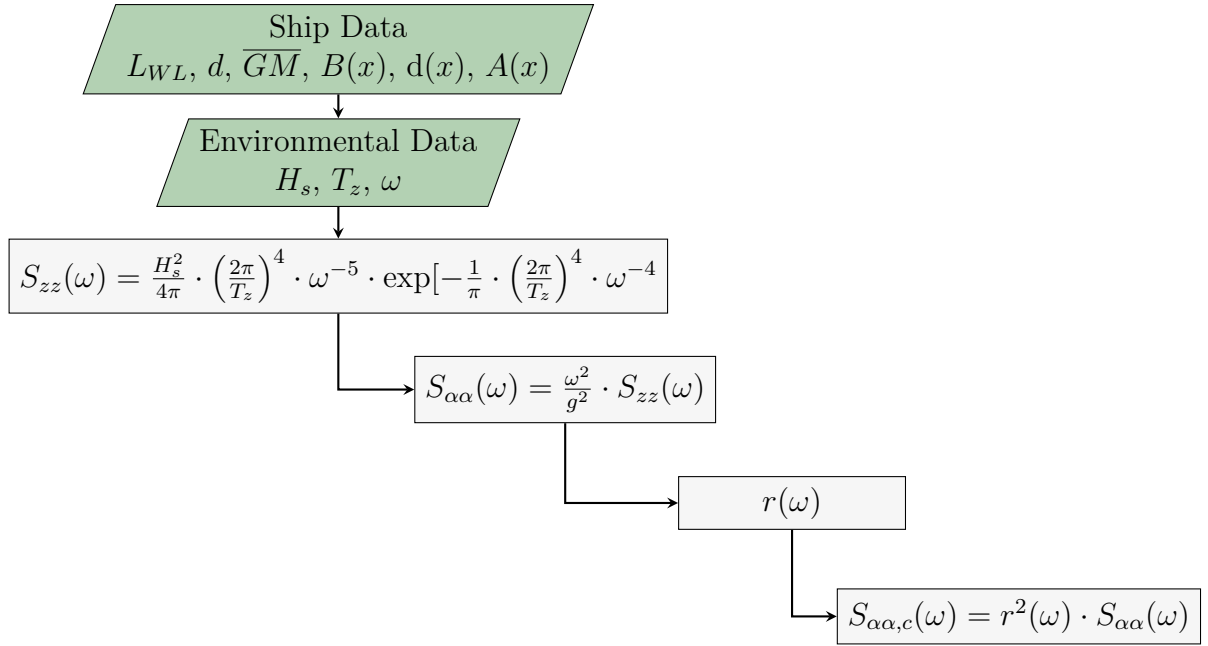
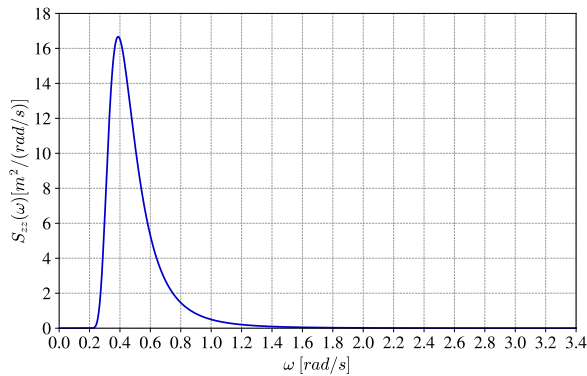
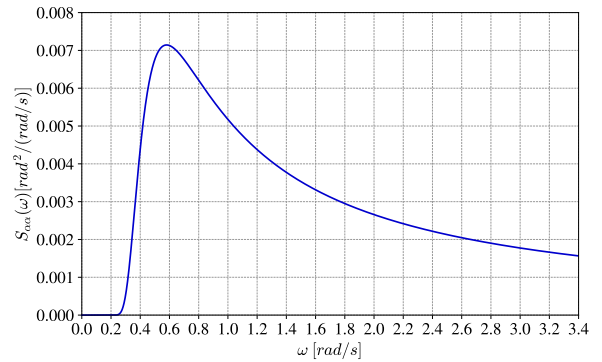


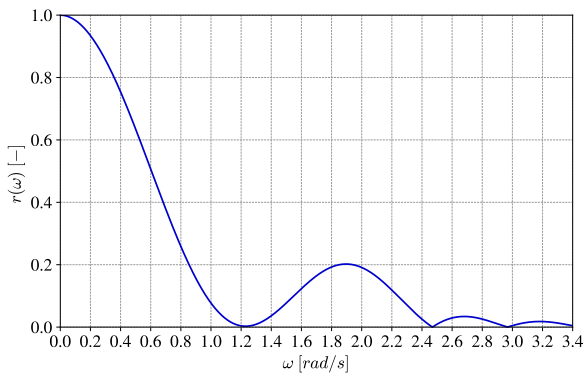
Figure 6.3: Flowchart of the calculation of the effective wave slope spectrum.



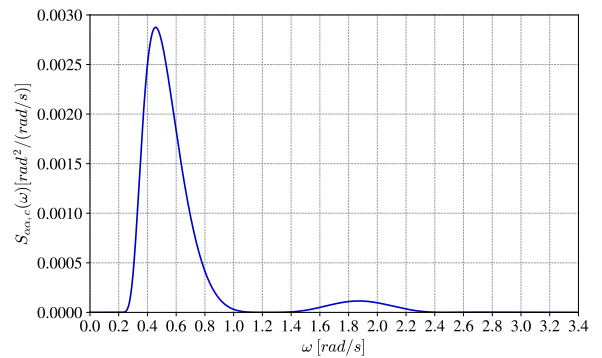
(a) Sea elevation spectrum.



(b) Wave slope spectrum.



(c) Effective wave slope.



(d) Effective wave slope spectrum.

Figure 6.4: Impact of waves on worked example. Environmental condition : $H_s = 8.5 \text{ m}$ and $T_z = 11.5 \text{ s}$.

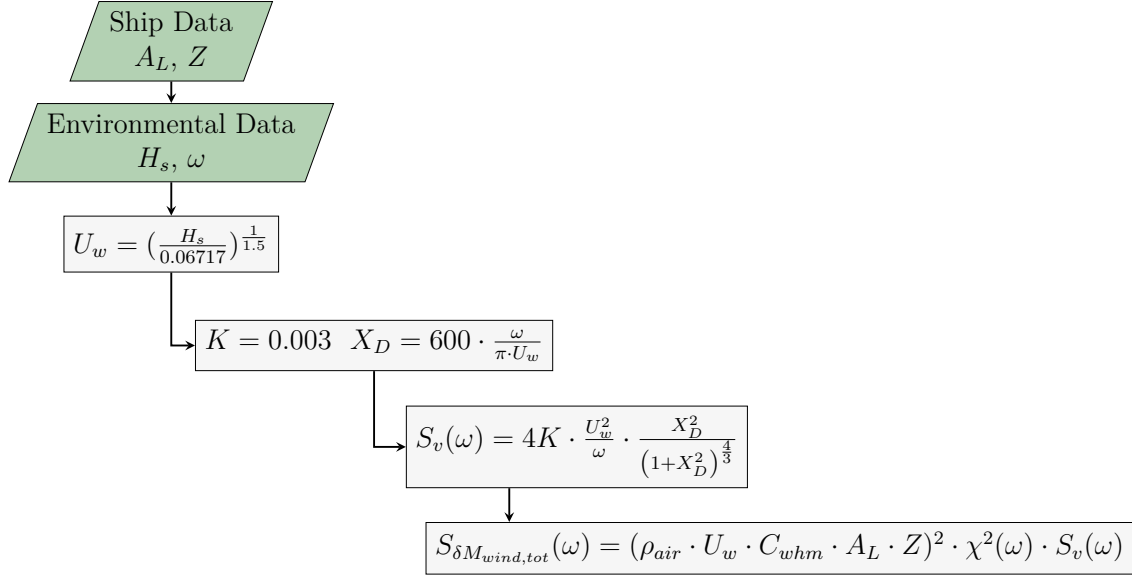


Figure 6.5: Flowchart of the calculation of the spectrum of the wind gust moment.

Furthermore, apart from the influence of waves, the ship's rolling is also affected by wind gusts. To assess the wind effects on the considered loading condition, it is necessary to estimate them for each value of significant wave height, i.e. mean wind speed (see *Figure 6.5*). The wind gustiness spectrum $S_v(\omega)$ is derived using the Davenport spectrum (see *Equation (4.9)*), while the spectrum of the roll moment $S_{\delta M_{wind,tot}}(\omega)$ induced by gustiness (including the drift reaction) can be determined using *Equation (4.11)*. In *Figure 6.6*, $S_v(\omega)$ and $S_{\delta M_{wind,tot}}(\omega)$ are presented for one mean wind speed.

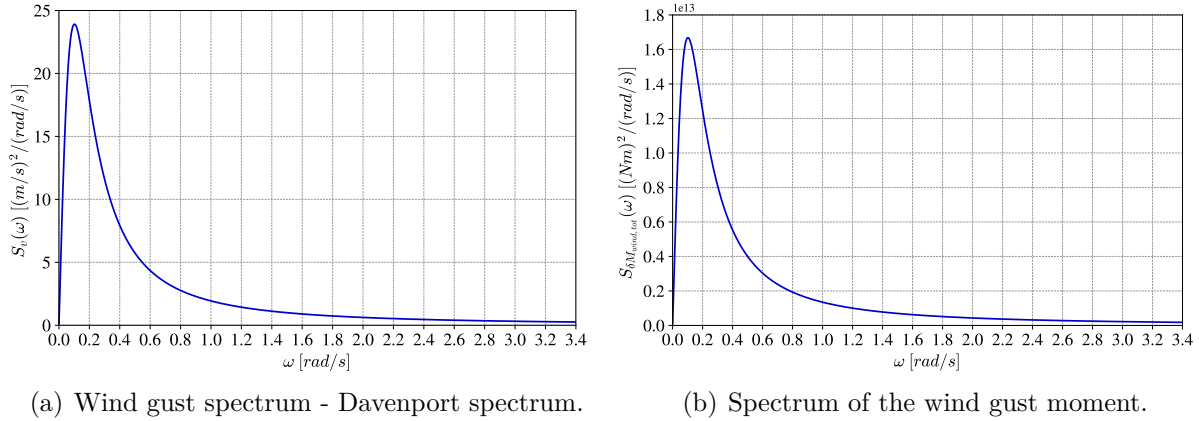


Figure 6.6: Impact of winds on worked example. Environmental condition : $H_s = 8.5 \text{ m}$ ($U_w = 25.21 \text{ m/s}^2$).

6.3. Equivalent Linear Roll Damping Coefficients

Roll damping coefficient \hat{B}_{44} is calculated according to Simplified Ikeda's method, as explained in *Section 4.2.4*. Furthermore, the roll damping \hat{B}_{44} is assessed as a function of roll amplitude function (see *Equation (4.28)*), followed by deriving of three damping coefficients, μ , β , and δ (linear, quadratic, and cubic), using a least square fitting method.

According to *Kawahara et al., 2011*, Simplified Ikeda's method has a limitation of applicability. There are no application limits for B_F component. Applicable ranges of vessel parameters such as B/d , C_B , C_M , and \overline{OG}/d which are associated with B_W , B_E , and B_{BK} roll damping components are follows:

1. $2.5 \leq B/d \leq 4.5$
2. $0.5 \leq C_B \leq 0.85$
3. $0.9 \leq C_M \leq 0.99$
4. $0.01 \leq b_{BK}/B \leq 0.06$
5. $0.05 \leq l_{BK}/L_{BP} \leq 0.4$

In this thesis, as per the guidelines *IMO, 2023*, the code is written to manage scenarios where a ship's parameter exists outside the applicable range. In such cases, the parameter value is kept at the corresponding maximum or minimum limit value to ensure the accurate use of the associated formula.

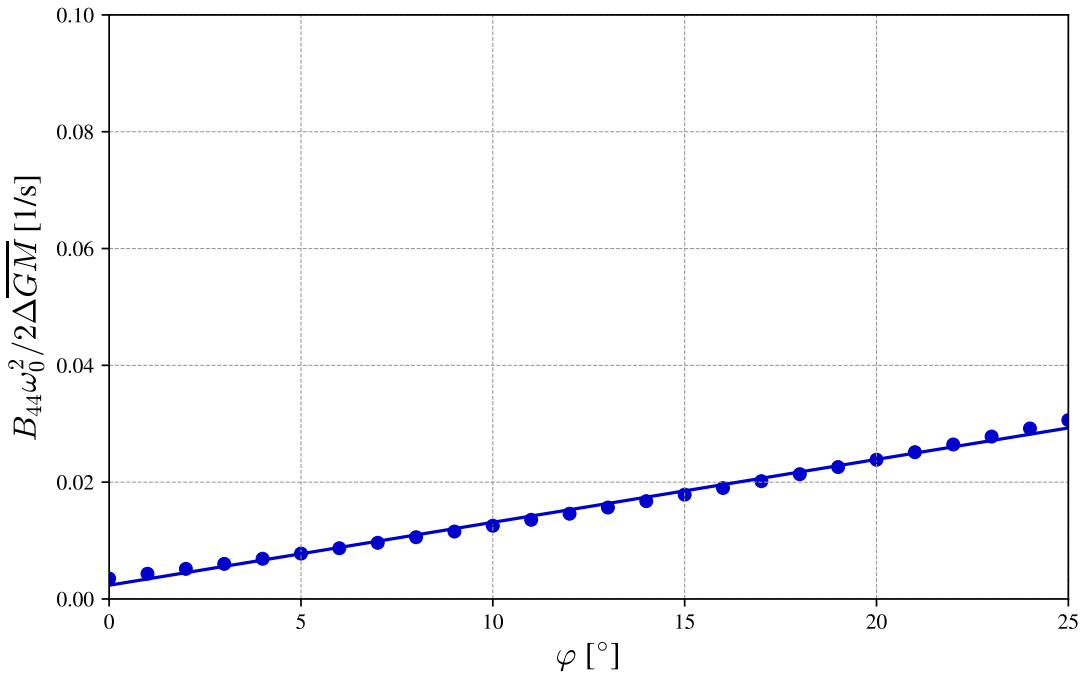


Figure 6.7: Damping coefficients of the worked example. Calculated data with the presence of the bilge keels ($b_{bk} = 0.22 \text{ m}$, $l_{bk} = 0.4 \cdot L_{BP} \text{ m}$) and a fitting curve are represented with (\bullet) and $(—)$, respectively. Roll damping coefficients: $\mu = 0.002351[1/s]$; $\beta = 0.384547[1/rad]$; $\delta = 0[s/rad^2]$.

To ensure future extrapolations of the fitted polynomial can be avoided, a wide range of roll amplitudes is employed, following the guidelines of *IMO, 2013*. In this thesis, the range spans from 0° to 25° , with a step size of 1° . To prevent any numerical issues, the value at 0° is approximated as $0 \approx 1 \times 10^{-16}$. Moreover, for simplicity, the cubic damping coefficient δ is considered negligible, and only the linear coefficient μ and quadratic coefficient β roll damping coefficient are utilized. However, the calculated data with the fitting curve is represented in *Figure 6.7*.

Once rolling damping coefficients are determined, an iterative procedure can be applied to calculate the equivalent roll damping coefficient μ_e . The algorithm to access this iterative process is shown in *Figure 6.8* and has to be implemented for each environmental condition. In *Table 6.5* is presented the equivalent linear roll damping coefficient μ_e for the worked example under different combinations of H_s and T_z . In the table color gradient visually illustrates how the equivalent roll damping coefficient changes under various sea conditions. Darker cells represent higher damping coefficients, which means higher resistance to rolling motion, whereas lighter cells represent lower damping coefficients, indicating lower resistance. Generally, as the significant wave height increases as well average zero-crossing wave period, the roll damping coefficient μ_e increases as well. This means that the impact of roll damping on rolling motion becomes stronger in rougher sea conditions.

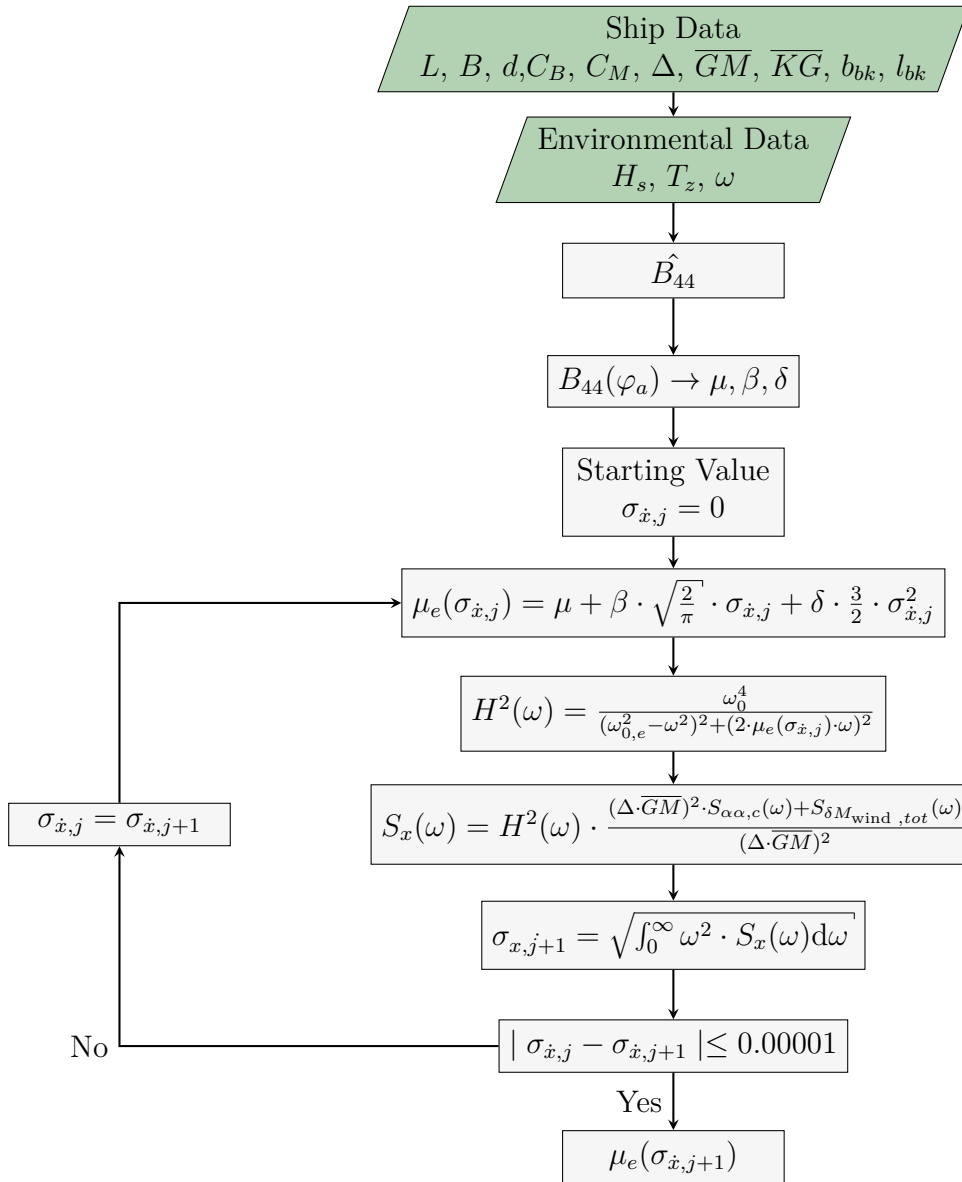


Figure 6.8: Flowchart of the calculation for the equivalent linear roll damping coefficient. Spectrum $S_{\alpha\alpha,c}(\omega)$ and $S_{\delta M_{wind,tot}}(\omega)$, as well as natural roll frequency ω_0 and modified roll frequency $\omega_{0,e}$ should be defined earlier.

Table 6.5: Equivalent linear roll damping coefficient μ_e for the worked example across all environmental conditions.

H_s [m] - Significant Wave Height	T_z [s] - Average Zero-Crossing Wave Period															
	3.5	4.5	5.5	6.5	7.5	8.5	9.5	10.5	11.5	12.5	13.5	14.5	15.5	16.5	17.5	18.5
0.5	2.555E-03	2.550E-03	2.569E-03	2.606E-03	2.703E-03	3.048E-03	3.486E-03	3.804E-03	3.970E-03	4.022E-03	4.002E-03	3.941E-03	3.858E-03	3.768E-03	3.676E-03	3.587E-03
1.5	3.260E-03	3.251E-03	3.286E-03	3.360E-03	3.559E-03	4.291E-03	5.229E-03	5.897E-03	6.242E-03	6.349E-03	6.303E-03	6.170E-03	5.993E-03	5.798E-03	5.600E-03	5.407E-03
2.5	4.100E-03	4.087E-03	4.135E-03	4.230E-03	4.507E-03	5.467E-03	6.729E-03	7.631E-03	8.092E-03	8.229E-03	8.160E-03	7.973E-03	7.726E-03	7.455E-03	7.180E-03	6.913E-03
3.5	4.981E-03	4.964E-03	5.026E-03	5.156E-03	5.489E-03	6.628E-03	8.131E-03	9.201E-03	9.746E-03	9.890E-03	9.806E-03	9.571E-03	9.264E-03	8.929E-03	8.589E-03	8.261E-03
4.5	5.863E-03	5.843E-03	5.919E-03	6.082E-03	6.507E-03	7.860E-03	9.565E-03	1.075E-02	1.133E-02	1.146E-02	1.133E-02	1.104E-02	1.067E-02	1.028E-02	9.879E-03	9.497E-03
5.5	6.747E-03	6.724E-03	6.813E-03	7.009E-03	7.521E-03	9.054E-03	1.092E-02	1.220E-02	1.280E-02	1.293E-02	1.275E-02	1.241E-02	1.199E-02	1.154E-02	1.109E-02	1.066E-02
6.5	7.622E-03	7.596E-03	7.700E-03	7.930E-03	8.541E-03	1.026E-02	1.227E-02	1.361E-02	1.422E-02	1.432E-02	1.411E-02	1.372E-02	1.324E-02	1.274E-02	1.224E-02	1.177E-02
7.5	8.482E-03	8.452E-03	8.573E-03	8.843E-03	9.569E-03	1.149E-02	1.362E-02	1.500E-02	1.560E-02	1.567E-02	1.540E-02	1.496E-02	1.443E-02	1.388E-02	1.334E-02	1.283E-02
8.5	9.293E-03	9.261E-03	9.404E-03	9.735E-03	1.070E-02	1.295E-02	1.519E-02	1.653E-02	1.704E-02	1.701E-02	1.666E-02	1.614E-02	1.554E-02	1.494E-02	1.435E-02	1.379E-02
9.5	1.011E-02	1.008E-02	1.024E-02	1.063E-02	1.178E-02	1.426E-02	1.657E-02	1.790E-02	1.837E-02	1.827E-02	1.786E-02	1.727E-02	1.663E-02	1.597E-02	1.534E-02	1.475E-02
10.5	1.089E-02	1.085E-02	1.104E-02	1.152E-02	1.299E-02	1.579E-02	1.813E-02	1.937E-02	1.972E-02	1.952E-02	1.901E-02	1.835E-02	1.763E-02	1.692E-02	1.625E-02	1.563E-02
11.5	1.170E-02	1.166E-02	1.187E-02	1.240E-02	1.403E-02	1.697E-02	1.936E-02	2.060E-02	2.092E-02	2.068E-02	2.013E-02	1.942E-02	1.866E-02	1.791E-02	1.720E-02	1.655E-02
12.5	1.251E-02	1.247E-02	1.269E-02	1.327E-02	1.500E-02	1.805E-02	2.050E-02	2.175E-02	2.207E-02	2.180E-02	2.121E-02	2.047E-02	1.968E-02	1.889E-02	1.816E-02	1.748E-02
13.5	1.334E-02	1.329E-02	1.353E-02	1.413E-02	1.585E-02	1.892E-02	2.145E-02	2.278E-02	2.313E-02	2.287E-02	2.227E-02	2.151E-02	2.070E-02	1.990E-02	1.913E-02	1.843E-02
14.5	1.416E-02	1.411E-02	1.437E-02	1.498E-02	1.666E-02	1.971E-02	2.233E-02	2.373E-02	2.414E-02	2.391E-02	2.332E-02	2.255E-02	2.172E-02	2.089E-02	2.011E-02	1.939E-02
15.5	1.506E-02	1.500E-02	1.525E-02	1.583E-02	1.723E-02	2.003E-02	2.273E-02	2.434E-02	2.493E-02	2.483E-02	2.432E-02	2.360E-02	2.279E-02	2.197E-02	2.119E-02	2.045E-02
16.5	1.601E-02	1.594E-02	1.618E-02	1.670E-02	1.775E-02	2.001E-02	2.269E-02	2.456E-02	2.544E-02	2.557E-02	2.523E-02	2.462E-02	2.388E-02	2.310E-02	2.233E-02	2.160E-02

6.4. Long-term Failure Index of Worked Example

In the final step, the determined equivalent linear roll damping coefficient is used to define several parameters for estimating the short-term stability failure index under various sea conditions and considered exposure time. The algorithm for this purpose is presented in *Figure 6.9*, and the relevant formulas can be found in *Chapter 4*.

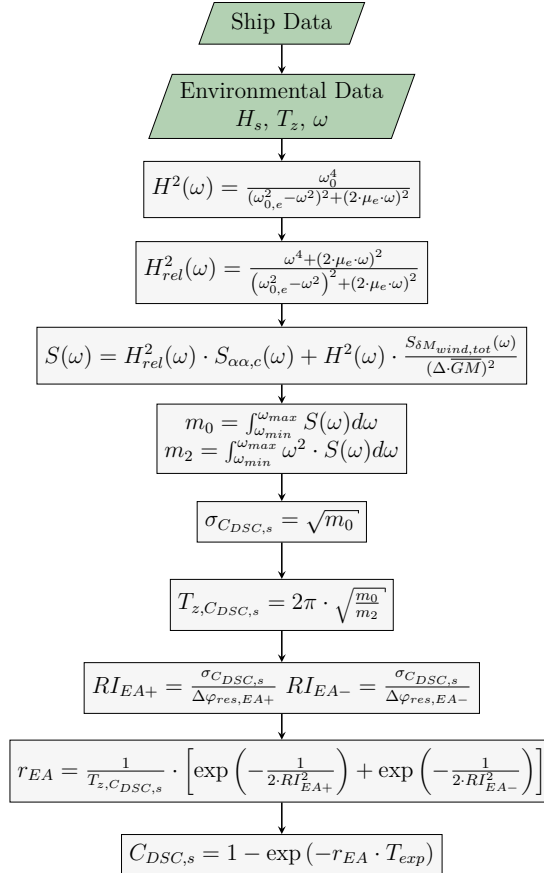


Figure 6.9: Flowchart of the calculation of the short-term failure stability index. Spectrum $S_{\alpha\alpha,c}(\omega)$ and $S_{\delta M_{wind,tot}}(\omega)$, residual range of stability to leeward $\Delta\varphi_{res,EA+}$ and windward $\Delta\varphi_{res,EA-}$, equivalent linear roll damping coefficient μ_e , as well as natural roll frequency ω_0 and modified roll frequency $\omega_{0,e}$ should be defined earlier.

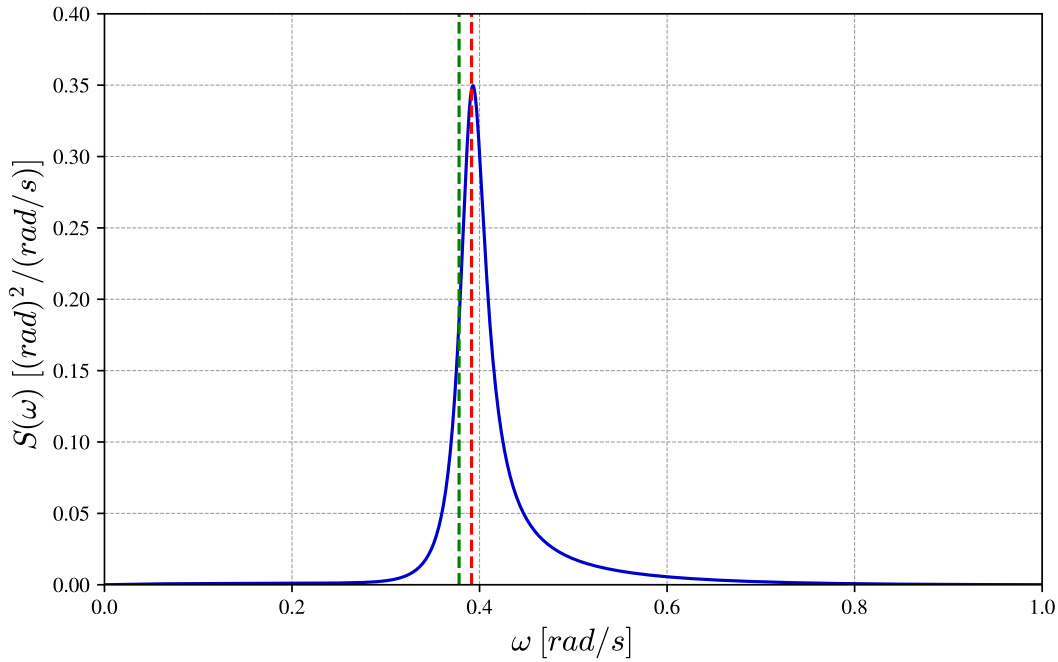


Figure 6.10: Spectrum of effective relative roll motion for $\overline{GM} = 1\text{ m}$ and Loading Condition 1. Environmental condition : $H_s = 8.5\text{ m}$ and $T_z = 11.5\text{ s}$. The spectrum $S(\omega)$ is denoted with (—), while with (---) and (-.-) are represented natural roll frequency (ω_0) and modified natural frequency ($\omega_{0,e}$), respectively.

To visually display all spectrums, the effective relative roll angle spectrum $S(\omega)$ is shown in *Figure 6.10* for a specific environmental condition. This spectrum represents the ship’s response to the combined influence of waves and gustiness.

Due to the extensiveness of the results, only short-term Dead Ship Condition failure index $C_{DSC,s}$ is given (see *Table 6.6*). The $C_{DSC,s}$ is a measure of the probability of the ship exceeding specified heel angles during the considered exposure time, taking into account an effective relative angle between the ship and the waves.

Table 6.6: Short-term Dead Ship Condition failure index $C_{DSC,s}$ for the worked example across all environmental conditions.

		$T_z[s]$ - Average Zero-Crossing Wave Period																
		3.5	4.5	5.5	6.5	7.5	8.5	9.5	10.5	11.5	12.5	13.5	14.5	15.5	16.5	17.5	18.5	
$H_z[m]$ - Significant Wave Height	0.5	0.000E+00	0.000E+00	0.000E+00	0.000E+00	0.000E+00	0.000E+00	0.000E+00	0.000E+00	0.000E+00	0.000E+00	0.000E+00	0.000E+00	0.000E+00	0.000E+00	0.000E+00	0.000E+00	
	1.5	0.000E+00	0.000E+00	0.000E+00	0.000E+00	0.000E+00	0.000E+00	0.000E+00	0.000E+00	0.000E+00	0.000E+00	0.000E+00	0.000E+00	0.000E+00	0.000E+00	0.000E+00	0.000E+00	
	2.5	0.000E+00	0.000E+00	0.000E+00	0.000E+00	0.000E+00	0.000E+00	0.000E+00	0.000E+00	0.000E+00	0.000E+00	0.000E+00	0.000E+00	0.000E+00	0.000E+00	0.000E+00	0.000E+00	
	3.5	0.000E+00	0.000E+00	0.000E+00	0.000E+00	0.000E+00	0.000E+00	0.000E+00	0.000E+00	0.000E+00	0.000E+00	0.000E+00	0.000E+00	0.000E+00	0.000E+00	0.000E+00	0.000E+00	
	4.5	0.000E+00	0.000E+00	0.000E+00	0.000E+00	0.000E+00	0.000E+00	0.000E+00	0.000E+00	0.000E+00	0.000E+00	0.000E+00	0.000E+00	0.000E+00	0.000E+00	0.000E+00	0.000E+00	
	5.5	0.000E+00	0.000E+00	0.000E+00	0.000E+00	0.000E+00	0.000E+00	0.000E+00	0.000E+00	0.000E+00	0.000E+00	0.000E+00	0.000E+00	0.000E+00	0.000E+00	0.000E+00	0.000E+00	
	6.5	6.189E-12	0.000E+00	0.000E+00	0.000E+00	0.000E+00	0.000E+00	0.000E+00	1.110E-16	1.233E-12	2.904E-11	3.880E-11	1.021E-11	9.021E-13	3.475E-14	6.661E-16	0.000E+00	0.000E+00
	7.5	8.077E-08	2.623E-12	9.115E-14	5.943E-13	1.232E-10	7.342E-07	1.882E-04	1.833E-03	3.559E-03	3.001E-03	1.527E-03	5.461E-04	1.490E-04	3.277E-05	6.031E-06	9.607E-07	0.000E+00
	8.5	4.435E-05	1.988E-08	1.698E-09	8.428E-09	7.876E-07	4.196E-04	1.390E-02	5.237E-02	7.063E-02	5.583E-02	3.143E-02	1.379E-02	4.975E-03	1.530E-03	4.141E-04	1.010E-04	0.000E+00
	9.5	2.822E-03	7.687E-06	1.166E-06	4.239E-06	1.590E-04	1.497E-02	1.528E-01	3.308E-01	3.736E-01	3.068E-01	1.998E-01	1.069E-01	4.845E-02	1.922E-02	6.872E-03	2.266E-03	0.000E+00
	10.5	5.650E-02	5.591E-04	1.304E-04	4.186E-04	9.733E-03	2.339E-01	7.157E-01	8.799E-01	8.865E-01	8.165E-01	6.679E-01	4.658E-01	2.744E-01	1.394E-01	6.331E-02	2.652E-02	0.000E+00
	11.5	3.693E-01	1.126E-02	3.447E-03	8.602E-03	9.620E-02	6.970E-01	9.761E-01	9.954E-01	9.952E-01	9.860E-01	9.483E-01	8.430E-01	6.548E-01	4.349E-01	2.513E-01	1.310E-01	0.000E+00
	12.5	8.807E-01	1.000E-01	3.819E-02	7.527E-02	4.065E-01	9.670E-01	9.997E-01	1.000E+00	1.000E+00	9.998E-01	9.980E-01	9.849E-01	9.287E-01	7.931E-01	5.933E-01	3.913E-01	0.000E+00
	13.5	9.986E-01	4.288E-01	2.105E-01	3.189E-01	7.898E-01	9.988E-01	1.000E+00	1.000E+00	1.000E+00	1.000E+00	1.000E+00	9.995E-01	9.942E-01	9.646E-01	8.768E-01	7.219E-01	0.000E+00
	14.5	1.000E+00	8.709E-01	6.158E-01	7.315E-01	9.738E-01	1.000E+00	1.000E+00	1.000E+00	1.000E+00	1.000E+00	1.000E+00	1.000E+00	9.999E-01	9.978E-01	9.840E-01	9.357E-01	0.000E+00
	15.5	1.000E+00	9.953E-01	9.310E-01	9.534E-01	9.968E-01	1.000E+00	1.000E+00	1.000E+00	1.000E+00	1.000E+00	1.000E+00	1.000E+00	1.000E+00	9.999E-01	9.984E-01	9.898E-01	0.000E+00
16.5	1.000E+00	1.000E+00	9.972E-01	9.970E-01	9.996E-01	1.000E+00	1.000E+00	1.000E+00	1.000E+00	1.000E+00	1.000E+00	1.000E+00	1.000E+00	1.000E+00	9.998E-01	9.985E-01	0.000E+00	

The table again employed a color gradient to convey the results visually, green cells signify very low failure indices, while red cells indicate higher failure indices. Cells with a yellow shade represent intermediate probabilities. A failure index of 0 suggests that there is no probability of the ship exceeding the specified heel angles under the given combination of significant wave height and wave period. Conversely, as the failure index approaches 1, the likelihood of the ship exceeding the specified heel angles increases, signifying a higher risk of failure. Notably, a failure index value of 1 represents the utmost probability of failure, indicating that the ship exceeds the specified roll angle in that specific condition, which leads to capsizing.

Table 6.7: Weighted short-term Dead Ship Condition failure index $C_{DSC,s}$ for the worked example across all environmental conditions.

$H_w[m]$ - Significant Wave Height	$T_z[s]$ - Average Zero-Crossing Wave Period																
	3.5	4.5	5.5	6.5	7.5	8.5	9.5	10.5	11.5	12.5	13.5	14.5	15.5	16.5	17.5	18.5	
0.5	0.000E+00	0.000E+00	0.000E+00	0.000E+00	0.000E+00	0.000E+00	0.000E+00	0.000E+00	0.000E+00	0.000E+00	0.000E+00	0.000E+00	0.000E+00	0.000E+00	0.000E+00	0.000E+00	0.000E+00
1.5	0.000E+00	0.000E+00	0.000E+00	0.000E+00	0.000E+00	0.000E+00	0.000E+00	0.000E+00	0.000E+00	0.000E+00	0.000E+00	0.000E+00	0.000E+00	0.000E+00	0.000E+00	0.000E+00	0.000E+00
2.5	0.000E+00	0.000E+00	0.000E+00	0.000E+00	0.000E+00	0.000E+00	0.000E+00	0.000E+00	0.000E+00	0.000E+00	0.000E+00	0.000E+00	0.000E+00	0.000E+00	0.000E+00	0.000E+00	0.000E+00
3.5	0.000E+00	0.000E+00	0.000E+00	0.000E+00	0.000E+00	0.000E+00	0.000E+00	0.000E+00	0.000E+00	0.000E+00	0.000E+00	0.000E+00	0.000E+00	0.000E+00	0.000E+00	0.000E+00	0.000E+00
4.5	0.000E+00	0.000E+00	0.000E+00	0.000E+00	0.000E+00	0.000E+00	4.283E-18	3.116E-14	3.509E-13	1.675E-13	1.265E-14	2.714E-16	2.252E-18	8.660E-21	0.000E+00	0.000E+00	0.000E+00
5.5	0.000E+00	0.000E+00	0.000E+00	0.000E+00	0.000E+00	3.559E-18	3.797E-12	8.358E-10	2.970E-09	1.255E-09	1.461E-10	6.937E-12	1.665E-13	2.338E-15	1.984E-17	1.608E-19	
6.5	0.000E+00	0.000E+00	0.000E+00	0.000E+00	7.416E-19	1.121E-12	9.662E-09	3.273E-07	6.446E-07	2.721E-07	4.351E-08	3.493E-09	1.658E-10	5.149E-12	1.084E-13	1.847E-15	
7.5	0.000E+00	0.000E+00	0.000E+00	1.305E-17	5.574E-14	1.872E-09	1.082E-06	1.256E-05	1.825E-05	8.116E-06	1.665E-06	1.954E-07	1.479E-08	7.953E-10	3.504E-11	9.275E-13	
8.5	0.000E+00	0.000E+00	0.000E+00	4.683E-14	1.098E-10	3.942E-07	3.472E-05	1.803E-04	2.062E-04	9.583E-05	2.396E-05	3.747E-06	4.093E-07	3.290E-08	2.020E-09	9.831E-11	
9.5	0.000E+00	0.000E+00	0.000E+00	7.101E-12	6.389E-09	4.813E-06	1.529E-04	5.222E-04	5.621E-04	3.007E-04	9.525E-05	1.970E-05	2.907E-06	3.209E-07	2.694E-08	2.217E-09	
10.5	0.000E+00	0.000E+00	0.000E+00	1.105E-07	2.449E-05	2.691E-04	5.918E-04	6.336E-04	4.186E-04	1.811E-04	5.262E-05	1.085E-05	1.650E-06	1.870E-07	2.607E-08		
11.5	0.000E+00	0.000E+00	0.000E+00	2.763E-07	2.275E-05	1.297E-04	2.647E-04	3.124E-04	2.434E-04	1.344E-04	5.375E-05	1.561E-05	3.016E-06	4.968E-07	1.293E-07		
12.5	0.000E+00	0.000E+00	0.000E+00	3.944E-07	9.648E-06	4.399E-05	9.900E-05	1.280E-04	1.100E-04	6.786E-05	3.248E-05	1.205E-05	3.158E-06	5.891E-07	0.000E+00		
13.5	0.000E+00	0.000E+00	0.000E+00	0.000E+00	0.000E+00	2.996E-06	1.400E-05	3.500E-05	5.000E-05	4.600E-05	3.100E-05	1.599E-05	6.957E-06	1.927E-06	8.742E-07	0.000E+00	
14.5	0.000E+00	0.000E+00	0.000E+00	0.000E+00	0.000E+00	1.000E-06	4.000E-06	1.200E-05	1.800E-05	1.800E-05	1.300E-05	7.000E-06	3.000E-06	9.977E-07	0.000E+00	0.000E+00	
15.5	0.000E+00	0.000E+00	0.000E+00	0.000E+00	0.000E+00	0.000E+00	1.000E-06	4.000E-06	6.000E-06	7.000E-06	5.000E-06	3.000E-06	1.000E-06	9.999E-07	0.000E+00	0.000E+00	
16.5	0.000E+00	0.000E+00	0.000E+00	0.000E+00	0.000E+00	0.000E+00	0.000E+00	1.000E-06	2.000E-06	2.000E-06	2.000E-06	1.000E-06	1.000E-06	0.000E+00	0.000E+00	0.000E+00	

In *Table 6.7*, can be found the weighted short-term failure index, which considers the probability of occurrence for specific environmental conditions in the North Atlantic. Or, in another hand, *Table 4.2* and *Table 6.6* are combined. By factoring $C_{DSC,s}$, the analysis becomes more representative of real scenarios. Similarly, green cells indicate a weighted index of 0, while the color transitions towards yellow and then to red, the probability increases.

The long-term probability index (C_{DSC}) of the worked example can be obtained by summarizing the weighted short-term failure index from *Table 6.7*. The calculation is as follows:

$$C_{DSC} = \sum_{i=1}^n C_{DSC,s,i} \cdot W_i = 0.006485 \quad (6.3)$$

According to the *Equation (4.27)*, the worked example meets the vulnerability criteria at Level 2 for the Dead Ship Condition failure mode. This is because the long-term stability failure index is less than the long-term standard R_{DS0} , which is 0.06.

As mentioned above, in the following chapter, the same procedure will be repeated for different freeboard heights of the sample vessel, with variations of metacentric height. This approach allows us to evaluate the freeboard impact on dynamic stability under different conditions and identify potential vulnerabilities across the range of metacentric heights.

Analysis and Interpretation of Results

7.1. Research Outcome

In this Chapter, the impact of freeboard as a design parameter on dynamic ship stability will be examined. The analysis is based on comparing the Dead Ship Condition failure indices obtained for the sample ship with different freeboard heights, with and without bilge keels, and with different container arrangements. The code made for the purpose of the thesis is validated with the available IMO data (*IMO, 2013*) and cross-checked with the corresponding code used at the Department of Naval Architecture of the Faculty of Mechanical Engineering, University of Belgrade (*Rudaković, 2021*).

In *Figure 7.1*, *Figure 7.2*, *Figure 7.3*, and *Figure 7.4* the long-term stability failure index C_{DSC} of the sample ship is reported as a function of metacentric height. Each curve corresponds to a specific freeboard height, which ranges from 1.5 to 3 m with a step of 0.5 m, as previously explained in *Chapter 5*. A ship is considered to be safe if the values of the failure indices are lower than the long-term standard $R_{DS0} = 0.06$. Correspondingly, the red-shaded areas represent unacceptable levels of safety. The points plotted on the curves indicate the minimum values of initial metacentric heights calculated in compliance with the Vulnerability Level 1 criterion, as described in *Section 4.1*.

Remark: : Loading Conditions and Bilge Keels Dimensions

1. The projected lateral area for Loading Condition 1 (LC1) is $A_L = 1880.55 \text{ m}^2$ and the vertical distance between the center of the windage and underwater area is $Z = 11.89 \text{ m}$.
2. The projected lateral area for Loading Condition 2 (LC2) is $A_L = 1735.63 \text{ m}^2$ and the vertical distance between the center of the windage and underwater area is $Z = 11.25 \text{ m}$.
3. It is assumed that the bilge keel (BK) dimensions correspond to the maximum values of applicability of Simplified Ikeda's method. The width is 0.22 m, and the length of the bilge keels is 40% of the ship's length.

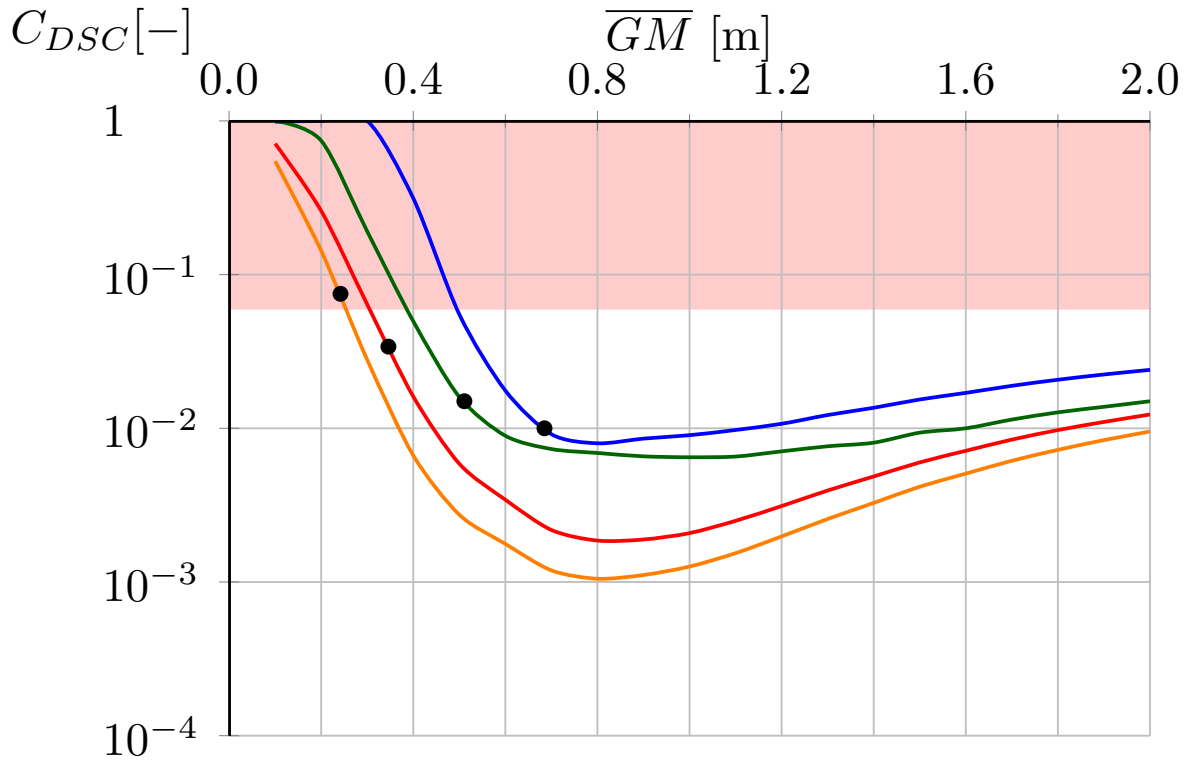


Figure 7.1: Long-term probability index for Loading Condition 1, ship with bilge keels. $F_B = 1.5$ m (—), $F_B = 2$ m (—), $F_B = 2.5$ m (—), and $F_B = 3$ m (—).

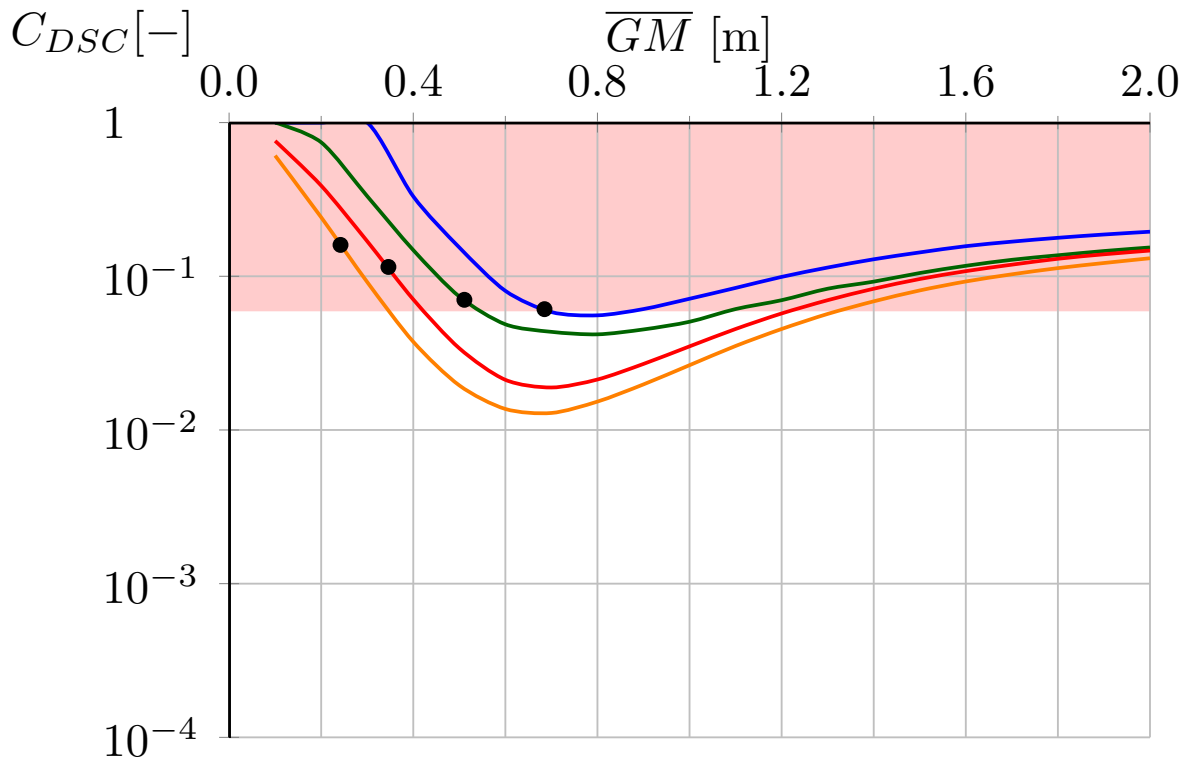


Figure 7.2: Long-term probability index for Loading Condition 1, ship without bilge keels. $F_B = 1.5$ m (—), $F_B = 2$ m (—), $F_B = 2.5$ m (—), and $F_B = 3$ m (—).

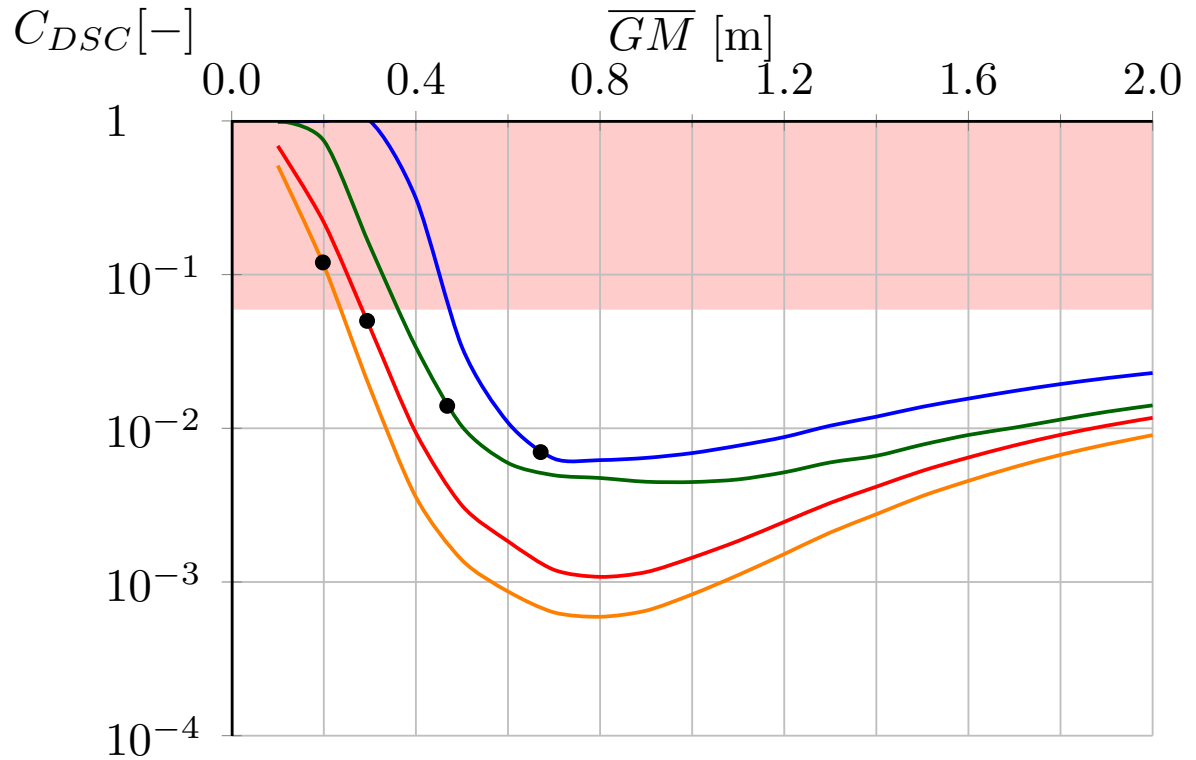


Figure 7.3: Long-term probability index for Loading Condition 2, ship with bilge keels. $F_B = 1.5$ m (—), $F_B = 2$ m (—), $F_B = 2.5$ m (—), and $F_B = 3$ m (—).

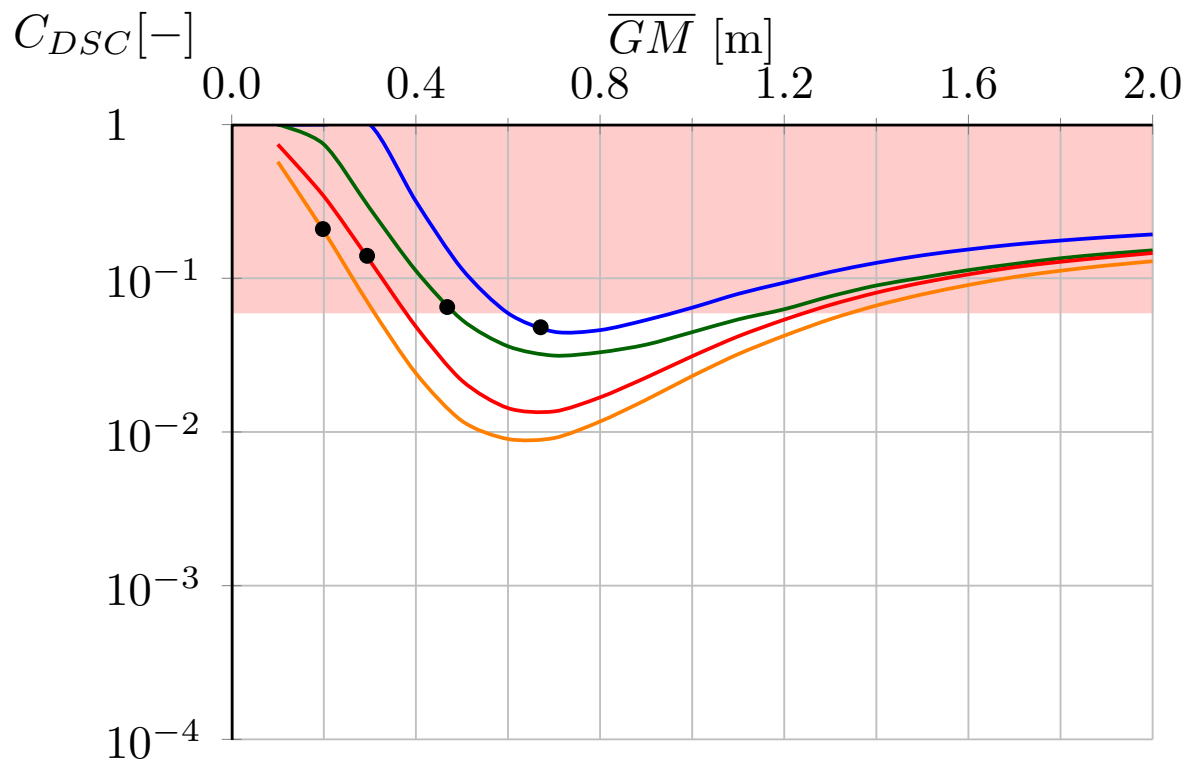


Figure 7.4: Long-term probability index for Loading Condition 2, ship without bilge keels. $F_B = 1.5$ m (—), $F_B = 2$ m (—), $F_B = 2.5$ m (—), and $F_B = 3$ m (—).

7.2. Interpretation

Each examined case indicates that the vessels with higher freeboards exhibit better dynamic stability in Dead Ship Condition failure mode. Or, to put it differently, as the freeboard increases, the long-term stability failure index decreases for the same metacentric height and container arrangement. It may be noticed that the influence of freeboard is more pronounced in the region corresponding to smaller metacentric heights. This may be explained by the fact that in the range of small metacentric heights, the \overline{GZ} curve is dominated by the residual lever \overline{GZ}_{res} which depends on the hull form geometry. However, as the metacentric height increases, so does the influence of the other term (\overline{GZ}_c) in [Equation \(2.2\)](#). Aside from hull form, \overline{GZ}_c also depends on the vertical distribution of the masses as mentioned before. Increasing the freeboard height provides sufficient stability for a wider range of \overline{GM} when the ship is exposed to the beam waves and gust wind. Using a different probabilistic approach, similar results were obtained in the study of *Bačkalov and Rudaković, 2017*. The Authors also assert that an increase in the metacentric height does not always improve the ship's stability, contrary to the classic ship stability concept. In addition to the minimal, the maximal metacentric height can be determined as well; a further increase of the metacentric height would make the ship even more vulnerable to this stability failure mode than with lower values. It can be arrived at the same conclusion using the probabilistic approach given in SGISC. Similar observations are found in *Bulian and Francescutto, 2011*.

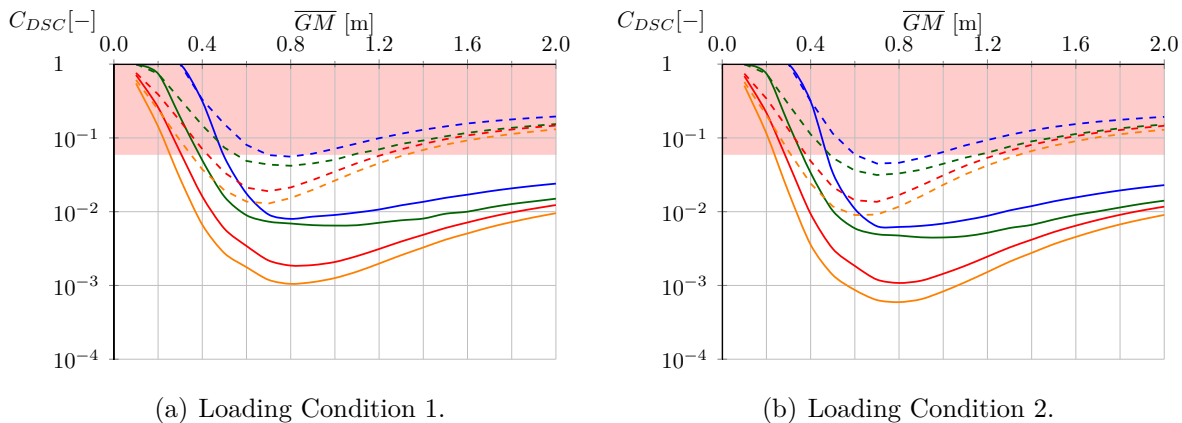


Figure 7.5: Impact of bilge keels. With bilge keel : $F_B = 1.5 \text{ m}$ (—), $F_B = 2 \text{ m}$ (—), $F_B = 2.5 \text{ m}$ (—), and $F_B = 3 \text{ m}$ (—). Without bilge keel : $F_B = 1.5 \text{ m}$ (- - -), $F_B = 2 \text{ m}$ (- - -), $F_B = 2.5 \text{ m}$ (- - -), and $F_B = 3 \text{ m}$ (- - -).

The impact of bilge keels on ship safety is noticeable, as the probability of failure calculated for the ship with bilge keels is by an order of magnitude lower, on average, in comparison to the results obtained for the ship without them. In the framework of SGISC, the conventional "axiom" of static ship stability ("greater the metacentric height, better the stability") is no longer valid. Namely, it may be observed that an optimal \overline{GM} value can correspond to the lowest value of the long-term failure index be determined for each of the curves given in [Figure 7.1](#), [Figure 7.2](#), [Figure 7.3](#), and [Figure 7.4](#). The C_{DSC} corresponding to optimal \overline{GM} may be up to two orders of magnitude lower than the values obtained for other metacentric heights; such is the case for the highest freeboard

analyzed, $F_B = 3 \text{ m}$ (see *Figure 7.1* and *Figure 7.3*). For the case when the sample ship is equipped with bilge keels, the optimal \overline{GM} approximately appears around 0.8 m , while without the bilge keels, it shifts to around 0.7 m . The impact of bilge keels is summarized in *Figure 7.5*. In the region of lower metacentric heights, before reaching the optimal metacentric height, the curves of C_{DSC} are much steeper when the ship is equipped with bilge keels. This indicates that the effects of roll damping due to bilge keels decrease with higher values of metacentric heights.

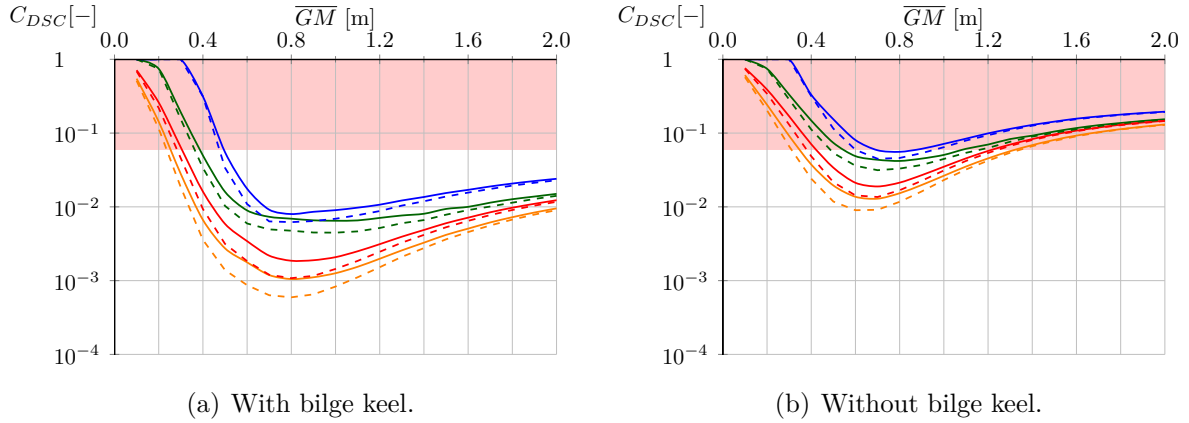


Figure 7.6: Comparison between different loading conditions. Loading Condition 1 : $F_B = 1.5 \text{ m}$ (—), $F_B = 2 \text{ m}$ (—), $F_B = 2.5 \text{ m}$ (—), and $F_B = 3 \text{ m}$ (—). Loading Condition 2 : $F_B = 1.5 \text{ m}$ (- - -), $F_B = 2 \text{ m}$ (- - -), $F_B = 2.5 \text{ m}$ (- - -), and $F_B = 3 \text{ m}$ (- - -).

In Loading Condition 2, a case where the number of container tiers is reduced, the positive influence of wind on the C_{DSC} is noted within certain areas. Furthermore, comparison between LC1 and LC2, when considering the presence of bilge keels, reveals a decreased wind influence starting at around $\overline{GM} \approx 0.6 \text{ m}$, contrasted to $\overline{GM} \approx 0.5 \text{ m}$ when bilge keels are absent. These observations lead to the conclusion that the metacentric height reduction corresponds to increased wind influence. Regarding acceptable range, the minimum metacentric height (\overline{GM}_{min}) according to Vulnerability L2 is not significantly shifted to smaller values for LC2 than for LC1 with the presence of bilge keels as shown in *Figure 7.6* (a). More specifically, \overline{GM}_{min} begins before 0.25 m for the highest freeboard and before 0.5 m for the smallest freeboard. However, an upper limit (\overline{GM}_{max}) does not exist for the considered range of metacentric heights in this analysis. Contrary to the case of the absence of bilge keels (see *Figure 7.6* (b)), where the acceptable range of metacentric height (\overline{GM}_{min} and \overline{GM}_{max}) can be clearly defined. Furthermore, as the freeboard height increases, the acceptable range also widens, approximately 5 cm on each side. Considering $F_B = 1.5 \text{ m}$ in both loading cases, only a small segment of \overline{GM} meets the acceptable safety level. This suggests that for ships operating with lower metacentric heights and without bilge keels, higher freeboards can be extremely beneficial. For instance, if a ship with $F_B = 1.5 \text{ m}$ is exposed to rough weather, it must maintain a very narrow acceptable range of approximately $\overline{GM}_{min} \approx 0.7 \text{ m}$ to $\overline{GM}_{max} \approx 0.9 \text{ m}$ to avoid excessive rolling angles. In contrast, for $F_B = 3 \text{ m}$, this range expands significantly, spanning from $\overline{GM}_{min} \approx 0.3 \text{ m}$ to $\overline{GM}_{max} \approx 1.3 \text{ m}$.

In order to examine the consistency and correlation between the vulnerability criteria L1 and L2, values of the minimum acceptable metacentric height according to the Weather Criterion (L1) are calculated. Results according to L1 and L2 for Loading Condition 1 and Loading Condition 2 are given in *Table 7.1*. The increase in the freeboard is accompanied by a decrease in the minimum metacentric height according to both vulnerability criteria, which means certain flexibility in the exploitation of the ship. However, the safety levels attained with \overline{GM}_{min} differ for all examined cases using criteria at L1 and L2.

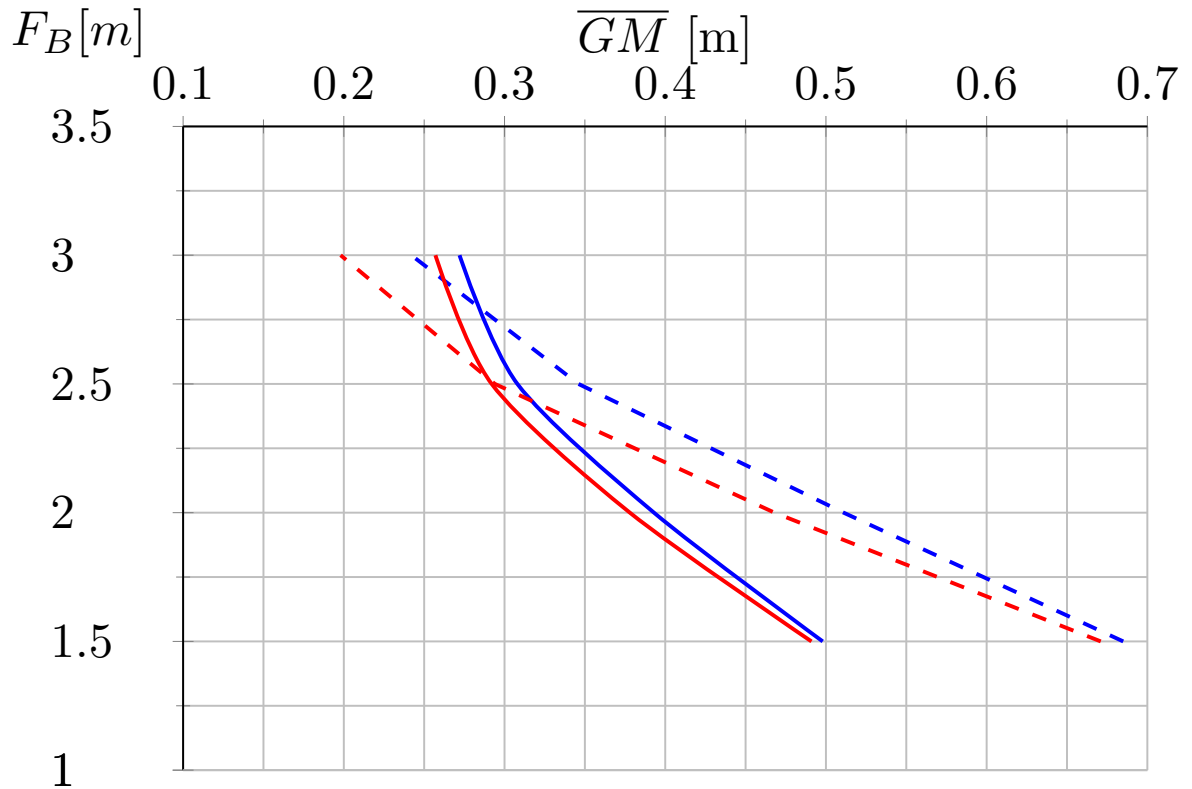
Table 7.1: Minimum metacentric height $\overline{GM}[m]$ according to Level 1 (L1) and Level 2 (L2) under Loading Conditions 1 (LC1) and Loading Conditions 2 (LC2), with and without bilge keels (BK).

F_B m	LC1				LC2			
	With BK		Without BK		With BK		Without BK	
	L1	L2	L1	L2	L1	L2	L1	L2
1.5	0.685	0.498	0.685	0.693	0.671	0.491	0.671	0.599
2	0.511	0.393	0.511	0.555	0.468	0.378	0.468	0.489
2.5	0.346	0.308	0.346	0.429	0.294	0.292	0.294	0.386
3	0.242	0.272	0.242	0.359	0.198	0.257	0.198	0.315

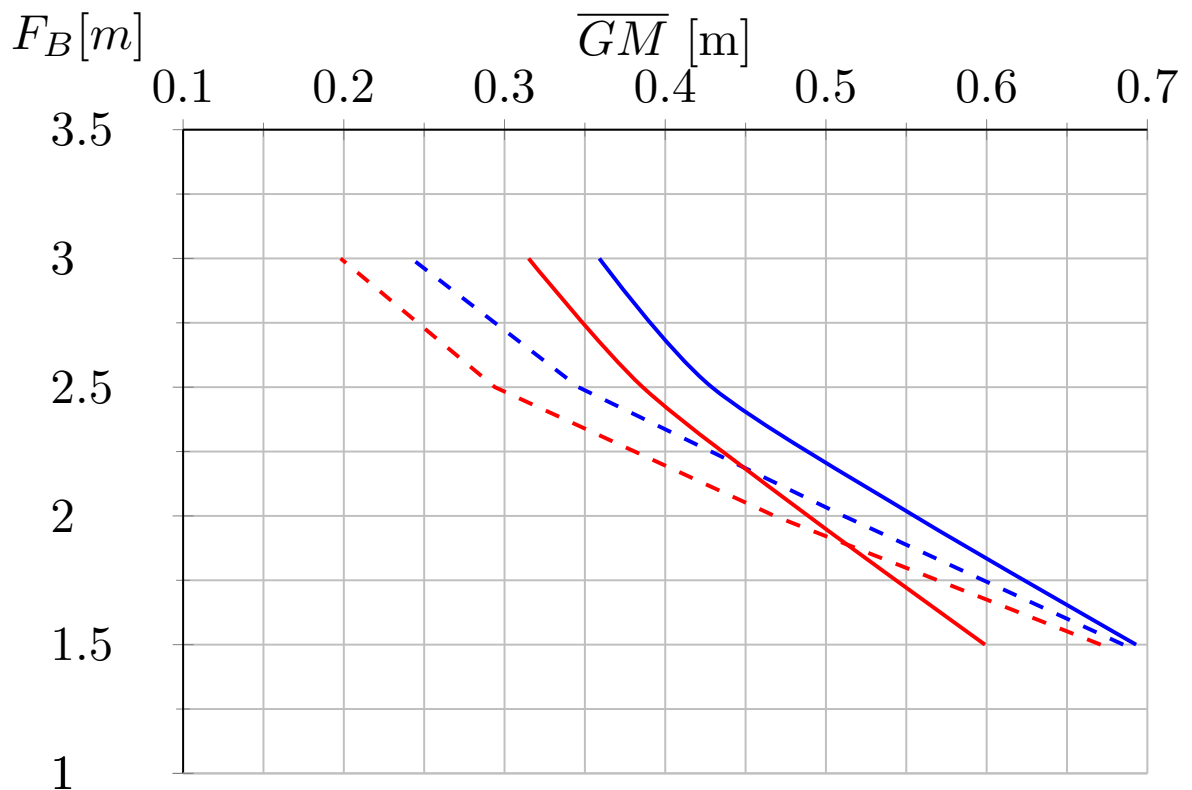
Vulnerability Level 1 should be more rigorous than Vulnerability Level 2, having stricter standards and ensuring higher safety. Or in simple terms, \overline{GM}_{min} calculated by L2 should be smaller than L1. Therefore, in the case of the absence of a bilge keel, the expected results are only achieved for the lowest freeboard $F_B = 1.5 m$ if the number of containers is reduced, while if the ship is equipped with bilge keels the consistency is achieved for all freeboards, except for the highest one ($F_B = 3 m$) for both container arrangements. The possible existence of inconsistencies between L1 and L2 is acknowledged in *IMO, 2020*.

As previously noted, minimum metacentric heights are higher for the cases which are showing that L2 is more conservative than L1. However, deterministic regulations are satisfied in those cases but L2 is not met. This implies a potential unreliability with L1, as the probabilistic approach provides a more accurate mathematical model in depicting the ship's rolling when it is exposed to a storm from the beam. The question remains open why is Weather Criteria chosen for the first level? The minimum metacentric heights, as determined by L1 for both container arrangements, remain constant regardless of the presence or absence of bilge keels on the ship. Moreover, the most failed requirement is a limitation of the static angle of the heel to 80% of the angle at which the deck enters to water. It's observable that both levels obtain the impact of wind, as evidenced by the smaller \overline{GM}_{min} for LC2 in comparison to LC1.

The analysis also indicated that if the ship has bilge keels and lower F_B , the flexibility of operation with lower metacentric height can be raised by applying the probabilistic approach. For instance, applying L2 for $F_B = 1.5 m$ gives $0.18 m$ smaller \overline{GM}_{min} . However, differences between levels from this point of view are decreasing with increasing the height of freeboards. Depending on freeboard height, loading condition, and with or without the presence of bilge keels, minimum metacentric heights \overline{GM}_{min} according to Vulnerability L1 and L2 which are necessary to operate in rough seaways can be determined using *Figure 7.7*.



(a) With bilge keels.



(b) Without bilge keels.

Figure 7.7: Minimum metacentric height for different freeboard heights according to Vulnerability Level 1 and Level 2. Loading Condition 1: Level 1(---), Level 2(—). Loading Condition 2 : Level 1(---), Level 2(—).



Conclusions and Future Work

The thesis investigated the influence of the freeboard on the dynamic stability of a small container vessel (a feeder) in intact condition exposed to gusty wind and irregular waves. Specifically, the analysis addressed the vulnerability of the examined ship to the Dead Ship Condition (DSC) which is one of the five stability failure modes considered in the framework of Second Generation Intact Stability Criteria (SGISC). SGISC represents the novel, multi-tier stability criteria put forward by the International Maritime Organization (IMO) which are based on a physically more realistic relation between ship motion and environmental conditions than the first generation of the stability criteria. SGISC was completed in 2020 and is to be included in the Intact Stability Code after a period of trials and verification.

The DSC scenario implies that the ship has lost its power and that it is, consequently, turned into beam seas where it rolls and drifts under rough seaways. Within this thesis, the stability assessment of the examined ship is accomplished at Vulnerability Level 1 (L1) and Vulnerability Level 2 (L2). For the purpose of the thesis, the computer codes for L1 and L2 assessments were made and verified using the data made available by IMO and the international ship stability community.

During the validation phase, in accordance with the SGISC Guidelines *IMO, 2013*, and the cross-checking process with *Rudaković, 2021*, certain discrepancies in obtained results occurred. These discrepancies are primarily attributed to the absence of clear instructions in the SGISC Guidelines *IMO, 2020* and Explanatory notes *IMO, 2023* regarding the exact discretization step or interpolation method necessary for accurately defining the \overline{GZ} curve. The difference between the short-term failure index $C_{DSC,s}$ calculated from the developed code and that of the IMO data amounts to a relative error of 6.923%. Similarly, the computation of the local metacentric height \overline{GM}_{res} at the equilibrium angle (φ_s) lacks an explicit method of determination. Therefore, discrepancies in results arise from utilizing different methodologies. Furthermore, the magnitudes of discrepancies depend on the complexity and precision of the used method. While the discretization steps could be refined or alternative, more precise interpolation methods could be adopted, it is crucial to consider the equilibrium between computational efficiency and accuracy when selecting these approaches.

The inconsistencies between L1 and L2, as highlighted in *IMO, 2020*, were also observed in this study across various examined cases. The inconsistencies occurred when minimum metacentric heights corresponding to L2 assessment were found to be greater than the minimum metacentric heights calculated in compliance with L1, meaning that in such cases L2 was more conservative than L1. These findings emphasize a potential reliability issue with L1 since the probabilistic L2 approach delivers a more precise mathematical model representing the ship's rolling motions in rough sea.

As expected, the analyses confirmed that an increase in freeboard improves intact dynamic stability. However, the probabilistic analysis performed at L2 of SGISC allows for quantification of this improvement. Higher freeboard leads to a marked reduction in the probability of stability failure in Dead Ship Condition: up to two orders of magnitude in some of the examined cases. Higher freeboard also allows for the lowering of the minimum metacentric heights. If the ship is equipped with bilge keels, \overline{GM}_{min} corresponding to the highest freeboard ($F_B = 3\text{ m}$) is approximately 0.23 m lower than the \overline{GM}_{min} corresponding to the lowest freeboard ($F_B = 1.5\text{ m}$); this applies to both container arrangements (i.e. Loading Condition 1 and 2). In case the examined ship does not have bilge keels, \overline{GM}_{min} corresponding to the highest ($F_B = 3\text{ m}$) is approximately 0.33 m lower than the \overline{GM}_{min} corresponding to the lowest freeboard ($F_B = 1.5\text{ m}$) in Loading Condition 1; this difference is 0.28 m in Loading Condition 2 (smaller lateral area). Such findings would not be possible within the framework of the first generation of intact stability criteria. Furthermore, the use of the probabilistic analysis enables the calculation of the optimum \overline{GM} (corresponding to the lowest probability of stability failure) as well as the maximum \overline{GM} . That is, a range of "acceptable" metacentric heights complying with the L2 DSC standard can be calculated. This range is also expanded with the increase of freeboard. In case there are no bilge keels, the range of acceptable metacentric heights corresponding to the highest freeboard ($F_B = 3\text{ m}$) is almost 1 m (from 0.33 m to 1.3 m), while the range of acceptable metacentric heights corresponding to the lowest freeboard ($F_B = 1.5\text{ m}$) is barely 0.15 m in Loading Condition 1. In Loading Condition 2, the range of acceptable metacentric heights is a bit over 1 m (from 0.3 m to 1.35 m) when $F_B = 3\text{ m}$, as compared to just 0.35 m (from 0.6 m to 0.95 m) when $F_B = 1.5\text{ m}$.

However, in case the ship is equipped with bilge keels, the range of acceptable metacentric heights is considerable even for the lowest freeboard analyzed in the study (in fact, there seems to be no upper limit of metacentric heights; nevertheless, the actual range of realistic metacentric heights is limited by the available loading options and possible vertical distribution of cargo). In addition, the probability of stability failure for the same metacentric height and the same freeboard reduces by approximately an order of magnitude due to bilge keels. Thus, the question arises: how cost-efficient is the increase of freeboard (which requires a different ship structure, increases gross tonnage, and may decrease payload) if similar effects in terms of intact stability are achieved by bilge keels that are simple and inexpensive?

The answer to this question is not straightforward. Although the addition of bilge keels itself considerably decreases the probability of stability failure in Dead Ship Condition (at a low cost) the increase of freeboard pushes \overline{GM}_{min} further towards lower values. Lower metacentric heights are beneficial from the point of view of roll motion (leading to *soft* rolling) and could be particularly important for container ships as a measure for mitigation of excessive lateral accelerations.

The effectiveness of the freeboard in the improvement of intact dynamic stability in seaway requires further research. It is deemed that the present L2 DSC mathematical model may not be entirely appropriate for studying the dynamic stability of ships with low freeboards (e.g. lower than required by the International Convention on Load Line), considering that a number of phenomena related to deck-in-water/water-on-deck effects are not taken into account by the model. Furthermore, it should be examined how the freeboard affects the other stability failure modes recognized by SGISC. Freeboard is one of the most fundamental concepts of ship safety and, thus, one of the most important design parameters. Therefore, its selection requires a holistic approach which is facilitated by the Second Generation Intact Stability Criteria framework. It is hoped that this thesis contributes to a better understanding of the importance of application of the novel stability methods for ship safety.

Bibliography

- Bačkalov, I. (2017). *International maritime regulations: Ship safety* [In Serbian].
Belgrade, Serbia, Faculty of Mechanical Engineering, University of Belgrade.
- Bačkalov, I., & Rudaković, S. (2017).
Influence of freeboard on ship stability in rough weather: A probabilistic analysis.
FME Transactions, 45(1), 45–50.
- Bulian, G., & Francescutto, A. (2004). A simplified modular approach for the prediction of the roll motion due to the combined action of wind and waves.
Proceedings of the Institution of Mechanical Engineers, Part M: Journal of Engineering for the Maritime Environment, 218(3), 189–212.
- Bulian, G., & Francescutto, A. (2011). Considerations on parametric roll and dead ship conditions for the development of second generation intact stability criteria,
In *Proc. 12th international ship stability workshop, washington, usa*.
- Francescutto, A. (2023).
Rahola criterion and the development of the intact stability code,
In *Contemporary ideas on ship stability: From dynamics to criteria*. Springer.
- Hofman, M. (2020). *Seakeeping* [In Serbian].
Belgrade, Serbia, Faculty of Mechanical Engineering, University of Belgrade.
- Hofman, M., & Bačkalov, I. (2005).
Weather criterion for seagoing and inland vessels—some new proposals,
In *Proceedings of international conference on marine research and transportation, icmrt '05, university of naples "federico ii*.
- IACS/LL. (2008). *Interpretations of the international convention on load lines, 1966*,
International Association of Classification Societies. London.
- IMO. (2008).
Adoption of the international code on intact stability, 2008 (MSC.267(85)).
International Maritime Organization. London.
- IMO. (2013).
Vulnerability assessment for dead-ship stability failure mode (SDC 1/INF.6).
International Maritime Organization. London.

- IMO. (2019). *Finalization of second generation intact stability criteria* (SDC 7/5). International Maritime Organization. London.
- IMO. (2020). *Interim guidelines on second generation intact stability criteria* (MSC.1/Circ/1627). International Maritime Organization. London.
- IMO. (2022). *Development of explanatory notes to the interim guidelines on second generation intact stability criteria* (SDC 8/WP.4/Add.2). International Maritime Organization. London.
- IMO. (2023). *Explanatory notes to the interim guidelines on the second generation intact stability criteria* (MSC.1/Circ.1652). International Maritime Organization. London.
- Kawahara, Y., Maekawa, K., & Ikeda, Y. (2011). A simple prediction formula of roll damping of conventional cargo ships on the basis of ikeda's method and its limitation. *Contemporary Ideas on Ship Stability and Capsizing in Waves*, 465–486.
- Kobyliński, L. (2014). Stability criteria-present status and perspectives of improvement. *TransNav: International Journal on Marine Navigation and Safety of Sea Transportation*, 8(2), 281–286.
- Lloyd, A. (1998). *Seakeeping: Ship behaviour in rough weather*. Gosport, Hampshire, United Kingdom.
- Munakata, S., Takagaki, K., Umeda, N., Koike, H., Sakai, M., Maki, A., Manabe, K., & Matsuda, A. (2022). An investigation into false-negative cases for low-freeboard ships in the vulnerability criteria of dead ship stability. *Ocean Engineering*, 266, 113130.
- Nechaev, Y. (1978). *Modelling of ship stability in waves* [In Russian]. Leningrad.
- Rahola, J. (1939). *The judging of the stability of ships and the determination of the minimum amount of stability—especially considering the vessels navigating finnish waters*. Aalto University.
- Ribar, B. (1986). *Ship theory* [In Serbian]. Belgrade, Serbia, Faculty of Mechanical Engineering, University of Belgrade.
- Rudaković, S. (2014). *Influence of freeboard on the stability of a small multipurpose cargo ship* (Master's thesis) [In Serbian]. Faculty of Mechanical Engineering, University of Belgrade. Belgrade, Serbia. In Serbian.

Rudaković, S. (2021). *A novel approach to stability assessment of river-sea ships*
(Doctoral dissertation).
Faculty of Mechanical Engineering, University of Belgrade. Belgrade, Serbia.

Schneekluth, H., & Bertram, V. (1998).
Ship design for efficiency and economy (Vol. 218).
Butterworth-Heinemann Oxford.